“Au-Ag-telluride-selenide deposits”

Field Trip Notes

Field workshop of IGCP-486

Sponsored by:

SE European Geoscience Foundation

IVANHOE HEREWARD BULGARIA EAD

Organized by:

Sofia University “St. Kl. Ohridski”
Geological Institute at Bulgarian Academy of Sciences
University of Mining and Geology “ St. I. Rilski”
Bulgarian Mineralogical Society

14 - 19th September 2005

KITEN, BULGARIA

Organizing Committee

Nigel Cook, University of Oslo (IGCP-486 Project Leader)
Kamen Bogdanov, Sofia University “St. Kl. Ohridski”
Ivan Bonev, Geological Institute at Bulgarian Academy of Sciences
Strashimir Strashimirov, University of Mining and Geology “St. I. Rilski”

www.segweb.org

Sofia SEG Student Chapter

Introduction

The ore deposits described in the following pages and in the enclosed copies of scientific papers have been chosen to emphasize different ideas concerning the geology, petrology, mineralogy, ore genesis, and metallogeny of the most important porphyry and epithermal systems in three parts of Bulgaria (Panagyurishte ore district, Rhodopes and Burgas district).

During the first day of the field trip the participants will tour the Late Cretaceous Chelopech and Vlaykov Vruh epithermal and porphyry-copper deposits (Fig. 1), learn about local geology, see and sample host-rock alteration styles and important ore types, and discuss their genesis.

The second day of the field trip is devoted to the Tertiary LS type gold deposits Chala and Ada Tepe, as new and important targets for gold exploration and exploitation in the Eastern Rhodopes of Bulgaria.

Following the scientific session in Kiten, participants will have the opportunity to examine Late Cretaceous epithermal vein mineralization at Zidarovo, in the eastern district of Burgas.

Kamen Bogdanov, Strashimir Strashimirov, Ivan Bonev and Nigel Cook
- organizers and editors

******

The Srednogorie metallogenic zone in Bulgaria (Fig. 1) is part of the global Tethyan-Eurasian copper belt. The Panagyuirishte ore region, the most important element of the Srednogorie metallogenic zone, contains characteristic calc-alkaline magmatism that hosts the Bulgaria's most important economic porphyry and epithermal ore deposits. Significant examples of discrete Upper Cretaceous volcano-plutonic centres with porphyry-copper deposits (Elatsite, Medet, Assarel, Tsar Assen, Vlaykov Vruh) closely associated with intermediate- to high-sulphidation Cu-Au epithermal deposits (Chelopech, Krassen, Radka, Elshitsa) occur in the Panagyurishte ore district (Fig. 1).

The copper ore deposits in Bulgaria have been known since ancient times. One of the oldest known copper mines in Europe, which dates from the 4th Century B.C., was located in the central part of the Srednogorie metallogenic zone near the town of Stara Zagora. Copper-gold epithermal ore deposits (Radka, Elshitsa, Krassen) attracted geological studies and exploration during the twentieth century. Modern geological exploration and mining exploitation started in 1922. During the last 50 years active mining operations have been carried out in the Elatsite,

Medet, Assarel, Tsar Assen, and Vlaikov Vruh porphyry deposits as well as in the Chelopech, Krassen, Elshitsa, and Radka Cu-Au epithermal deposits. Operations at present are in decline, and most of the deposit sites are being abandoned. Since 1950 more than 460 Mt of ore have been mined from these deposits, which have produced about 2 Mt Cu and 2.5 million oz of gold.

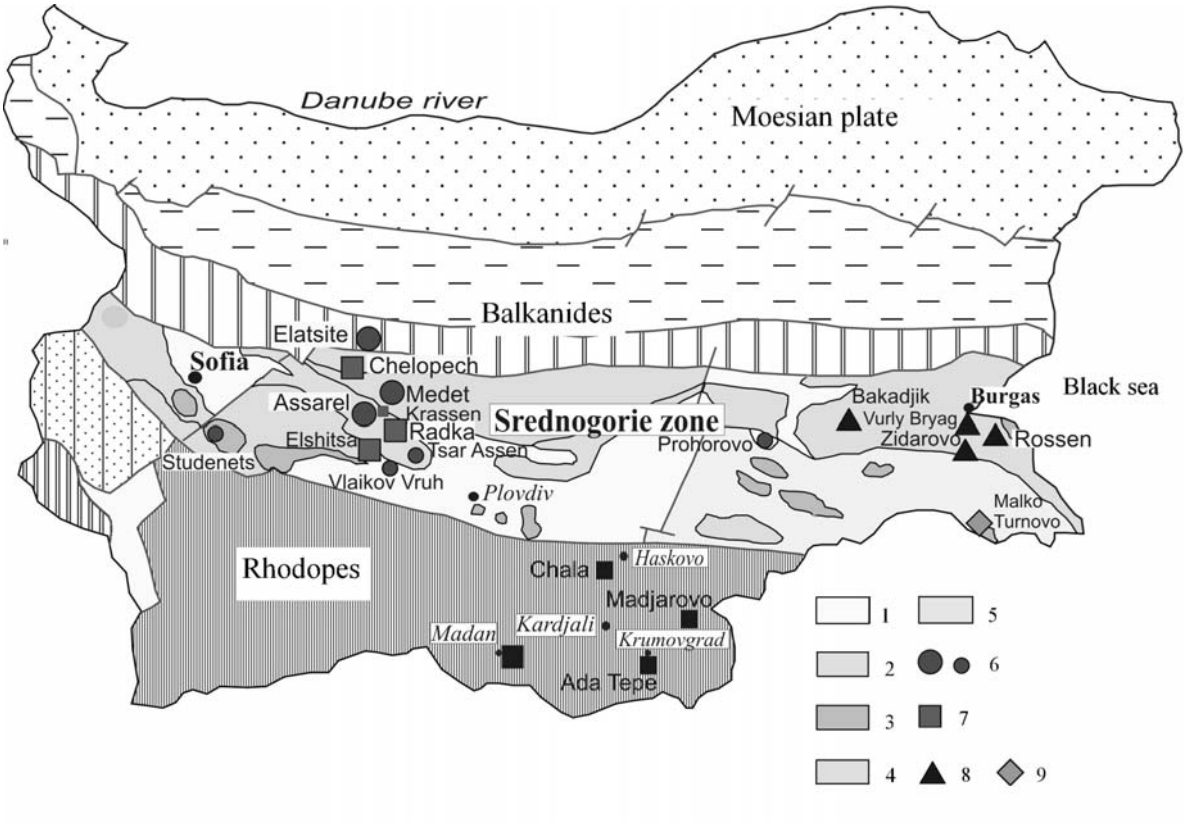

Fig. 1. Location of Cu and Au ore deposits in the Srednogorie metallogenic zone and the Rhodopes. 1 = Cenozoic sediments, 2 = Late Cretaceous volcanic rocks, 3 = Late Cretaceous intrusions, 4 = Paleozoic granites and metamorphic rocks, 5 = Paleozoic and Mesozoic metamorphic rocks, 6 = Porphyry copper deposits, 7 = Epithermal deposits, 8 = Vein copper deposits, 9 = Skarn deposits (Modified after Bogdanov and Strashimirov, 2003).

Porphyry deposits in the central and southern part of the Panagyurishte ore region

Strashimir Strashimirov* and Kamen Bogdanov**

**University of Mining and Geology "St. Ivan Rilski," Sofia, Bulgaria*

***Sofia University "St. Kliment Ohridski,"*

Department of Mineralogy, Petrology and Economic Geology, Sofia, Bulgaria

The Srednogorie part of the metallogenic zone in Bulgaria developed during the Mesozoic as a copper-rich, andesite-dominated island arc system (Fig. 1) that continues eastwards through Turkey to Iran. (Jankovic, 1977, 1997; Bogdanov, 1987; Dabovski et al., 1991; Heinrich and Neubauer, 2002). According to Popov et al. (2000, 2002, 2003), the Panagyurishte ore region is part of the Late Cretaceous Apuseni-Banat-Timok-Srednogorie magmatic and metallogenic belt (Fig. 2).

The Panagyurishte ore district is located in a 30 x 50 km belt trending N-NW and S-SE of the town of Panagyurishte in the central Srednogorie, Bulgaria (Fig. 2). The district belongs to the Late Cretaceous Banat-Srednogorie metallogenic zone, part of the European Alpine belt (De Boorder et al., 1998; Neubauer et al., 2002). The zone (Fig. 2), also known as the Banatititic magmatic and metallogenetic belt (BMMB) (Berza et al., 1998, Ciobanu et al., 2002; Heinrich and Neubauer, 2002) was formed as a result of Late Cretaceous subduction-related magmatic activity. Porphyry Cu-(Au)-(Mo) and intimately associated epithermal massive sulphides dominate in the central segments (Fig. 2, Table 1) of the belt (Ciobanu et al., 2002; Bogdanov et al., 2004), in southernmost Banat (Romania), Serbia and NW Bulgaria (Moldova Nouă in Romania, Majdanpek, Veliki Krivelj and Bor in Serbia, and Elatsite, Assarel and Chelopech in Bulgaria) Fe, Cu and Zn-Pb skarns occur mainly at the two ends of the belt (Fig. 2), in Eastern Bulgaria (Malko Turnovo: Burdtzeto, Mladenovo, Velikovets) and in Romania (Apuseni Mts., N.Banat). Vein deposits are present in the easternmost districts (Fig. 2) of Yambol (Bakadjik), Burgas (Zidarovo, Vurly Bryag, Rossen).

Two groups of porphyry copper deposits (Fig. 3) can be distinguished in the Panagyurishte ore region (Bogdanov, 1984, 1987; Strashimirov et al., 2002, 2003; Popov et al., 2003). The first group includes deposits of intrusives within the basement rocks. Ore mineralisation and hydrothermal alteration in this group are mainly in the apical part of the intrusive bodies and partly in the basement rocks (Medet, Elatsite). The second group includes deposits developed in

intrusive bodies located in effusive rocks. Hypabyssal to subvolcanic-hypabyssal porphyry intrusions controls the spatial position of the porphyry copper deposits in both groups. In some cases they are intruded into the central parts of the volcanic structures (Assarel, Petelovo) or into volcanic slopes (Tsar Assen, Vlaikov Vruh) and in other cases they are developed in basement rocks (Elatsite) or in the apical part of the intrusives (Medet, partly Elatsite). The orebodies are cone-like or column-like, rarely of linear stockwork type.

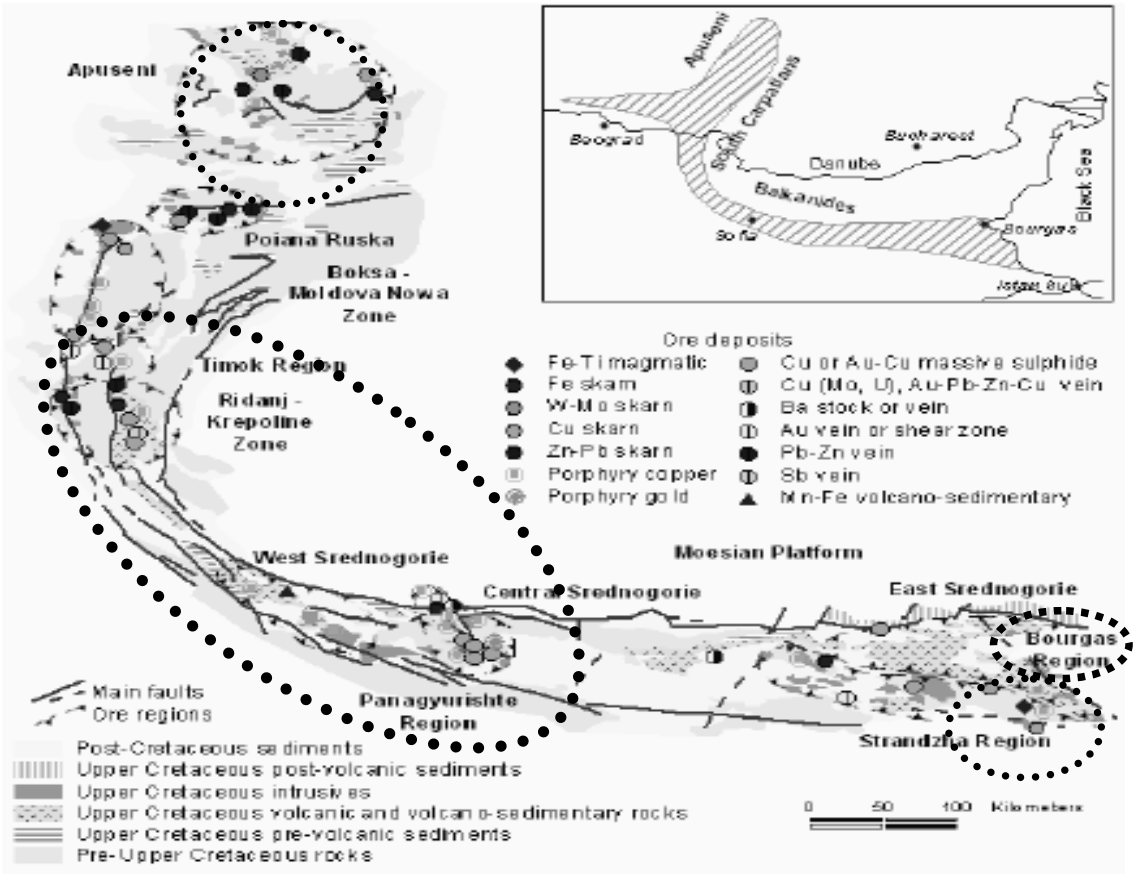

Fig.2. Late Cretaceous Apuseni-Banat-Timok-Srednogorie magmatic and metallogenic belt (After Popov et al., 2003).

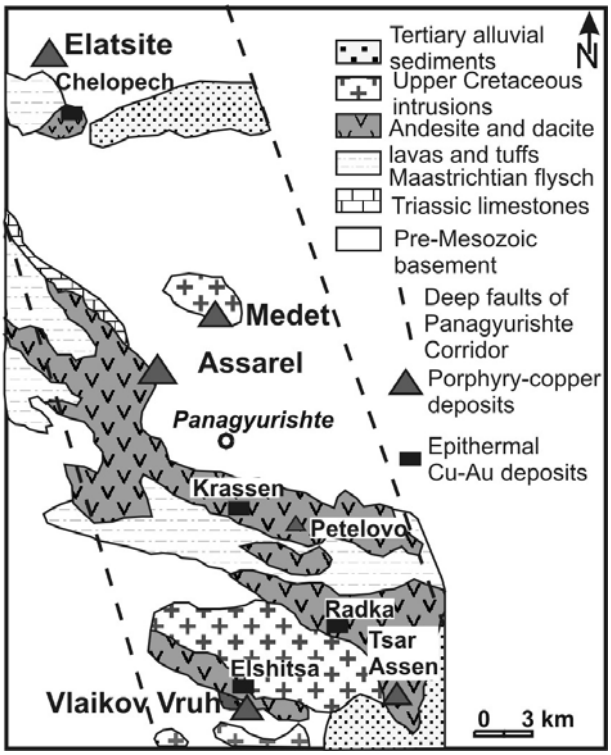

Fig. 3. Location of the porphyry copper deposit in the Panagyurishte ore region (modified after Bogdanov, 1987).

Table 1. Copper Deposits in the Panagyurishte Ore District and Their Production and Resources (data provided by the Bulgarian Ministry of Environment and Waters)

Deposit type and name	Remaining resources	Past production
Porphyry		
Assarel	254 Mt at 0.41% Cu In production since 1976	100 Mt at 0.53% Cu, trace Au
Elatsite	154 Mt at 0.33% Cu In production since 1981	165 Mt at 0.38% Cu, 0.21 g/t Au
Medet	Mined out (1984–1993)	163 Mt at 0.32% Cu, 0.1 g/t Au
Vlaikov Vruh	Mined out (1962–1979)	9.8 Mt at 0.46% Cu
Tsar Assen	Mined out (1980–1995)	6.6 Mt at 0.47% Cu
High sulphidation		
Chelopech	31 Mt at 1.39% Cu, 3.5 g/t Au In production since 1954	11.5 Mt at 1.0% Cu 3.0g/t Au
Intermediate to high sulphidation		
Krassen	Mined out (1962–1973)	0.30 Mt at 0.76% Cu
Intermediate sulphidation		
Elshitsa	Mined out (1947–1996) (1.5 Mt at 1.27% Cu)	2.5 Mt at 1.0% Cu
Radka	Mined out (1942–1997) (2.5 Mt at 0.6% Cu)	6.4 Mt at 1.0% Cu

(After Strashimirov et al., 2002; Popov et al., 2003)

Vlaikov Vruh Porphyry Copper Deposit

The Vlaikov Vruh porphyry copper deposit (Fig. 4) is located in the central part of Elshitsa ore field, about 1.5 km south of Elshitsa village and about 80 km SE of Sofia city (Fig. 3). It covers an area of about 0.5 km diameter. The deposit was open-pit mined from 1962 to 1979. During that time, 9,793,400 t copper ore with 0.46% average copper content was extracted (Milev et al., 1996). Resources of 22,700 t copper ore with 0.32% average copper contents still remain in the deposit. The porphyry-copper mineralisation is hosted in porphyry granodiorite to quartz diorite, which is intruded along the contact of Upper Cretaceous andesites, dacites, breccias and tuffs and in the pre-Mesozoic metamorphic and granitic basement (Figs. 4, 5). The intrusion extends E-W and is intersected by north-trending dacitic dykes. The geology of the Vlaikov Vruh deposit and the entire Elshitsa ore field is controlled by the setting and evolution of the Elshitsa volcano-intrusive complex (Bogdanov et al., 1970, 1972; Popov et al., 2000c). The Elshitsa effusive suite, numerous volcano-tectonic faults and later minor intrusives within the area of deposit compose this complex. The Vlaikov Vruh deposit is related to the granodiorite porphyry intrusion, which cuts the effusive rocks from the southern slope of Elshitsa stratovolcano as well as the basement rocks (Fig. 4).

The pre-Upper Cretaceous basement consists of Precambrian (?) muscovite-biotite and biotite gneisses. Garnet-two-mica, granitized biotite, muscovite and aplitic gneisses as well as layers from biotite and two-mica gneissic schists and schists are rarely observed. These rocks are assigned to the Pre-Rhodopian Supergroup with probable Archaean-Lower Proterozoic age (Katskov and Iliev, 1993). The Elshitsa effusive suite contains lava flows, lava-breccias, agglomerate, lapilli and rarely ash tuffs with 100°–130° strikes and 10°–30° N-NE dips overlying the highly metamorphosed basement rocks. Two sequences, andesitic (lower) and dacitic (upper), are distinguished in the suite (Boyadjiev and Chipchakova, 1963). The subvolcanic intrusions are mainly dacitic but rarely andesitic in composition. They are intruded mostly along E-SE faults and less along N-NW and E-NE faults in both the northern and the southern flanks of the deposit. The Vlaikov Vruh intrusion is subvolcanic to hypabyssal and consists of porphyry granodiorite (with transitions to porphyry quartz-monzodiorite, porphyry granite and porphyritic plagiogranite) with dacitic enclaves in the poorly crystallized parts around the contacts (Figs. 4, 5). Xenoliths from the metamorphic and rarely from the volcanic rocks (up to 170 x 420 mm in size) have also been observed. The major axis of the intrusion trends 115°–120°, its length is over 2 km and width is 100–150 m in the western part to 750–800 m in the eastern part. Meandering contacts and numerous apophyses penetrated into the host

rocks are typical of the intrusive. The late dacitic dykes with N-NW and E-SE trends crosscut all rock types including the altered propylitic rocks and the ore mineralization.

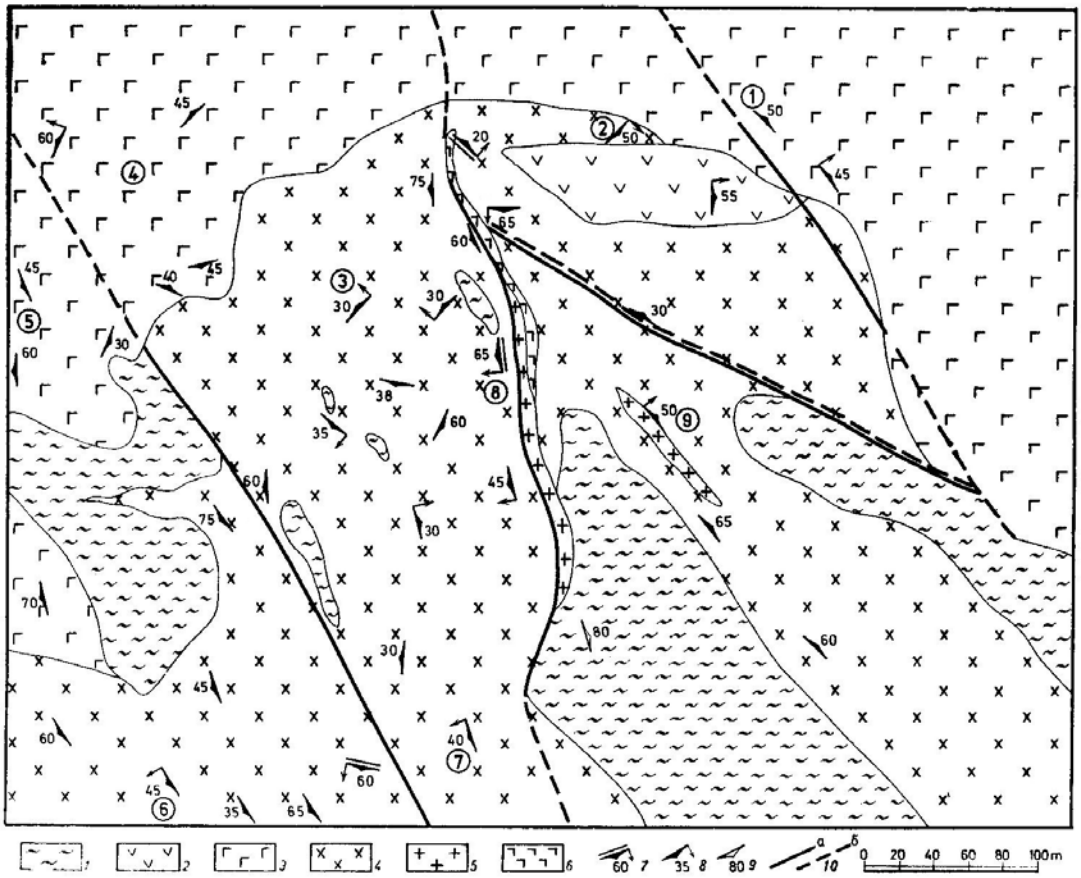

Fig. 4. Geological map of the Vlaykov Vruh porphyry copper deposit (after Bogdanov et al., 1972). 1 = gneisses; 2 = andesite; 3 = dacite; 4 = granodiorite; 5 = granodiorite porphyry dykes; 6 = dacite dykes; 7 =lineation; 8 = schistosity ; 9 = magmatic foliation; 10 = faults.

Longitudinal E-SE (100°–135°) and diagonal N-NW (330°–350°) faults (Figs. 4, 5) are developed in the area of the Vlaikov Vruh deposit as an important element of the Elshitsa volcano-intrusive complex. The Vlaikov Vruh fault and several smaller sub-parallel structures represent the E-SE trending faults (100°–135°). The longitudinal faults are characterized by steep sub-vertical to north dips. Normal and strike-slip movements and uplift of the southern blocks occurred along these faults during volcano-tectonic deformation. N-NW–trending dextral strike-slip faults (330°–350°) belonging to the Panagyurishte fault zone are characteristic of the southern margin of the Vlaikov Vruh open pit. An almost meridional fault hosts granodiorite-porphyritic and dacitic dykes (Figs. 4, 5). The porphyry Cu vein-like and disseminated ore mineralisation with minor molybdenite is hosted by the porphyry granodiorite and partly in the basement metamorphic and the dacite and andesite volcanic rocks. K-silicate, sericitic (phyllic)

and propylitic pre-ore hydrothermal alteration have been recognized in the deposit (Bogdanov, 1987; Tsonev et al., 2000). Four vertically elongated stockwork ore bodies can be distinguished in the deeper parts, coalescing into a single ore body in the upper parts of the deposit. The main ore body is oxidized to a depth of some 10–20 m, characterized by the development of malachite-azurite ores, below which is a zone of secondary enrichment, up to 40–50 m in depth, which is characterized by bornite-chalcocite-covellite ores. The tectonic jointing and faulting occurred after solidification of the intrusive controlled the development and localization of ore mineralization. Volcano-tectonic faults were reactivated along the E-SE trends as well as along

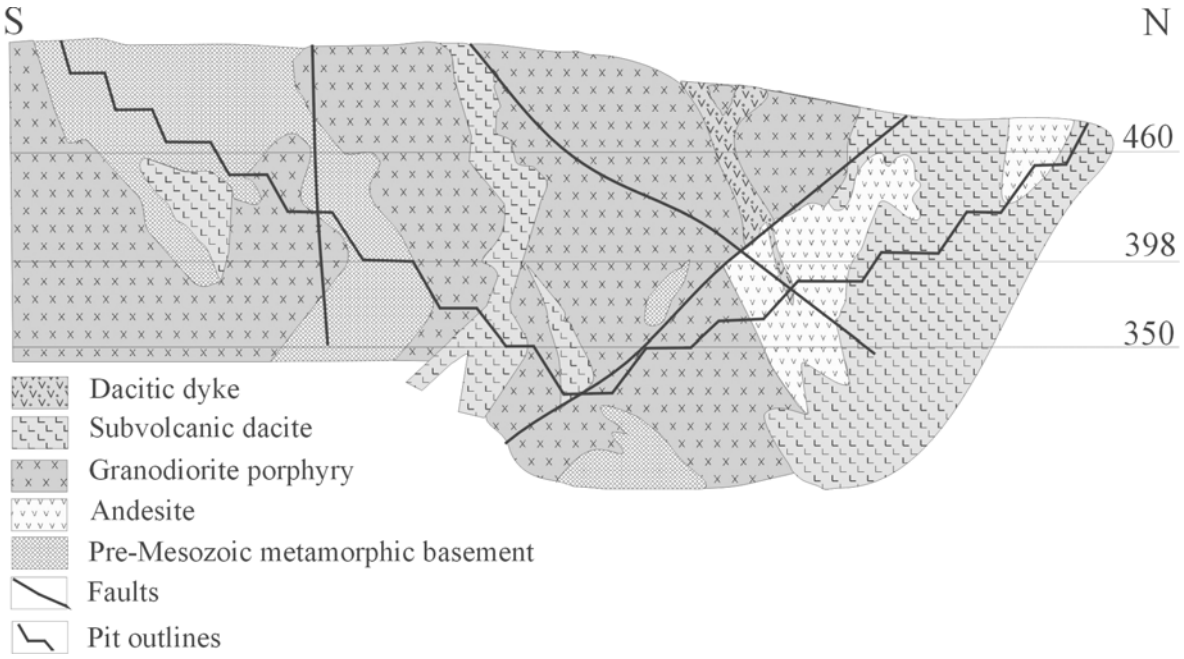

Fig. 5. Cross-section of the Vlaykov Vruh porphyry copper deposit (modified after Popov et al., 2000c). 1 = dacitic dyke; 2 =subvolcanic dacite; 3 = porphyry granodiorite; 4 = pre-Mesozoic basement; 5 = primary Cu-Mo mineralisation; 6 = zone of secondary Cu-sulphide enrichment.

the diagonal NE and N-NW trends (Figs. 4, 5). The jointing is expressed by reactivation of the primary sub-parallel and branch joints around the faults. Part of the new small faults is sub-parallel to the primary bedding joints. The jointing and faulting determines the development of economically significant mineralization mainly within the intrusive bodies, due to their greater brittleness.

Mineral Composition

The porphyry Cu vein-like and disseminated ore mineralisation with minor molybdenite was deposited at a very early stage in the evolution of the hydrothermal system. Pyrite-chalcopyrite

and molybdenite mineralization occurs in thin veinlets and in veins up to 2 cm wide, crosscutting late-magmatic aplite-pegmatite veins and the granodiorite. In addition, the veinlets contain quartz, minor amounts of titanite, rutile, and isolated inclusions of pyrrhotite.

The oxidizing zone is well expressed and is up to 10–20 m thick, and it contains Fe-hydroxides and minor amounts of cuprite, native copper, malachite, chrysocolla and azurite. The secondary enrichment zone built up an almost-horizontal zone 300 x 30 m in the central part of the deposit, which consists mainly of chalcocite with minor bornite and covellite (Bogdanov, 1987). According to Kouzmanov et al. (2001) the early hydrothermal fluids are represented by high-temperature (325°–370°C) and high-salinity (up to 48 wt % NaCl equiv) liquid-rich, and medium- to high-temperature (260°–310°C) and low-salinity (4.7–5.9 wt % NaCl equiv) fluid inclusions with variable liquid/vapour ratios. In addition the high-salinity fluid inclusions usually contain numerous solid phases, such as NaCl, anhydrite, chalcopyrite, hematite and two unidentified solids. The fluid inclusions studied are interpreted to represent an orthomagmatic fluid that boiled, causing sulphide precipitation. Preliminary results from Re-Os dating on molybdenite with relatively low Re content (0.02–0.96 wt%) (Kouzmanov, 2001) suggest that the mineralizing process took place at ca. 82 Ma.

Features of the porphyry copper deposits of the Panagyurishte ore region

Similarities and differences in mineral associations and fluid inclusions from the hydrothermal systems in porphyry copper deposits from the Panagyurishte region of the central Srednogorie zone reflect the geologic position of ore mineralisation within the framework of the Upper Cretaceous volcanic-intrusive complexes.

Although depths and fluid pressures have not been quantified at this stage, the deposits may together represent a continuum from relatively deep basement-hosted deposits centered on intrusive stocks (Elatsite, Medet) to rather shallower and lower-temperature hydrothermal systems associated with subvolcanic stocks intruding their own volcanic superstructures (Assarel). The porphyry style of wallrock alteration from these deposits contains K-silicate and propylitic alteration as an early stage of the hydrothermal-metasomatic processes (Tables 1, 2). The outer parts of the deposits are generally affected by propylitic alteration developed proximally to a K-silicate zone (Medet deposit), a sericitic zone (Elatsite deposit), or a sericite-advanced argillic alteration zone (Assarel deposit). The zone of K-silicate alteration in the Elatsite deposit is replaced at the upper levels by a zone of K-silicate-sericitic alteration, where the main sulphide mineralisation and quartz-pyrite veins are developed (Table 2). Sericitic and

advanced argillic assemblages (acid-chlorine and acid-sulphate sub-types) could be developed at the upper levels and are representatives of an epithermal style of alteration (e.g., Assarel). This type of alteration overprints the K-silicate and propylitic

Table 2. Ore Mineral Associations and Geochemical Assemblages (after Strashimirov et al., 2002)

Ore mineral association	Location and structure of ore aggregates	Specific geochemical assemblages	Characteristic minerals		
			Elatsite	Assarel	Medet
Mgt-hem ± brunt, chpy	Central parts; veinlets, aggregates, lenses	1. Fe-Ti	Mgt, hem, rut, ilm	Mgt, hem, ilm	Mgt, hem, ilm, rut
		2. Cu-PGE-Fe-Co-Ni-Te-Bi-Se-Au-Ag	Brnt, chpy, mer, ln, car, ws, mch, au	-	--
		3. Ag-Se ± Te, Bi	Hs, cls, kz, nm, euc, bcz, te, bi	-	
Qtz-py-chpy	Whole ore body; veinlets, short veins, dissem. and aggregates	1. Fe-Cu ± Mo, Au	Py, chpy, mol, gld	Py, chpy, gld	Py, chpy, mol, gld
		2. Co-Ni	Car, vaes	Brvt	Car, vaes, co-ni-pyr
		3. Ni-Pd-As	Pd-ars, pd-ramm	-	-
		4.Cu-As (Te)	-	En, gldfd, cal	-
		5.Cu-Sn-V	-	Colus, sulv, as-sulv	Colus, sulv
		6. Cu-Pb-Bi	-	Alkin, witch	-
		7.-Bi-Ag-Te	-	-	Hs, tetr
Qtz-mol	Inner parts; thin veinlets	Mo-Re	Qtz, mol	-	Qtz, mol
Qtz-py ±calc	Medium and outer parts; short veins	Fe ± Au	Qtz, pyr, calc, ± gld	Qtz, pyr, ± gld	Qtz, pyr, calc
Qtz-gal-sph	Marginal and upper levels; short veins	Pb-Zn-Ag ± Se	Qtz, gal, sph	Qtz, gal, sph	Qtz, gal, sph
Cov-chal (secondary)	Upper levels, (zone of secondary enrichment in Asarel)	Cu- Fe	Cov, chal, brnt	Cov, chal, brnt	Cov, chal, brnt

alkin = alkinite, brnt = bornite, bcz = bohdanowiczite, brvt = bravoite, cal = calaverite, calc = calcite, car = carrollite, chal = chalcocite, chpy = chalcopyrite, cls = clausthalite, colus = colusite, cov = covellite, en = enargite, euc = eucairite, gal = galena, Au = native gold, gldf = goldfieldite, hem = hematite, hs = hessite, ilm = ilmenite, kz = kawazulite, ln = linnaeite, mgt = magnetite, mch = michenerite, mer = merenskyite, mol = molybdenite, nm = naumannite, Bi = native Bi, Te = native Te, Pd-ars = Pd-arsenide, Pd-ramm = Pd-rammelsbergite, py = pyrite, pyrh = pyrrhotite, qtz = quartz, rut = rutile, sph = sphalerite, sulv = sulvanite, tetr = tetradymite, vaes = vaesite, ws = weissite, witch = witticheniite

alteration as the second stage of wallrock alteration. This stage is only weakly expressed in the Medet deposit due to the deeper erosion level of this deposit. Apart from differences of the erosion level, the differences in the types of the wallrock alteration are probably due to variable proportions of vapour and brine fluids derived from a magmatic source and low-salinity fluids of meteoric origin (Table 3). However, more data have to be collected to apply precise modeling of the development of these systems.

The characteristic features of the ore mineralisation common in all three deposits are (1) the appearance of Fe-Ti-oxide mineralisation at the beginning of the ore-forming process, (2) the wide distribution of pyrite-chalcopyrite association as the main economic stage, (3) and the presence of quartz-molybdenite, quartz-pyrite and quartz-galena-sphalerite veins at the later stages of the development of the systems (Tables 2, 3). The most significant differences among the deposits are the presence of PGE and gold mineralisation in the Elatsite deposit, as well as the occurrence of an epithermal style of mineralisation and the very rare distribution of molybdenite in the Assarel deposit. These characteristics indicate differences of the primary source of the ore elements. PGE mineralisation and Co-Ni assemblages found in the Elatsite deposit and Co-Ni assemblage in the Medet deposit suggest probable participation of fluids influenced by mafic/ultramafic materials. Enargite and numerous rare minerals including tellurides and selenides occur at Assarel, emphasizing the nature of this deposit as transitional to the high-sulphidation epithermal environment. Major pyrite-rich epithermal "massive-sulphide" Cu-Au deposits are spatially associated within a few kilometers of the large and some of the smaller porphyry-copper deposits in the Panagyurishte ore district. They are of medium- to high-sulphidation style and have a similarly complex element association with abundant arsenic, bismuth and other sulphides and tellurides (Cook et al., 2002; Kouzmanov et al., 2002, 2003; Bogdanov et al., 2004). Heinrich et al (1999) suggested that in some cases this could be an indication of a relationship-between magmatic vapour condensates from subjected porphyry-copper deposits and epithermal fluids forming high-sulphidation deposits. It is assumed that in the Medet and Elatsite deposits only limited participation of meteoric waters occurred in the initial stages. In contrast, the shallower volcanic level of the Assarel system facilitated intense re-working of the host rocks in an environment that was more open to the incursion of meteoric water. Interactions of low- and high-salinity magmatic fluids with meteoric waters within a composite cross-section, extending from basal intrusives up into to the subvolcanic domain, might explain the close spatial relationships between porphyry copper and intermediate- to high-sulphidation epithermal styles of mineralisation, which are a characteristic of the Panagyurishte district and of the Balkan-Carpathian belt in general.

Table 3:

Table 7. Temperature of Homogenization, Composition and Salinity in the Porphyry Copper Deposits Elatsite, Medet and Assarel (data from Strashimirov et al., 2002; Kehayov et al., 2003; Tarkian et al., 2003)

	Fluid inclusion data T_h (°C) / (wt % NaCl equiv)		
Mineral association	Elatsite	Medet	Assarel
Quartz-K-feldspar	>500 n.d.	>500 n.d.	n.d. n.d.
Quartz-magnetite-hematite (± born, chlpy, pyrrh)	600–450 H_2O-NaCl ± $FeCl_2$ ± $CaCl_2$ 64–42	400–380 H_2O-NaCl ± $FeCl_2$ 20–12	n.d. n.d.
Quartz-pyrite- chalcopyrite	450–330 H_2O- NaCl-KCl to H_2O- NaCl 50–44	390–320 H_2O-NaCl-KCl to H_2O-NaCl	310–290 n.d.
Quartz-molybdenite Quartz-pyrite	360–310 300–260 43–40	330–300 310–280	not found 230–215
Quartz-galena-sphalerite	240–200 25–20	280–240	195–150

* n. d. = no data

Schweizerische Mineralogische und Petrographische Mitteilungen 84, 79–99, 2004

Late Cretaceous Cu–Au epithermal deposits of the Panagyurishte district, Srednogorie zone, Bulgaria

Robert Moritz[1], *Kalin Kouzmanov*[2,1] and *Rumen Petrunov*[3]

Abstract

This review compiles geologic al, mineralogical, and isotopic data from the four largest Cu–Au epithermal deposits of the Late Cretaceous Panagyurishte mineral district, Bulgaria, including from north to south: the producing Chelopech, and the past-producing Krassen, Radka and Elshitsa deposits. Epithermal Cu–Au deposits of the northern and older part of this district are mainly hosted by andesites, whereas those from the southern and younger district are hosted by dacites. Advanced argillic alteration is described in the majority of the deposits, with the most complex alteration assemblage occurring at Chelopech. In all deposits, mineralization is the result of replacement and open-space deposition producing massive sulphide lenses surrounded by disseminated mineralization. Additionally at Chelopech, stockwork vein zones are also an important ore type. At Elshitsa, Radka and Krassen, the mineralized zones are controlled by WNW-oriented faults, and at Chelopech there is a supplementary control by NE-oriented faults. A three-stage paragenesis is recognized in all deposits, including an early disseminated to massive pyrite stage; an intermediate, Au-bearing Cu–As–S stage, which forms the economic ore; and a late Zn–Pb–Ba stage. Sulphur isotopic compositions of sulphide and gangue minerals are consistent with similar data sets from other high-sulphidation deposits. Variations in Sr and Pb isotope data among the deposits are interpreted in terms of fluid interaction with different host-rocks, additionally variability in Pb isotopic compositions can be attributed to differences in composition of the associated magmatism. Throughout the Panagyurishte district, there is a coherent and continuous sequence of events displayed by the epithermal Cu–Au deposits indicating that they result from similar ore forming processes. However, latitudinal differences in ore deposit characteristics are likely related to emplacements at different depths, differences in degrees of preservation as a function of post-ore tectonics and/or sedimentary processes, efficiency of ore formation, and/or modifications of regional controls during the 14 Ma-long geological evolution of the Panagyurishte district, such as magma petrogenesis and/or tectonic regimes.

Keywords: Cu–Au high-sulphidation epithermal deposits, Panagyurishte district, Srednogorie zone, Bulgaria.

Introduction

The Panagyurishte district is a major metallogenic region in Eastern Europe (Fig. 1a), which has supplied about 95% of the recent Bulgarian copper and gold production (Mutafchiev and Petrunov, 1996), and where Late Cretaceous porphyry-Cu and Cu–Au epithermal deposits form the most significant deposits. Within the Tethyan region, the Panagyurishte mineral district displays some of the best examples of the porphyry-Cu and high-sulphidation epithermal ore deposit association recognized in other tectonic settings such as the circum-Pacific region (Sillitoe, 1991, 1999; Hedenquist and Lowenstern, 1994; Corbett and Leach, 1998). The Panagyurishte district is located 60–90 km east of Sofia, between the towns of Etrepole and Pazardzhik (Fig. 1c), and belongs to the Late Cretaceous Banat-Timok-Srednogorie belt extending from Romania through Serbia to Bulgaria (Fig. 1a), a major ore province within the Alpine-Balkan-Carpathian-Dinaride collision belt (Berza et al., 1998; Ciobanu et al., 2002; Heinrich and Neubauer, 2002). While the genesis of porphyry-Cu deposits has been relatively undisputed in the Panagyurishte district (e.g. Strashimirov et al., 2002; von Quadt et al., 2002; Tarkian et al., 2003), the Cu–Au epithermal deposits have remained subject to debate for some time, since they were interpreted as volcanogenic massive sulphide (VMS) deposits in early studies (Bogdanov, 1984), and their high-sulphidation nature has only been recognized in recent years (Petrunov, 1994, 1995; Mutafchiev and Petrunov, 1996).

[1] Section des Sciences de la Terre, Université de Genève, rue des Maraîchers 13, CH-1205 Genève, Switzerland. <robert.moritz@terre.unige.ch>
[2] Institut für Isotopengeologie und Mineralische Rohstoffe, ETH-Zentrum, CH-8092 Zürich, Switzerland. Present address: (1). <kalin.kouzmanov@terre.unige.ch>
[3] Geological Institute, Bulgarian Academy of Sciences, Acad. G. Bonchev Street, Bl. 24, 1113 Sofia, Bulgaria. <petrunov@geology.bas.bg>

0036-7699/04/0084/79

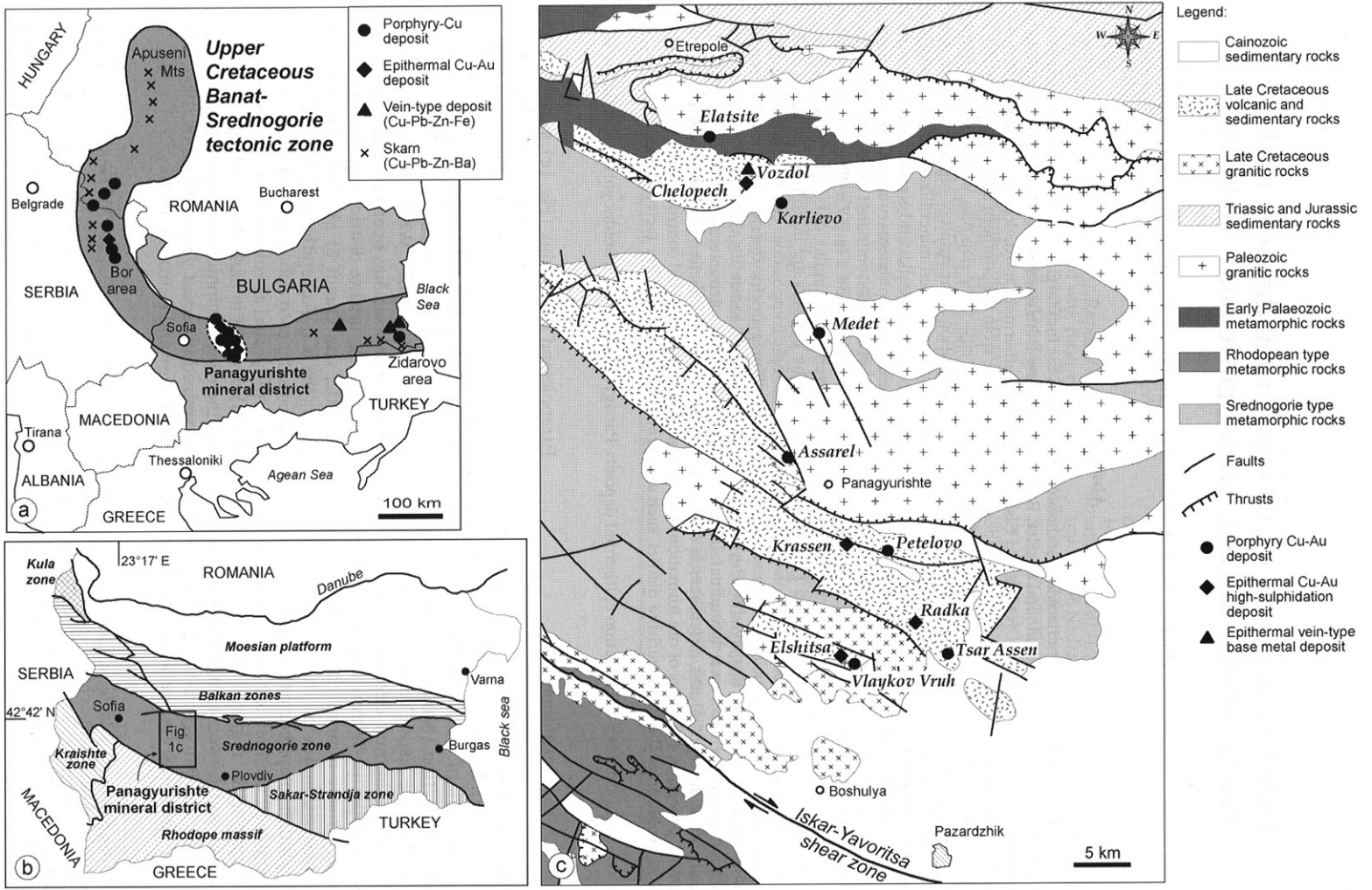

Fig. 1 (a) Location of the Late Cretaceous Banat-Srednogorie Belt in Eastern Europe (after Berza et al., 1998; Ciobanu et al., 2002; Heinrich and Neubauer, 2002). (b) Major tectonic zones of Bulgaria (after Ivanov, 1998). (c) Simplified geology of the Panagyurishte ore district (after Cheshitev et al., 1995).

This review compiles geological, mineralogical, and isotopic information from the four largest Cu–Au epithermal deposits of the Panagyurishte district (Table 1), including Chelopech, Krassen, Radka and Elshitsa (Fig. 1c). It shows that these deposits were formed by similar processes, typical for high-sulphidation epithermal deposits, during the evolution of the Srednogorie belt. However, latitudinal variations of the ore deposit characteristics are recognized, and their significance is discussed as a function of emplacements at different depths, differences in the degree of preservation, efficiency of ore formation processes at the local scale, and fundamental changes in regional geological controls in space and with time.

Regional geological setting

The Srednogorie tectonic zone is an 80 to 100 km wide and east–west oriented zone in Bulgaria, located between the Balkan Zone in the north, and the Rhodopes and the Sakar-Strandja Zone in the south (Fig. 1b; Boncev, 1988; Ivanov, 1988, 1998). The Panagyurishte ore district belongs to the Central Srednogorie zone, and is characterised by a north-northwest oriented alignment of porphyry-Cu and Cu–Au epithermal ore deposits, which is oblique with respect to the east-west trending Srednogorie tectonic zone in Bulgaria (Fig. 1b).

The geology of the Panagyurishte mineral district consists of metamorphic and igneous basement rocks, abundant Late Cretaceous magmatic rocks and subsidiary sedimentary rocks, and subordinate Tertiary sedimentary rocks (Fig. 1c; Popov et al., 2003). The oldest basement rocks are two-mica migmatites, amphibolites and gneisses of uncertain Precambrian age, known as Pirdop Group (Dabovski, 1988), Srednogorie type metamorphic rocks (Cheshitev et al., 1995) or pre-Rhodopean Supergroup (Katskov and Iliev, 1993). Younger metamorphic rocks are Late Precambrian to Cambrian phyllites, chlorite schists and diabases of the Berkovitsa Group (Haydoutov, 2001). Palaeozoic basement intrusions are gabbrodiorites, quartz-diorites, tonalites, and granodiorites-granites (Dabovski et al., 1972; Kamenov et al., 2002).

The type and composition of the Late Cretaceous magmatic rocks vary as a function of latitude in the Panagyurishte district, with sub-volcanic and effusive rocks becoming progressively more abundant from south to north with respect to intrusive rocks (Fig. 1c). Andesites predominate in the northern and central Panagyurishte district, whereas dacites are more abundant in its southern part (Boccaletti et al., 1978; Stanisheva-Vassileva, 1980). Rhyodacites and rhyolites only occur in the central and southern Panagyurishte district (Dimitrov, 1983; Nedialkov and Zartova, 2002). In the south, andesites are the earliest volcanic rocks, followed by dacites, and a final stage of dacitic-rhyodacitic subvolcanic intrusions (Bogdanov et al., 1970; Popov et al., 2000a). Small, subvolcanic dacite, quartz-monzodiorite and granodiorite intrusions (mostly <1km^2 in size), with subsidiary aplites and mafic dykes are comagmatic with the Late Cretaceous volcanic rocks. Porphyry-Cu deposits of the Panagyurishte district are typically centred on such intrusions (Strashimirov et al., 2002; von Quadt et al., 2002; Popov et al., 2003; Tarkian et al., 2003). Larger sized, northwest-elongated, syntectonic, Late Cretaceous granodioritic-granitic intrusions are restricted to the southernmost Panagyurishte district along the Iskar-Yavoritsa Shear Zone (Ivanov et al., 2001; Peytcheva et al., 2001), which corresponds to the transition between the Srednogorie zone and the Rhodope Massif (Fig. 1b,c). The Late Cretaceous magmatic rocks are calc-alkaline to high-K calc-alkaline with a local transition to subalkaline (Fig. 2), and their trace element data are coherent with destructive continental margin and/or volcanic arc related magmatism (Popov and Popov, 1997; Nedialkov and Zartova, 2002; Stoykov et al., 2002, 2003; Kamenov et al., 2003a,b).

U–Pb zircon geochronology reveals a 14 Ma-long protracted Cretaceous magmatic and ore-forming activity in the Panagyurishte district (Fig. 1c). The oldest activity is recorded in its northern part, where the age of the Elatsite porphyry-Cu deposit is bracketed by dykes dated at 92.1 ± 0.3 Ma and 91.84 ± 0.3 Ma (von Quadt et al., 2002), in line with recent Re–Os ages of 92 Ma (Zimmerman et al., 2003). At the Chelopech deposit, andesite pre-dating mineralization and latite yield an age of 91.45 ± 0.15 Ma (Chambefort et al., 2003a; Stoykov et al., 2004). Ages decrease southward with 86.62 ± 0.02 and 86.11 ± 0.23 Ma, respectively, for the Elshitsa granite and subvolcanic dacites, and 85 ± 0.15 Ma for the Vlaykov Vruh porphyry-Cu deposit (Peytcheva et al., 2003), 84.6 ± 0.3 and 82.16 ± 0.1 Ma, respectively, for granodiorite and gabbro at Boshulya (Peytcheva and von Quadt, 2003), and 78.54 ± 0.13 Ma for the Capitan-Dimitrievo pluton (Kamenov et al., 2003c).

The Late Cretaceous sedimentary rock succession in the Panagyurishte district starts with Cenomanian-Turonian conglomerate and sandstone, which transgressively overly the basement rocks, contain metamorphic rock fragments and coal-bearing interbeds, and are devoid of volcanic

rock fragments. They are postdated by Late Cretaceous intrusive and volcanic rocks, which are interbedded with early Senonian argillaceous limestone, calcarenite and sandstone with abundant volcanic rock fragments. This interbedded rock assemblage is transgressively overlain by Santonian-Campanian red marl of the Mirkovo Formation, and Campanian-Maastrichtian calcarenite and mudstone flysch of the Chugovo Formation (Aiello et al., 1977; Moev and Antonov, 1978; Popov, 2001a; Stoykov and Pavlishina, 2003).

Three predominant fault orientations are recognized in the Panagyurishte district (Fig 1c; Cheshitev et al., 1995; Popov, 2001b; Popov et al., 2003): (1) regional WNW-oriented faults, which are partly thrusts with both northward and southward vergences, and which control the geometry of the distribution of the Late Cretaceous magmatic and sedimentary rocks; (2) shorter NW to NNW-oriented faults, recognized within the entire district, including in the ore centres, and which are parallel to the characteristic ore deposits alignment of the Panagyurishte district; and (3) subordinate NE-oriented faults, also recognized in some deposits (Popov, 2001b; Jelev et al., 2003). According to Dobrev et al. (1967) and Tsvetkov (1976), gravity and magnetic data reveal a regional, deep-seated NNW-oriented fault-zone that coincides with the ore deposit alignment of the district.

Regional tectonic evolution

The Alpine evolution of the Bulgarian tectonic zones is intimately linked to the tectonic evolution and closure of the Tethys (Dabovski et al., 1991; Ricou et al., 1998). Ivanov (1988) interprets the Srednogorie tectonic zone as an island arc that was formed during northward Late Cretaceous subduction of the African Plate beneath the Eurasian Plate. Boccaletti et al. (1974), Berza et al. (1998) and Neubauer (2002) suggest post-collisional detachment of the subducted slab as the trigger for the Late Cretaceous calc-alkaline magmatism and associated ore deposit formation in the Srednogorie zone. In contrast, based on the observation that subduction ceased in the early Cretaceous (Barremian), Popov (1987, 2002) has interpreted the Banat-Timok-Srednogorie zone as a rift. This appears to be in apparent conflict with the subduction-related scenario, but the arguments raised by Popov (1987) could be reconciled with the scenario of Boccaletti et al. (1974), Berza et al. (1998) and Neubauer (2002), if one considers the time lag between cessation of subduction and post-collisional slab break-off. More recently, based on regional lithogeochemical and radiometric age data from magmatic rocks, Kamenov et al. (2003a,b) and von Quadt et al. (2003 a,b) propose a roll-back scenario to explain the geodynamic setting of the Panagyurishte district. However, both slab detachment and roll-back scenarios are disputed by Lips (2002), who argues that conditions for such geodynamic settings were unfavourable in the Late Cretaceous due to the relatively low density and limited length of the young subducted slab, and he favours typical subduction-related calc-alkaline magmatism and associated ore formation processes. A consensus might be difficult to reach, because, as admitted by Neubauer (2002), distinction between subduction-related and slab break-off magmatism remains ambiguous. During the Early to Middle Eocene, continuous tectonic plate convergence resulted in the collision of the Rhodopes with the Srednogorie zone, whereby allochthonous units of the former were thrusted northward on the southern Srednogorie zone (Ivanov, 1988; Ricou et al., 1998).

Evolution of genetic concepts for the Panagyurishte Cu–Au epithermal ore deposits

Early contributions (see Dimitrov, 1960, and references therein) have interpreted the Cu–Au hydrothermal deposits as epithermal to mesothermal deposits genetically linked to porphyry-Cu deposits in the Panagyurishte district. Dimitrov (1960) describes the ore deposits as epigenetic, formed by replacement and open space deposition processes, with a preferential development of alteration zones and ore bodies in volcanic tuffs and sedimentary rocks.

Later, based on the observation that massive pyrite fragments from the early ore paragenesis were set in a matrix of dacitic tuffs in some deposits of the Panagyurishte district, Bogdanov (1984) interpreted the early massive pyrite stage of the Cu–Au hydrothermal deposits as synchronous with volcanic activity and sedimentation in water basins, followed by epigenetic polymetallic ore. Bogdanov (1984) concluded that porphyry-Cu deposits post-dated Cu–Au hydrothermal ores based on K–Ar ages of 90–94 Ma for the volcanic rocks and 75–87 Ma for the intrusions hosting the porphyry-Cu deposits (Chipchakova and Lilov, 1976).

More recently, Petrunov (1995), and Mutafchiev and Petrunov (1996) recognized that the Cu–Au Chelopech deposit of the northern Panagyurishte district (Fig. 1c) shares alteration and opaque mineral associations with typical high-sulphidation epithermal deposits (Hedenquist et al., 2000), also known as acid sulphate or alunite-kao-

linite deposits (Heald et al., 1987; Berger and Henley, 1989). Petrunov (1995), and Mutafchiev and Petrunov (1996) proposed a succession of events with submarine formation of early massive sulphide ore, followed by uplift of the volcanic edifice and formation of the high-sulphidation ore in an aerial setting, overprinting the volcanogenic massive sulphide ore. Therefore, they classified the Chelopech deposit as a volcanic-hosted epithermal deposit of high-sulphidation type.

Recent contributions (Popov and Kovachev, 1996; Popov and Popov, 1997; Strashimirov et al., 2002), based on modern genetic concepts (e.g. Hedenquist and Lowenstern, 1994; Hedenquist et al., 2000), interpret the Cu–Au hydrothermal deposits as epithermal high-sulphidation systems genetically linked to porphyry-Cu deposits of the Panagyurishte district, therefore in agreement with the early interpretation by Dimitrov (1960).

Spatial association of the Cu–Au epithermal deposits with porphyry-Cu deposits

The Cu–Au hydrothermal deposit at Elshitsa is located about 1 km to the NW to the past-producing Vlaykov Vruh porphyry-Cu deposit (Fig. 1c). These two neighbouring deposits constitute the best example for the tight spatial association of high-sulphidation epithermal and porphyry-Cu deposits within the Panagyurishte ore district (Kouzmanov, 2001). Such a relationship is not as obvious at the Radka deposit, although granodioritic and quartz-diorite porphyries have been described in its vicinity. Cu–Au epithermal occurrences have also been described in the immediate proximity of the Assarel and Petelovo porphyry-Cu deposits (Petrunov et al., 1991; Sillitoe, 1999; Tsonev et al., 2000a; Fig. 1c). The Chelopech deposit belongs to an ore deposit cluster in the northern Panagyurishte district, which also includes the vein-type Vozdol base metal occurrence, the Karlievo porphyry-Cu occurrence, and the major producing porphyry-Cu Elatsite deposit (Popov et al., 2000b; Fig. 1c). This ore deposit cluster is centred on a major, regional geomagnetic anomaly of the northern Panagyurishte district, interpreted by Popov et al. (2002) as a shallow, large magmatic chamber.

Economic significance and metal ratios of the Cu–Au epithermal deposits

Chelopech is the largest and, at present, the only producing high-sulphidation deposit in the Panagyurishte mineral district (Table 1). It ranks among the major high-sulphidation deposits of

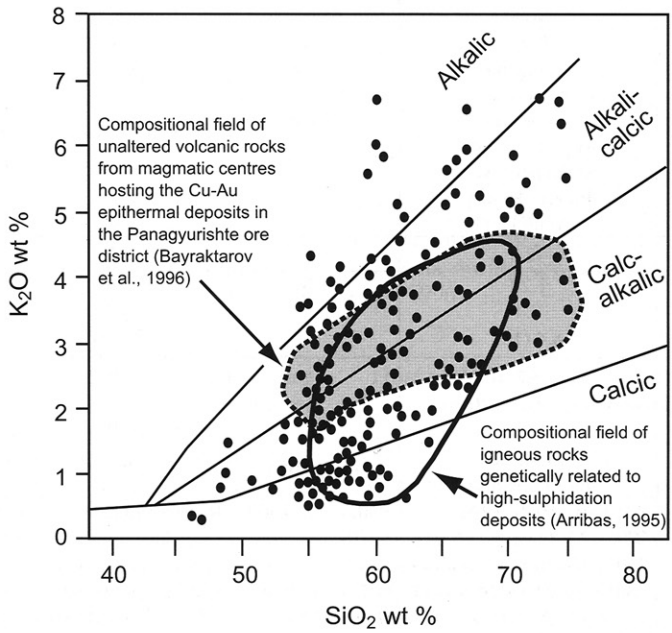

Fig. 2 K_2O vs. SiO_2 diagram for Late Cretaceous igneous rocks from the Panagyurishte ore district (black dots). Data for the Panagyurishte ore district from Bayraktarov et al. (1996), and data compilation of igneous rocks genetically related to high-sulphidation deposits from Arribas (1995).

Table 1 Major characteristics of high-sulphidation deposits from the Panagyurishte ore district.

Ore deposit	Chelopech	Krassen	Radka	Elshitsa
Immediate host rocks	Massive andesites; phreatomagmatic diatreme breccia; sedimentary rocks (oolithic, biodetrital and sandstone layers); volcanic tephra and tuff.	Andesitic breccia tuff, and lava.	Preferentially dacitic breccia (abundant) and dacitic tuff (rare). Subordinate lava flows.	Dacite subvolcanic body, dacitic tuff, volcanic breccia.
Alteration	Proximal to ore bodies: advanced argillic with vuggy silica (innermost part of silicic zone with pyrite and APS minerals*, followed laterally by quartz-kaolinite-dickite-pyrite-APS minerals*). Intermediate: phyllic. Distal: propylitic. At depth: diaspore, pyrophyllite, alunite and zunyite.	Proximal: advanced argillic (quartz-kaolinite/dickite). Intermediate: phyllic. Distal: propylitic (including adularia).	Proximal: phyllic (innermost part with quartz-sericite followed laterally by quartz-sericite-albite). Distal: propylitic.	Proximal to ore bodies: advanced argillic (quartz-sericite +/- diaspore). Intermediate: phyllic. Distal: propylitic
Orebody geometry & texture	Veins, dissemination, massive sulphide lenses with replacement textures, breccia.	Moderately dipping massive sulphide lenses, disseminations.	Mainly steeply dipping massive sulphide lenses surrounded by disseminations, breccia pipes, rare quartz-sulphide veins.	Mainly steeply dipping massive sulphide lenses, surrounded by disseminations, breccia and rare veins.
Ore & alteration control	Fault and lithological control.	Fault control (& lithological?)	Fault and lithological control.	Fault and lithological control.
Mineralogical differences				
Enargite	Abundant	Present	Rare, upper levels	Rare, upper levels
Luzonite	Abundant	Minor	None	None
Native Ag	None	Minor	Minor	Minor
Tetrahedrite	Rare	Present	Present	Present
APS minerals*	Abundant	None	None	None
Kaolinite/Dickite	Abundant	Present	None	None
Alunite	At deeper levels	None	None	Rare, upper levels
Diaspore	At deeper levels		None	Rare
Pyrophyllite	At deeper levels		None	Rare
Vuggy silica	Present locally		None	None
Chalcedony	Abundant		None	None
Tonnage* (Mt)	42.5	0.3	8.9	4.5
Ore grades				
Cu (%)	1.28	0.76	1.06	1.13
Au (g/t)	3.4		1.5-2.0	1.5
Ag (g/t)	8.4 (18)		25-30	15
Metal ratios				
Ag/Au	2.5		16	10
Au/Cu	2.7		1.7	1.3
Ag/Cu	7.8		26	13.3
Production period	1954- ... (still in operation)	1962-1973	1942-1995	1922-1999
Source of information (except tonnage and production mainly from Strashimirov et al., 2002)	Petrunov (1989, 1994, 1995); Moritz et al. (2001, 2003); Chambefort et al. (2002, 2003); Georgieva et al. (2002); Arisanov (pers. comm., 2002).	Radonova (1969, 1970); Radonova and Velinov (1974); Tsonev et al. (2000a).	Radonova (1962); Chipchakova et al. (1981); Tsonev et al. (2000b); Kouzmanov (2001); Kouzmanov et al. (2004).	Radanova (1967, 1970); Chipchakova and Stefanov (1974); Dimitrov (1985); Kouzmanov (2001).

APS minerals*: Aluminium-phosphate-sulphate minerals; Tonnage*: total of past production and remaining resources.

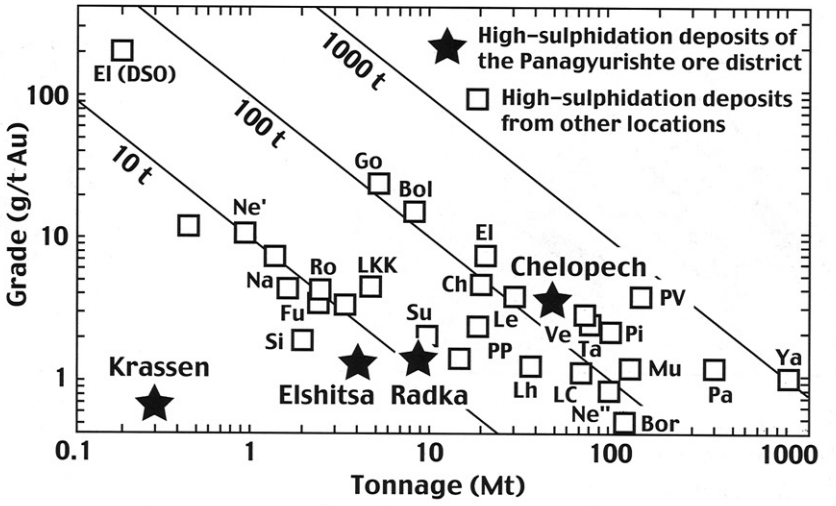

Fig. 3 Grade–tonnage diagram of high-sulphidation deposits from the Panagyurishte ore district in comparison to similar deposits from other localities. Grades and tonnages of the Bulgarian deposits are from Strashimirov et al. (2002). The diagram is modified from Hedenquist et al. (2000) with additional data from Sillitoe (1999) marked with an asterisk (*) in the following list. Bol — Boliden, Sweden; Bor — Bor*, Serbia; Chinkuashih, Taiwan; El — El Indio, Chile; El (DSO) — El Indio direct shipping ore; Fu — Furtei*, Italy; Go — Goldfield: U.S.A.; LC — La Coipa*, Chile; Le — Lepanto, Philippines; Lh — Lahoca, Hungary; LKK — Lerokis and Kali Kuning*, Indonesia; Mu — Mulatos, Mexico; Na — Nansatsu district (including Kasuga), Japan; Ne' and Ne" — Nevados de Famatina*, Argentina (high and low grade ore, respectively); Pa — Pascua, Chile; Pi — Pierina, Peru; PP — Paradise Peak, U.S.A.; PV — Pueblo Viejo, Dominican Republic; Ro — Rodalquilar, Spain; Si — Sipan*, Peru; Su — Summitville, U.S.A.; Ta — Tambo, Chile; Ve — Veladero, Argentina; Ya — Yanacocha, Peru.

the world, with a tonnage and a gold grade comparable to important deposits of the circum-Pacific region such as El Indio in Chile, Lepanto in the Philippines and Pierina in Peru (Fig. 3). By contrast, the past-producing Elshitsa and Radka deposits are on the borderline of economic deposits, and Krassen remains an uneconomic occurrence (Fig. 3).

The northern zone stands out as the more fertile part of the Panagyurishte ore district. Indeed, the location of the major high-sulphidation Chelopech deposit coincides with the geographic position of the economically significant porphyry-Cu deposits of the area (Fig. 1c), including Elatsite (354 Mt at 0.44% Cu and 0.2 g/t Au), Medet (163 Mt at 0.32% Cu and 80 g/t Mo), and Assarel (319 Mt at 0.36% Cu), whereas the southern porphyry-Cu deposits at Tsar Assen (6.6 Mt at 0.47% Cu) and Vlaykov Vruh (9.8 Mt at 0.46% Cu) are much smaller (Porphyry-Cu data from Strashimirov et al., 2002, total of past production and remaining resources), and correlate spatially with the lesser economic Elshitsa, Radka and Krassen epithermal deposits.

Chelopech is characterised by higher Cu and Au grades (1.28% and 3.4 g/t) relative to Krassen (0.76% and 0.69 g/t), Radka (1.06% and 1.5–2.0 g/t) and Elshitsa (1.13% and 1.5 g/t). Silver grades are on average lower at Chelopech (8.4 g/t) than at Radka (25–30 g/t) and Elshitsa (15 g/t), which is reflected by a low Ag/Au ratio of 2.5 at Chelopech in contrast to 16 and 10, respectively, at Radka and Elshitsa. The Chelopech deposit has a higher Au/Cu ratio of 2.7 than the Radka and Elshitsa deposits, respectively, with 1.7 and 1.3 (Table 1). Additionally, Chelopech is characterised by elevated contents of S, Ga and Ge that have been by-products during ore dressing (Popov and Kovachev, 1996).

Host rocks of the Cu–Au epithermal deposits in the Panagyurishte ore district

At Elshitsa, the ore bodies are hosted by an about 100 m wide breccia zone within a WNW-elongated and steeply dipping Late Cretaceous subvolcanic dacite body (Fig. 4c). This subvolcanic rhyodacite body crosscuts a belt of andesitic-dacitic volcanic rocks located between Palaeozoic granitoids to the south and the Late Cretaceous Elshitsa intrusion to the north (Fig. 1c). Dacitic volcanic rocks and breccia form the preferential rock environment for metasomatic replacement and hy-

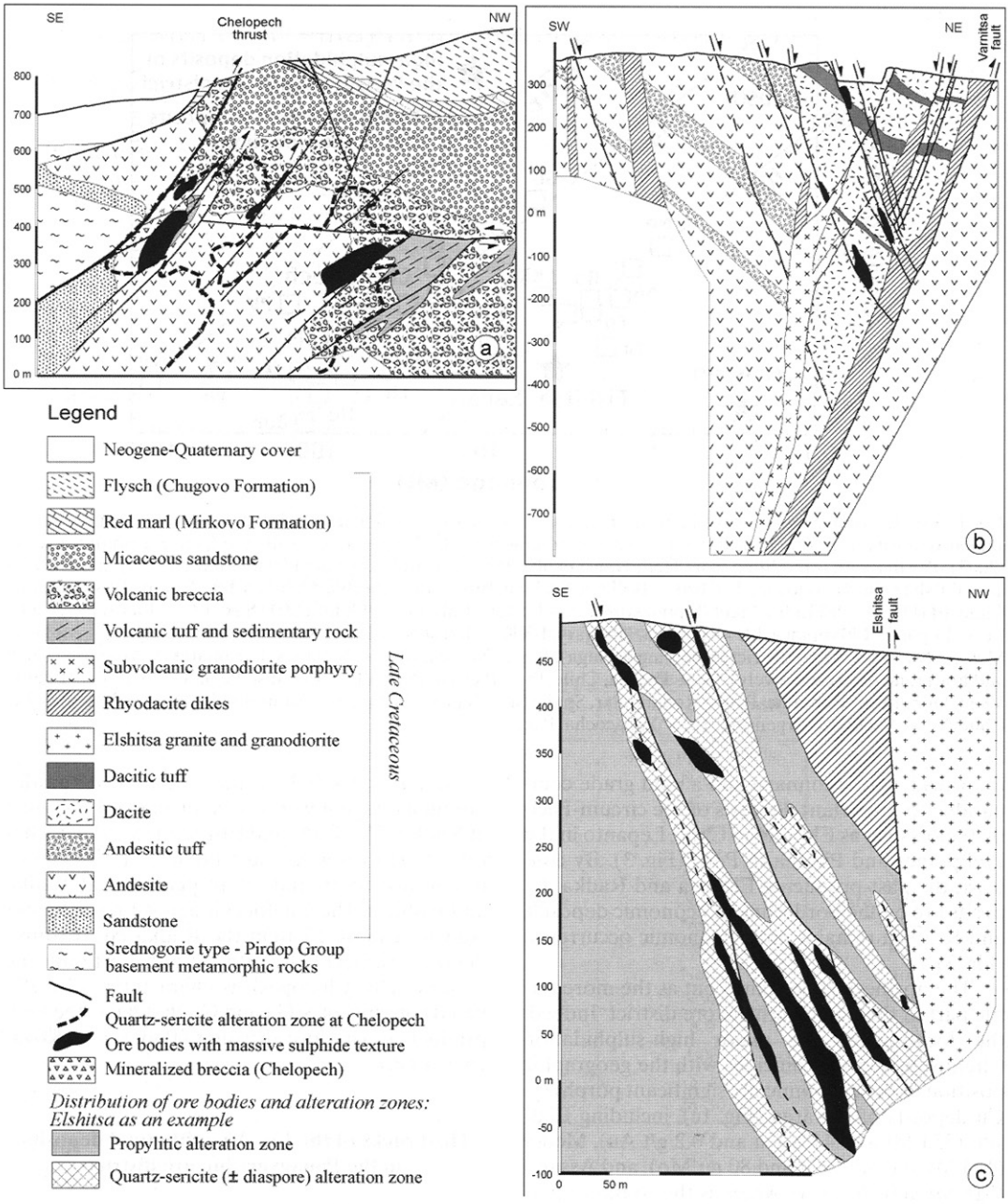

Fig. 4 (a) Cross sections of the Chelopech (after Chambefort, 2005), (b) Radka (after Popov and Popov, 1997; Tsonev et al., 2000b; Kouzmanov et al., 2002) and (c) Elshitsa deposits (after Chipchakova and Stefanov, 1974).

drothermal precipitation (Fig. 4c; Kouzmanov, 2001).

The Radka deposit occurs in an andesitic-dacitic volcanic belt, with subordinate rhyodacitic dykes and granodioritic and quartz dioritic porphyries (Fig. 4b), immediately to the northeast of the Late Cretaceous Elshitsa intrusion (Fig. 1c). The immediate host rocks of the mineralized zones are exclusively Late Cretaceous dacitic lava flows, volcanic breccia and tuffs (Fig. 4b). The lat-

ter two are preferential hosts to the mineralization (Bogdanov and Bogdanova, 1974; Kouzmanov, 2001; Kouzmanov et al., 2004).

In the Krassen deposit (Fig. 1c), the host rocks of the mineralized zones are andesitic breccia, tuffs and lava flows that have been overthrusted along the Krassen fault on the sedimentary rocks of the Chugovo Formation (Tsonev et al., 2000a).

The Chelopech deposit is hosted by a Late Cretaceous volcanic and volcano-sedimentary complex, transgressively overlaying Precambrian and Palaeozoic metamorphic rocks (Fig. 1c, Table 1; Popov et al., 2000b). The Late Cretaceous rock sequence consists of detrital sedimentary rocks derived from the basement, and andesitic, dacitic to trachyandesitic subvolcanic bodies, lava flows, agglomerate flows, tuffs and epiclastic rocks. They are transgressively covered by sandstone, argillaceous limestone, and the terrigenous flysch sequence of the Chugovo Formation (Fig. 4). The ore bodies are hosted by (1) an andesitic subvolcanic body, associated with phreatomagmatic, diatreme breccias, and (2) sedimentary rocks with oolithic, biodetrital and sandstone layers interbedded with (3) volcanic tephra-tuff containing accretionary lapilli and pumices (Chambefort et al., 2003b; Jacquat, 2003).

Unaltered volcanic rocks from the magmatic centres hosting the Cu–Au epithermal and porphyry-Cu deposits are enriched in K with respect to equivalent rock types in barren areas (Bayraktarov et al., 1996). Figure 2 shows that the K_2O vs. SiO_2 field of the volcanic host rocks of the ore deposits in the Panagyurishte district overlaps with the upper part of the field typical for volcanic rocks genetically related to high-sulphidation deposits (Arribas, 1995).

Wall rock alteration of the Cu–Au epithermal deposits in the Panagyurishte district

Alteration assemblages are variable among the different Cu–Au epithermal deposits of the Panagyurishte ore district (Fig. 5). Chelopech displays laterally and vertically the most complex alteration assemblages among these deposits (Fig. 5a). Laterally outward from the ore bodies, there are four alteration assemblages: (1) a silicic zone with massive silica, sparsely developed vuggy silica, disseminated pyrite and aluminium–phosphate–sulphate (APS) minerals; (2) a quartz–kaolinite–dickite zone with pyrite, APS minerals, and anatase; (3) a widespread quartz–sericite alteration zone; and (4) a propylitic zone. Below the present mining level (405 level, about 400 m below surface), samples from 2 km deep drill cores (from the surface) reveal that the alteration evolves into a diaspore, pyrophyllite, alunite, zunyite, rutile, and APS mineral assemblage (Petrunov, 1989, 1995; Georgieva et al., 2002).

Radonova (1970), Radonova and Velinov (1974), and Tsonev et al. (2000a) report an advanced argillic assemblage (quartz–kaolinite/dickite) in the immediate wall rocks of the mineralized zones at Krassen, followed laterally by a phyllic and propylitic alteration (Fig. 5b). At Elshitsa and Radka, the wall rock alteration of the mineralization consists predominantly of a phyllic assemblage (quartz–sericite in the immediate host rock of the sulphide bodies followed laterally by quartz–sericite–albite) and grades outwards into a propylitic alteration assemblage (Fig. 5). In addition at Elshitsa, subordinate diaspore and dumortierite have been recognized in the quartz–sericite alteration immediately next to the mineralized zones (Radonova, 1967, 1970), and alunite has been documented at shallow mining levels by Dimitrov (1985), thus revealing the occurrence of advanced argillic alteration in this deposit (Figs. 4 and 5). In contrast to the Chelopech deposit, neither vuggy silica, nor any hypogene kaolinite/dickite and APS minerals have been recorded at Elshitsa and Radka (Table 1, Figs. 5 and 6). Illite is the predominant clay mineral in the two later deposits.

Ore body geometry of the Cu–Au epithermal deposits in the Panagyurishte ore district

In all three deposits of the southern Panagyurishte ore district, i.e. Elshitsa, Radka and Krassen, the mineralized zones consist predominantly of massive sulphide lenses surrounded by a halo of disseminated mineralization (Tsonev et al., 2000a,b; Kouzmanov, 2001). In addition, at the Elshitsa and Radka deposits there is also subordinate veinlet-type ore (Kouzmanov, 2001). At the Chelopech deposit stockwork ore is also abundant, and in contrast to the high-sulphidation deposits of the southern Panagyurishte district, vein-type ore is volumetrically and economically as important as massive sulphide ore surrounded by disseminated ore (Petrunov, 1994; Jacquat, 2003).

Structural control of the ore bodies and the alteration zones

The Elshitsa and Radka deposits share similar structural controls on each side of the Elshitsa intrusion (Fig. 1). In both deposits, the ore bodies are steeply dipping and, together with the wall rock alteration, they are controlled by WNW-ori-

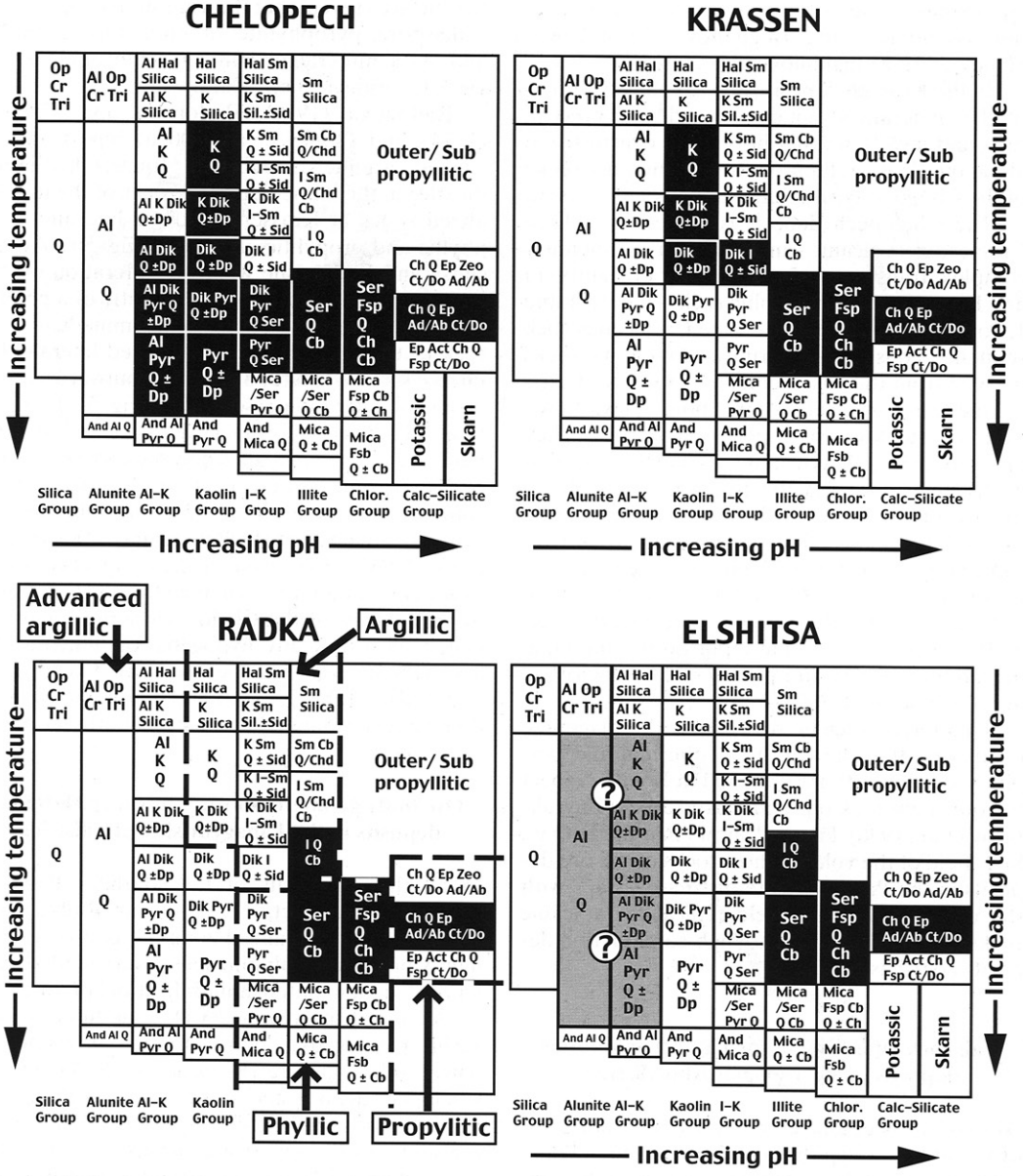

Fig. 5 Hydrothermal alteration assemblages described in the Chelopech (Petrunov, 1989, 1995; Georgieva et al., 2002), Krassen (Tsonev et al., 2000a), Radka (Tsonev et al., 2000b; Kouzmanov, 2001) and Elshitsa deposits (Radonova, 1967, 1970; Chipchakova and Stefanov, 1974; Dimitrov, 1985; Popov et al., 2000a; Kouzmanov, 2001) represented on diagrams after Corbett and Leach (Fig. 4.1, p. 71, 1998) showing the relative stability ranges of alteration mineral assemblages as a function of temperature and pH. The alteration zones (advanced argillic, argillic, phyllic, propylitic) defined in hydrothermal systems (Corbett and Leach, p. 73, 1998) are only represented for the Radka deposit, for the sake of clarity. The characteristic alteration assemblages of each deposit are highlighted with white letters on a black background. For Elshitsa, there is an additional grey background with questions marks, because Dimitrov (1985) reports an alunite facies without mentioning the other alteration minerals present in the same facies, therefore the alteration assemblage remains uncertain. Ab— albite; Act—actinolite; Ad—adularia; Al—alunite; And—andalusite; Bio—biotite; Cb—carbonate; Ch—chlorite; Chab—chabazite; Chd—chalcedony; Ch—chlorite; Cr—cristobalite; Ct—calcite; Do—dolomite; Dik—dickite; Dp—diaspore; Ep—epidote; Fsp—feldspar; Hal—halloysite; I—illite; K—kaolinite; Op—opaline silica; Pyr—pyrophyllite; Q—quartz; Ser—sericite; Sid—siderite; Sm—smectite; Tri—tridymite.

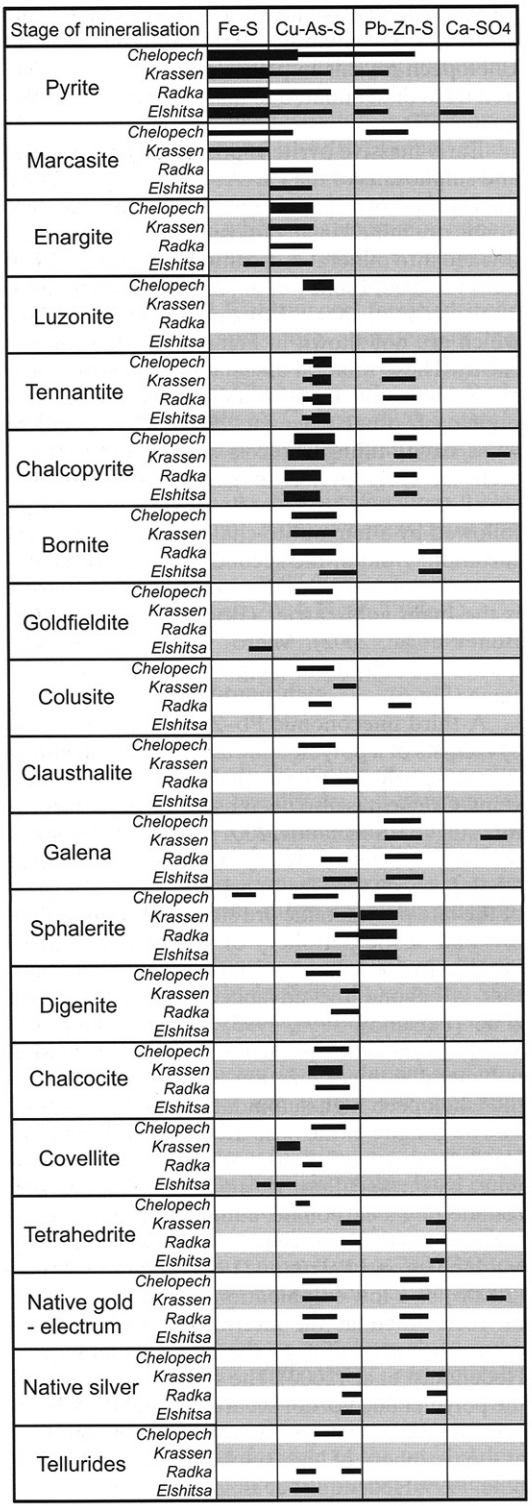

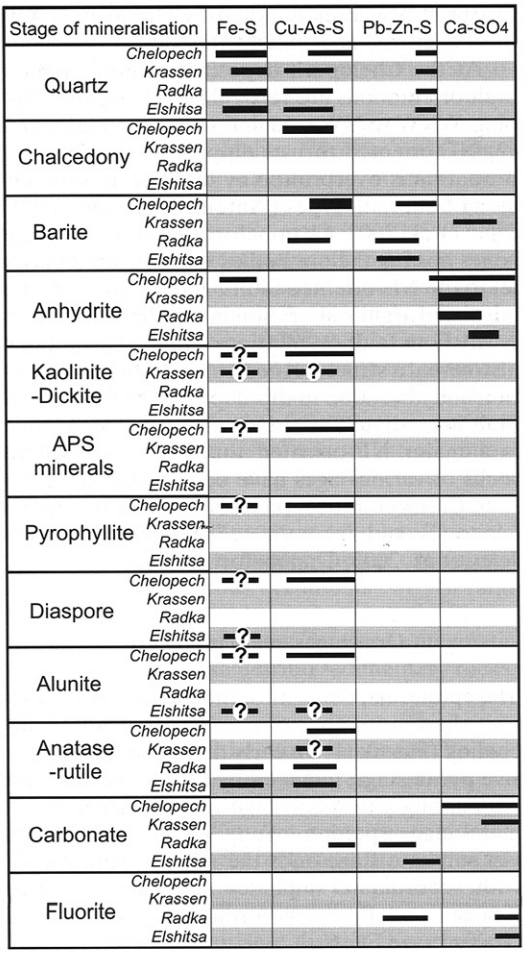

Fig. 6 Principal opaque and gangue mineral paragenesis of the Chelopech (Petrunov, 1989, 1994, 1995; Simova, 2000; Jacquat, 2003), Krassen (Tsonev et al., 2000a), Radka (Tsonev et al., 2000b; Kouzmanov, 2001) and Elshitsa deposits (Popov et al., 2000; Kouzmanov, 2001).

ented, sub-parallel normal faults dipping 65°–70° to the north (Fig. 4, Table 1). The mineralized faults merge with major, regional faults at depth, i.e. the Elshitsa fault in the homonymous deposit, and the Varnitsa fault at Radka (Fig. 4). At Elshitsa, there is a subsidiary set of NW-oriented strike-slip faults. The Krassen deposit shows a similar setting to these two deposits, where the mineralization is hosted by about an 80 to 100 m wide, and WNW-oriented breccia zone with a moderate dip of about 50° to the NE, and which is sub-parallel to the Krassen fault. Part of the massive sulphide bodies has been brecciated and overprinted by later tectonic movements along the latter (Tsonev et al., 2000a). This late tectonic

overprint was already noted by Dimitrov (1960) for the entire Panagyurishte district.

At the Chelopech deposit, two predominant fault orientations are recognized: (1) steeply dipping, WNW to NW-oriented strike-slip faults, and (2) NE-oriented thrusts dipping to the SE. Ore formation is overprinted by tectonic movements along both fault types (Antonov and Jelev, 2001; Jelev et al., 2003; Chambefort, 2005). The breccia zones hosting the ore bodies are elongated parallel to the NE-oriented faults, and the trend of the advanced argillic alteration in this deposit follows partly both fault orientations. These observations also reveal a structural control on both ore formation and alteration in this deposit. The Chelopech fault immediately to the southeast of the deposit is a major NE-oriented thrust (Fig. 4), where rocks of various ages have been thrusted on the Late Cretaceous host rocks of the Cu–Au deposit (Antonov and Jelev, 2001; Stoykov et al., 2002; Jelev et al., 2003; Chambefort, 2005).

Ore stages and paragenesis

The epithermal deposits of the Panagyurishte district share a number of paragenetic features including (Fig. 6): (1) an early disseminated to massive pyrite stage, followed by (2) an intermediate Au-bearing Cu–As–S stage and (3) a late base-metal stage (predominantly Zn, Pb and Ba). A last sulphate stage ends the mineral paragenesis with subordinate sulphides and native gold at Krassen and Radka according to Tsonev et al. (2000a,b; see Fig. 6).

In all four deposits, the first ore stage consists of pyrite with subordinate fine-grained quartz and marcasite, referred to as Fe–S ore stage and as massive sulphide ore (Fig. 6). Pyrite of this stage has a colloform, globular, fine-grained and fine-layered texture. On a macroscopic scale, the massive ore can be locally banded with centimetric alternations of massive pyrite layers and altered rock (Petrunov, 1994, 1995; Bogdanov et al., 1997; Simova, 2000; Tsonev et al., 2000a; Kouzmanov, 2001; Jacquat, 2003). The massive sulphide ore bodies are discordant with respect to the host rocks (Kouzmanov, 2001; Popov et al., 2003). At Elshitsa, the massive ore bodies and the alteration zones are controlled by faults (Fig. 4), and veins with colloform pyrite crosscut the host dacites (Kouzmanov, 2001). At Chelopech, sedimentary rocks and volcanic tuffs are the preferential host rocks of massive pyrite ore. Accretionary lapilli, oolithes, and microfossils are replaced by pyrite in these rocks (Chambefort et al., 2003b; Jacquat, 2003). Massive sulphide ore is typically surrounded by a halo of disseminated pyrite (Tsonev et al., 2000 a,b; Kouzmanov, 2001), and mapping at Chelopech reveals in places a progressive transition from disseminated to massive pyrite ore (Jacquat, 2003).

Early massive pyrite is postdated by sulphides and sulphosalts of the Cu–As–S ore stage (Fig. 6). This second ore stage is the Au-bearing and economic ore mined in all deposits. It is typically subdivided into mineral associations (Petrunov, 1994; Simova, 2000; Tsonev et al., 2000a,b; Kouzmanov, 2001; Jacquat, 2003; Kouzmanov et al., 2004), which are not shown in Figure 6 for the sake of clarity. These mineral associations constitute discrete, recurrent depositional events, which overprint each other (Jacquat, 2003). They occur as veins, cavity fillings, breccia matrix, and replacement of early pyrite. In general, enargite and covellite belong to an early depositional event, followed by a tennantite-chalcopyrite-bornite association. Gold of the second ore stage occurs as native metal and tellurides, but the native mineral is the main gold carrier (Bogdanov et al., 1997; Bonev et al., 2002). Micro- to cryptocrystalline quartz is a ubiquitous gangue mineral of this ore stage (Fig. 6).

A third uneconomic Pb–Zn–S ore stage (Fig. 6) consists of a polymetallic assemblage, including galena, sphalerite, pyrite, chalcopyrite, and barite veins. Calcite has also been reported at Elshitsa at this stage (Kouzmanov, 2001). Gold of this stage occurs as the native metal, and also as electrum at Chelopech. At the Chelopech deposit, a large part of the late polymetallic ore stage is developed below and at the periphery of the economic gold-bearing pyrite–enargite–chalcopyrite ore bodies, that is beyond the advanced argillic alteration zone (Petrunov, 1994, 1995; Jacquat, 2003). The Vozdol occurrence is such a physically separate, polymetallic mineralization about 1 km NNE to the Chelopech high-sulphidation ore bodies (Fig. 1). The gangue of the base metal sulphide veins at Vozdol consists of quartz, ankerite, calcite, dolomite, barite and fluorite, and the veins are surrounded by a carbonate, adularia and sericite alteration zone. This occurrence is considered by Mutafchiev and Petrunov (1995) and Popov et al. (2000b) as a low-sulphidation system, and would be reclassified as an intermediate-sulphidation occurrence according to the new terminology of Hedenquist et al. (2000). The spatial association of the polymetallic Vozdol occurrence and the Chelopech deposit is analogous to other base-metal veins at the periphery of high-sulphidation systems (Sillitoe, 1999; Hedenquist et al., 2000, 2001).

There are a number of major mineralogical differences among the Cu–Au epithermal depos-

its of the Panagyurishte district (Fig. 6; Table 1). Enargite is abundant at Chelopech (Petrunov, 1994; Simova, 2000; Jacquat, 2003) and predominant at Krassen (Tsonev et al., 2000a), but it is only a minor phase and restricted to the upper mine levels at Radka and Elshitsa (Tsonev et al., 2000b; Kouzmanov, 2001). Luzonite, the low-temperature dimorph of enargite, has only been reported at Chelopech, where it is a common mineral, and as a minor phase at Krassen. By contrast, native silver is absent at Chelopech, but present at Krassen, Radka and Elshitsa, and tetrahedrite is rare at Chelopech and more abundant in the three other deposits. This explains the distinctly lower Ag/Au ratios at Chelopech relative to Radka and Elshitsa (Table 1). Chelopech also stands out with its predominant gangue mineralogy, with chalcedony and barite being major to abundant phases during the Cu–As–S stage (Petrunov, 1994; Simova, 2000; Jacquat, 2003), whereas barite is only reported as a minor phase at Radka during this ore stage (Tsonev et al., 2000b; Kouzmanov, 2001; Kouzmanov et al., 2004; Fig. 6, Table 1).

Isotopic data

The sulphur isotopic compositions of sulphides and enargite from the high-sulphidation deposits of the Panagyurishte ore district fall between –9 and +1 ‰ (CDT), and sulphates yield higher $\delta^{34}S$ values between +15 and +28 ‰ (CDT) (Fig. 7a). Such isotopic compositions are consistent with similar data sets from other high-sulphidation epithermal deposits (see Arribas, 1995), and are typically interpreted in terms of sulphur isotope fractionation during hydrolysis of magmatic SO_2 and fluid oxidation with decreasing temperature (Rye, 1993). Temperatures obtained by sulphur isotope geothermometry in the deposits of the Panagyurishte district are typical for high-sulphidation epithermal systems (Arribas, 1995). At Chelopech, two pyrite-anhydrite pairs from deep drilling samples below the main mining level yield temperatures of 302° and 314°C (Jacquat, 2003), and one enargite–barite pair from the main Cu–As–S ore stage gives a temperature of 240°C (Moritz et al., unpublished data). One galena–barite pair at Chelopech and one chalcopyrite–barite at Elshitsa from the third base metal ore stage yield temperatures of 226° and 250°C, respectively (Jacquat, 2003; Kouzmanov et al., 2003).

Radiogenic isotopes show marked differences among the epithermal deposits of the ore district. The Sr and Pb isotopic compositions of gangue and ore minerals are more radiogenic in Chelopech than at Elshitsa and Radka (Figs. 7b and c). In the case of Sr, this difference cannot be explained by different magmatic sources, since Late Cretaceous magmatic rocks have similar Sr isotopic compositions throughout the Panagyurishte district (Fig. 7b). In all deposits, gangue minerals yield systematically higher $^{87}Sr/^{86}Sr$ ratios than the immediate Late Cretaceous volcanic host rocks (Fig. 7b). This reveals that the ore-forming fluid with a low $^{87}Sr/^{86}Sr$ ratio (~0.7045–0.7060; Fig. 7b), either of direct magmatic origin or equilibrated with the Late Cretaceous volcanic rocks, interacted with ^{87}Sr-enriched rocks such as Palaeozoic granites ($^{87}Sr/^{86}Sr \approx 0.708$–$0.712$; Fig. 7b) and metamorphic basement rocks or their sedimentary products, i.e. Turonian sandstones ($^{87}Sr/^{86}Sr > 0.715$; Fig. 7b). The higher $^{87}Sr/^{86}Sr$ ratios of sulphates at Chelopech reveal a more intense interaction of the ore-forming hydrothermal fluids with radiogenic metamorphic basement rocks and their detrital sedimentary products. The role of Late Cretaceous seawater during ore formation remains ambiguous, because its $^{87}Sr/^{86}Sr$ ratio (Koepnick et al., 1985) lies in-between the Sr isotopic compositions of Late Cretaceous magmatic rocks, and of Turonian detrital sedimentary rocks, Palaeozoic granites and metamorphic basement rocks (Fig. 7b).

Interpretation of the more radiogenic Pb isotopic composition of ore minerals from Chelopech relative to deposits of the southern Panagyurishte district (Fig. 7c) remains equivocal. Metamorphic basement rocks and Turonian sandstones contain more radiogenic Pb than Late Cretaceous magmatic rocks and Palaeozoic intrusions of the Panagyurishte district (Kouzmanov, 2001; Kouzmanov et al., 2001). Thus, akin to the Sr isotope data, a more intense leaching of metamorphic rocks and their detrital products by ore-forming hydrothermal fluids could explain the radiogenic nature of ore minerals at Chelopech. Alternatively, the variable Pb isotopic compositions of the epithermal ore minerals might be linked to differences in the composition of the genetically associated magmatism. Although the database is still fragmentary, sulphides from porphyry-Cu deposits of the northern Panagyurishte district apparently yield more radiogenic Pb isotopic compositions than the ones from the southern district (Fig. 7c: Elatsite-Medet-Assarel porphyries vs. Vlaykov Vruh porphyry). Safely assuming that Pb in the porphyry-Cu sulphides is totally to predominantly of magmatic origin, it must be concluded that the Pb isotopic composition of the magmatism is different in both areas, and that there is a larger crustal assimilation in the melts related to the Elatsite, Medet and Assarel porphyry-Cu deposits, and by extension to the Chelopech epither-

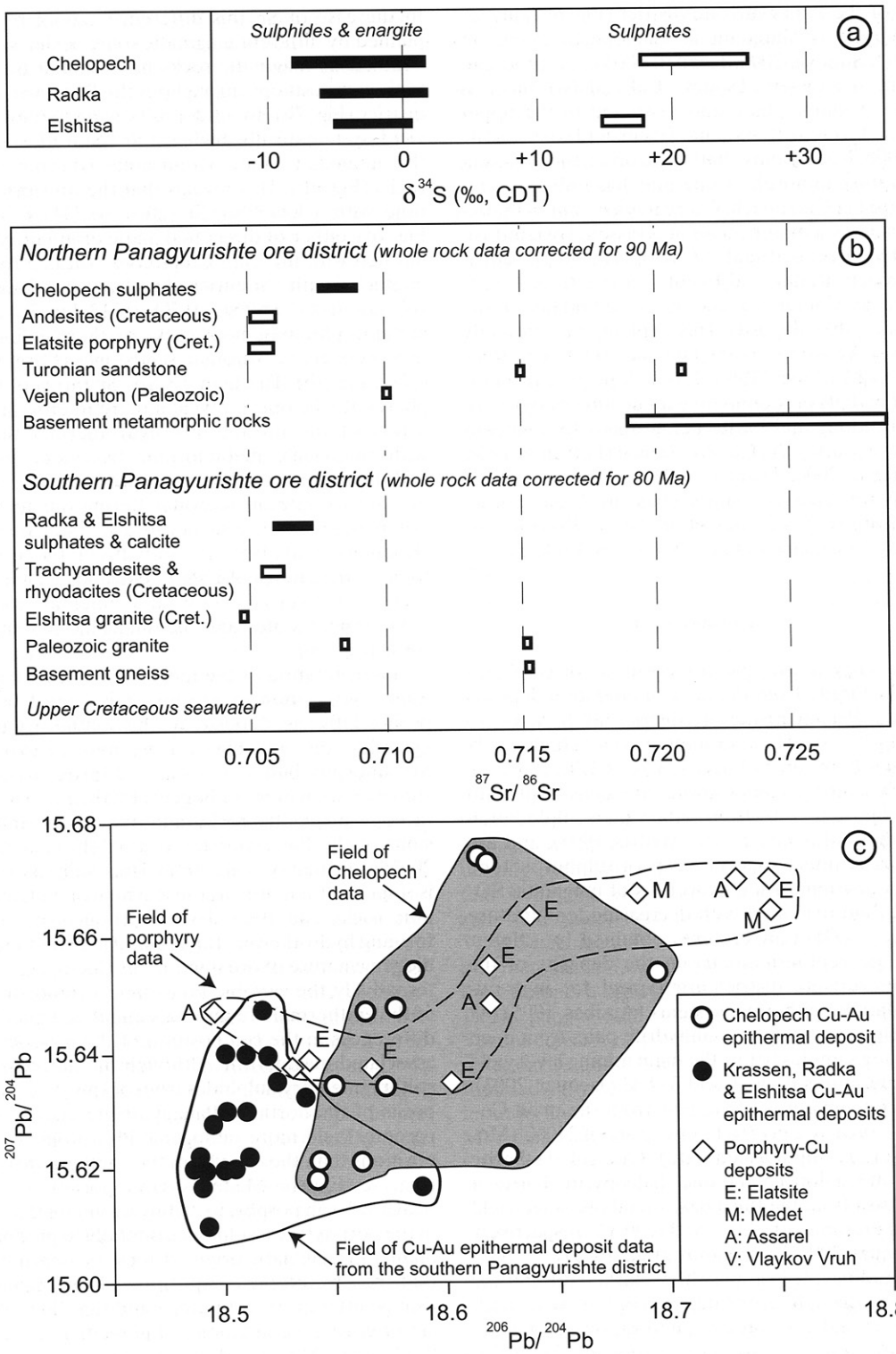
a
Sulphides & enargite
Sulphates
Chelopech
Radka
Elshitsa
-10
0
+10
+20
+30
δ 34S (‰, CDT)
b
Northern Panagyurishte ore district (whole rock data corrected for 90 Ma)
Chelopech sulphates
Andesites (Cretaceous)
Elatsite porphyry (Cret.)
Turonian sandstone
Vejen pluton (Paleozoic)
Basement metamorphic rocks
Southern Panagyurishte ore district (whole rock data corrected for 80 Ma)
Radka & Elshitsa sulphates & calcite
Trachyandesites & rhyodacites (Cretaceous)
Elshitsa granite (Cret.)
Paleozoic granite
Basement gneiss
Upper Cretaceous seawater
0.705
0.710
0.715
0.720
0.725
87Sr/86Sr
c
Field of Chelopech data
Field of porphyry data
Field of Cu-Au epithermal deposit data from the southern Panagyurishte district
Chelopech Cu-Au epithermal deposit
Krassen, Radka & Elshitsa Cu-Au epithermal deposits
Porphyry-Cu deposits
E: Elatsite
M: Medet
A: Assarel
V: Vlaykov Vruh
15.68
15.66
15.64
15.62
15.60
18.5
18.6
18.7
18.8
207Pb/204Pb
206Pb/204Pb

Fig. 7

mal deposit. This is in line with Kamenov et al. (2003a,b), who concluded that magmatism varies in composition from north to south in this district. However, even with additional Pb isotope data for whole rocks, it might be difficult to determine ultimately whether the more radiogenic Pb at Chelopech was leached from metamorphic basement rocks by the ore-forming fluid or if it was introduced into the ore deposit by a hydrothermal fluid of magmatic origin, where the magma has assimilated metamorphic basement rocks.

Discussion

The Panagyurishte Cu–Au epithermal deposits: witnesses of similar ore formation processes in space and time during the evolution of the Srednogorie belt

The epithermal Cu–Au deposits of the Panagyurishte district reveal a coherent and continuous sequence of events resulting from similar ore forming processes, typical for high-sulphidation epithermal deposits (Arribas, 1995; Cooke and Simmons, 2000; Hedenquist et al., 2000). Indeed, they share a common paragenesis including an early, massive pyrite stage, an intermediate Au-bearing Cu–As–S stage and a late base metal stage (Fig. 6). The textural and geometrical characteristics of the early, massive pyrite stage document its epigenetic nature, including both structural and lithological controls (Tsonev et al., 2000 a,b; Kouzmanov, 2001; Chambefort et al., 2003b; Jacquat, 2003; Popov et al., 2003). Early massive pyrite ore was formed by precipitation along fractures from a hydrothermal fluid, and by progressive replacement of more permeable rock units such as volcanic tuffs and sedimentary rocks. Such wallrock replacement and lithological control by permeable rock units and bedding planes are relatively common in high-sulphidation deposits (Arribas, 1995; White et al., 1995; Sillitoe, 1997, 1999; Corbett and Leach, 1998). Thus, it is not necessary to invoke profound changes in the geological environment with time, such as a transition from a submarine to an aerial setting, and early syngenetic processes (Bogdanov, 1984; Petrunov, 1995; Mutafchiev and Petrunov, 1996) to explain the genesis of the Cu–Au epithermal deposits of the Panagyurishte ore district. The economic and Au-bearing Cu–As–S stage shows an evolution from an early enargite event to a later tennantite-chalcopyrite-bornite event reflecting a temporal evolution from high to intermediate sulphidation states of the hydrothermal fluid during ore formation, and a low sulphidation state during the subsequent base metal stage (Einaudi et al., 2003). The sulphur isotopic compositions of ore and gangue minerals are coherent with disproportionation of magmatic SO_2 during ore formation (Rye, 1993).

The high ore grade - large tonnage Chelopech deposit: A giant amongst dwarfs in the Panagyurishte district

Despite descriptive and genetic similarities among the Cu–Au epithermal deposits of the Panagyurishte ore district, Chelopech clearly stands out as a giant and as the economically most attractive deposit in this area. The question about fundamental controls leading to the formation of large Cu–Au high-sulphidation epithermal deposits has been addressed in several contributions (e.g. Sillitoe, 1997, 1999; Hedenquist et al., 2000; Tosdal and Richards, 2002). The peculiarities of the Chelopech deposit in contrast to the southern Panagyurishte epithermal deposits are discussed below and may be explained by: (1) an emplacement in a shallower crustal environment, (2) its better preservation, (3) more efficient, local ore-formation processes, and (4) fundamental differences in regional geological controls.

Styles and characteristics of high-sulphidation epithermal systems vary with depth and temperature (Corbett and Leach, 1998; Sillitoe, 1999; Hedenquist et al., 2000). Collectively, several fea-

Fig. 7 Isotope data of epithermal deposits from the Panagyurishte ore district. (a) Sulphur isotope data for the Chelopech (Petrunov, 1994; Moritz et al., 2001; Jacquat, 2003), Radka (Angelkov, 1975; Velinov et al., 1978; Kouzmanov, 2001), and Elshitsa deposits (Kouzmanov, 2001; Kouzmanov et al., 2003). (b) Strontium isotope data for Chelopech sulphates (Moritz et al, 2001, 2003; Jacquat, 2003), Late Cretaceous andesites (Stoykov et al., 2003, 2004), the Vejen pluton and the Elatsite porphyry (von Quadt et al., 2002), Turonian sandstone and metamorphic basement rocks (Jacquat, 2003; Moritz et al., 2003), Radka and Elshitsa sulphates and calcite, and whole rocks from the southern Panagyurishte district (Kouzmanov, 2001; Kouzmanov et al., 2001), and Late Cretaceous seawater (Koepnick et al., 1985). (c) Lead isotope data of the Chelopech Cu–Au epithermal deposit (Moritz et al., 2001), the Elshitsa, Radka and Krassen Cu–Au epithermal deposits (Amov et al., 1974; Kouzmanov, 2001; Kouzmanov et al., 2001; except two data points from Moritz et al., 2001), and the porphyry-Cu deposits, including Vlaykov Vruh (Kouzmanov, 2001; Kouzmanov et al., 2001), Assarel (Amov et al., 1974; Moritz et al., 2001), Medet (Moritz et al., 2001) and Elatsite (von Quadt et al., 2002, except one data point from Moritz et al., 2001).

tures indicate a shallower depth and temperature environment of ore formation at Chelopech than for the other Cu–Au epithermal deposits of the Panagyurishte district (Table 1): (1) low temperature mineral polymorphs, such as chalcedony and luzonite, are confined to the Chelopech deposit, and luzonite is a subsidiary phase at Krassen, (2) vuggy silica is also restricted to the Chelopech deposit, and (3) the presence of enargite is only rarely reported at the Radka and Elshitsa deposits, and only in the upper mining levels. In addition, volcanic rocks are predominant in the northern part of the Panagyurishte district, whereas intrusive rocks become more abundant to the south (Fig. 1c), therefore revealing a progressively deeper crustal environment in the southern part. As reviewed by Sillitoe (1999), the largest high-sulphidation Au deposits are typically located in the shallow epithermal parts of high-sulphidation systems, where lithological permeability is more favourable.

Alternatively, the differences noted among the Cu–Au epithermal deposits of the Panagyurishte district might be related to different erosion levels, with Chelopech being the deposit with the better preservation. Typically, epithermal deposits have a poor preservation potential due to their shallow depth of formation, and the likelihood of their erosion increases with their age (Cooke and Simmons, 2000; Hedenquist et al., 2000). Thus, it appears as paradoxical that Chelopech, as the oldest epithermal deposit of the study area, had the best preservation potential, but this can be explained by local, late tectonics in each deposit. The overthrust on the Chelopech deposit, postdating ore formation, together with the late transgressive deposition of sandstone, limestone and a flysch sequence on top of the volcanic host rocks (Fig. 4a), were certainly key factors for its better degree of preservation. By contrast, the faults controlling the ore bodies at Elshitsa and Radka display a normal sense of movement (Figs. 4b,c), therefore an extensional tectonic setting, clearly less favourable for the preservation of epithermal deposits, possibly resulting in the loss of the upper parts of the Elshitsa and Radka deposits. Higher uplift and erosion rates in the southern Panagyurishte district could be due to the continuous, Tertiary plate tectonic convergence of the Rhodopes with the Srednogorie zone (Ivanov, 1988; Ricou et al., 1998). The subordinate presence or absence of advanced argillic mineral assemblages at Elshitsa and Radka, respectively (Fig. 5), may reflect the deeper erosion level of the epithermal deposits, thus preserving only their bottom parts (Hedenquist et al., 2000). In addition to erosion alone, catastrophic gravitational sector collapse of volcanic edifices, during or following ore formation may also explain the loss of the upper epithermal ore environment at Elshitsa and Radka (e.g. Sillitoe, 1991, 1995).

The formation of large epithermal Au deposits is the result of the confluence of magmatic and hydrothermal factors, the production of large volumes of Au-rich fluids, and an efficient hydrologic system for a focussed fluid flow to the ore site (White et al., 1995; Sillitoe, 1997; Hedenquist et al., 2000). The higher grade and tonnage of the Chelopech deposit reveal that such ore forming processes were particularly favourable in the northern part of the Panagyurishte district. Chelopech is also characterised by major lithological permeability contrasts, with the presence of a diatreme, a location close to a major discordance with basement rocks and a high abundance of sedimentary rocks in its environment (Fig. 4a). Such settings with major lithological permeability contrasts are favourable for the generation of large epithermal Au deposits (Sillitoe, 1997; Hedenquist et al., 2000). The laterally and vertically extensive advanced argillic alteration zone at Chelopech (Fig. 5) documents that the hydrology of its environment has been particularly propitious for the development of acidic conditions due to a large absorption of magmatic vapour by groundwater (Hedenquist et al., 2000).

The higher metallogenic fertility of the northern and older part of the Panagyurishte district reveals a temporal evolution in the ore formation environment on a regional scale. Fundamental variations in space and time of the regional geological context must have occurred between early porphyry-Cu and Cu–Au epithermal ore formation at about 92–90 Ma at Elatsite-Chelopech, Medet and Assarel, and later at about 86 Ma in the Krassen and Elshitsa-Vlaykov Vruh areas (Fig. 1c). The transition from predominantly andesitic volcanism in the northern Panagyurishte district to dacitic in the southern part, with subordinate rhyodacite and rhyolite, reveals a variation in space and time of magma petrogenesis, including a more important crustal input and/or higher degree of fractional crystallisation with time in the southern Panagyurishte district. Major and trace element data support a latitudinal variation in magma petrogenesis (Kamenov et al., 2003a,b), as well as the Pb isotope data of the ore deposits (Fig. 7c, see above). Chelopech has a distinctly lower Ag/Au ratio in comparison to the Cu–Au epithermal deposits of the southern Panagyurishte district (Table 1). According to Sillitoe (1999), magma chemistry is one of the basic controls on Ag/Au ratios in high-sulphidation epithermal deposits. Thus, the variable Ag/Au ratios

of the Panagyurishte epithermal deposits are possibly linked to the spatial and temporal variation of the magma chemistry throughout this ore district.

Although the regional tectonic evolution of the Panagyurishte ore district is not fully understood, one may speculate about the favourable tectonic environments that could explain the higher economic potential of its northern part. According to Tosdal and Richards (2002), the formation of porphyry-Cu and high-sulphidation epithermal deposits is favoured in a geological environment characterised by a near-neutral regional stress field, during transient periods of stress relaxation within a magmatic arc. In the Chelopech area, Jelev et al. (2003) suggest from their field studies a switch from a transtensional to a transpressional regime during the Late Cretaceous. Thus, the formation of the Chelopech deposit and, by geographical association, the Elatsite porphyry-Cu deposit may coincide with such a stress relaxation period. Although there is considerable tectonic overprint, the two predominant sets of fault orientations at Chelopech are nearly orthogonal (WNW–NW and NE), and maybe the relic of a regional stress field close to near-neutral during ore formation. Despite the fragmentary tectonic data, the southern Panagyurishte ore district appears to be essentially characterised by strike-slip tectonics along the dextral Iskar-Yavoritsa shear zone (Ivanov et al., 2001; Fig. 1c) that is a geological setting with a pronounced differential regional stress. The smaller Cu–Au epithermal deposits from the southern Panagyurishte district are essentially controlled by WNW-oriented subparallel faults (Figs. 4b–c), therefore consistent with the differential regional stress field. According to Tosdal and Richards (2002), the later tectonic environment is less propitious for the formation of high-sulphidation epithermal deposits, and may explain the lower economic potential of the southern Panagyurishte district.

Conclusions

Ore deposits are markers of specific tectonic, magmatic and fluid circulation events within the evolution of an orogen. The epithermal Cu–Au deposits of the Panagyurishte ore district are no exception to it. These deposits reveal a coherent and continuous sequence of similar ore forming processes, typical for high-sulphidation deposits throughout the regional geological evolution of the Srednogorie belt, characterised by a north to south younging of magmatic and tectonic events.

The variation in the composition of the dominant magmatism, the exposed structural level of the crust, and possibly the variation in tectonics from the northern to the southern part of the Panagyurishte ore district are paralleled by a latitudinal change in the characteristics of the epithermal Cu–Au deposits. Most notably, the northern Panagyurishte ore district appears as the economically fertile part of the Central Srednogorie belt. At this stage of knowledge, no unique explanation can be offered for this latitudinal change in ore deposit characteristics, but they are likely related to emplacements at different depths of the deposits, differences in degrees of preservation as a function of post-ore tectonics and/or sedimentary processes, efficiency of ore formation, and fundamental modifications of regional controls, such as magma petrogenesis and/or tectonic regimes. This study on the epithermal Cu–Au deposits clearly reveals that ore deposit genesis and their characteristics, in particular tonnage and grade, are very sensitive to variations of regional geological processes.

Further studies should try to understand why epithermal Cu–Au deposits in the northern Panagyurishte ore district, such as Chelopech and Krassen, are linked to a dominantly andesitic volcanism, whereas the same deposits in the southern Panagyurishte district are linked to or postdate dacitic magmatism, which itself postdates andesitic magmatism. An additional, open question is linked to the observation that a majority of the ore bodies within the Cu–Au epithermal deposits are controlled by WNW-oriented faults on a local scale, but that the ore deposit alignment on a regional scale has a NNW orientation. Paradoxically, it appears that, despite the north to south variation of geological and ore deposit characteristics within the Panagyurishte ore district, the deep crustal, fundamental control on episodic ore formation remained constant throughout its 14 Ma-long protracted Late Cretaceous magmatic and tectonic evolution.

Acknowledgements

This work was supported by the Swiss National Science Foundation through the SCOPES Joint Research Project 7BUPJ062276 and research grant 21-59041.99. The authors would like to thank I. Chambefort (University of Geneva) for discussions. The staff of the Geology Department from the Chelopech Mine, BIMAK AD mining group are gratefully acknowledged for arranging access to the mine, and sharing geological information. Critical reviews by Colin Andrew (Hareward Ventures, Sofia, Bulgaria) and Albrecht von Quadt (ETH-Zürich, Switzerland) helped us to improve the manuscript. This is a contribution to the ABCD-GEODE research program supported by the European Science Foundation.

References

Aiello, E., Bartolini, C., Boccaletti, M., Gocev, P., Karagjuleva, J., Kostadinov, V. and Manetti, P. (1977): Sedimentary features of the Srednogorie zone (Bulgaria): an Upper Cretaceous intra-arc basin. *Sedimentary Geol.* **19**, 39–68.

Amov, B.G., Bogdanov, B. and Baldjieva, C. (1974): Lead isotope composition and some features concerning the genesis and the age of the ore deposits in south Bulgaria. (in Russian), In: Problems of Ore Deposition, Proceedings of the 4th IAGOD Symposium, Varna, Bulgaria, **vol. 2**, 13–25.

Angelkov, K. (1975): Isotopic composition of sulfur in Radka, Chelopech, Medet and Vlaykov Vruh deposits (in Bulgarian), *Rudodobiv* **8**, 4–7.

Antonov, M. and Jelev, V. (2001): Transpression and oblique fold-and-thrust structures in the Chelopech ore field (Bulgaria). *Annual Univ. Mining Geol.* **43–44**, 45–49.

Arribas, A. (1995): Characteristics of high-sulfidation epithermal deposits, and their relation to magmatic fluid. In: Thompson, J.F.H. (ed.): Magmas, fluids and ore deposits. *Mineral. Assoc. Canada*, Short Course Series, **23**, 419–454.

Bayraktarov, I., Antova, N., Nikolov, G., Rankova, T. and Chemberski, H. (1996): Geodynamic environments during the Late Cretaceous in Bulgaria and their metallogeny. In: Popov P. (ed.): Plate tectonic aspects of the Alpine metallogeny in the Carpatho-Balkan region, UNESCO- IGCP project 356, Proceedings of the annual meeting, Sofia, Bulgaria, 1996, v. 2, 45–56.

Berger, B.R. and Henley, R.W. (1989): Advances in understanding of epithermal gold-silver deposits, with special reference to the Western United States. In: Keays, R.R., Ramsay, W.R.H. and Groves, D.I. (eds): The geology of gold deposits: the perspective in 1988, *Econ. Geol. Monograph* **6**, 405–423.

Berza, T., Constantinescu, E. and Vlad, S.-N. (1998): Upper Cretaceous magmatic series and associated mineralization in the Carpathian-Balkan region. *Resource Geology* **48**, 291–306.

Boccaletti, M., Manetti, P. and Peccerillo, A. (1974): The Balkanides as an instance of back-arc thrust belt: Possible relations with the Hellenides. *Geol. Soc. Am. Bull.* **85**, 1077–1084.

Boccaletti, M., Manetti, P., Peccerillo, A. and Stanisheva-Vassileva, G. (1978): Late Cretaceous high-potassium volcanism in eastern Srednogorie, Bulgaria. *Geol. Soc. Am. Bull.* **89**, 439–447.

Bogdanov, B. (1984): Hydrothermal systems of massive sulphide, porphyry-copper and vein copper deposits of Sredna Gora zone in Bulgaria. In: Proceed. VI Symp. IAGOD, Stuttgart, Germany, 63–67.

Bogdanov, B. and Bogdanova, R. (1974): The Radka copper-pyrite deposit. In: Dragov, P. and Kolkovski, B. (eds.): Twelve ore deposits of Bulgaria. IV symposium IAGOD, Varna, 1974, 114–133.

Bogdanov, B., Popov, P. and Obretenov, N. (1970): Structural features of the Elshitsa ore field. (in Bulgarian). *Rev. Bulg. Geol. Soc.* **31**, 303–313.

Bogdanov, K., Tsonev, D. and Kouzmanov, K. (1997): Mineralogy of gold in the Elshitsa massive sulphide deposit, Sredna Gora zone, Bulgaria. *Mineral. Deposita* **32**, 219–229.

Boncev, E. (1988): Notes sur la tectonique alpine des Balkans. *Bull. Soc. Géol. Fr.* **IV**, 241–249.

Bonev, I.K., Kerestedjian, T., Atanassova, R. and Andrew, C.J. (2002): Morphogenesis and composition of native gold in the Chelopech volcanic-hosted Au–Cu epithermal deposit, Srednogorie zone, Bulgaria. *Mineral. Deposita* **37**, 614–629.

Chambefort, I., von Quadt, A. and Moritz, R. (2003a): Volcanic environment and geochronology of the Chelopech high-sulfidation epithermal deposit, Bulgaria: regional relationship with associated deposits. European Union of Geosciences 12th Biennial Meeting, Nice, France, 6 – 11 Avril 2003. Abstract on CD: EAE03-A-00569.

Chambefort, I., Moritz, R., Jacquat, S. and Petrunov, R. (2003b): Influence of the volcanic environment on hydrothermal fluid circulation: Example of the Chelopech Au–Cu high-sulfidation epithermal deposit, Bulgaria. IAVCEI XXth meeting, Sapporo, Japan, 30 June–11 July 2003. Abstract volume A, p. 520.

Cheshitev, G., Milanova, V., Sapounov, I. and Choumachenko, P. (1995): Explanatory note to the geological map of Bulgaria in scale 1:100 000, Teteven map sheet (in Bulgarian). Avers, Sofia.

Chipchakova, S. and Stefanov, D. (1974): Genetic types of argillisites at the height of Golyamo Petelovo and in the Elshitsa-West copper-pyrite deposit in the Panagyurishte ore district (in Bulgarian). In: Alexiev, E., Mincheva-Stefanova, J. and Radonova, T. (eds.): Mineral Genesis, Geological Institute-Bulgarian Academy of Science, 437–454.

Chipchakova, S. and Lilov, P. (1976): About the absolute age of Upper Cretaceous magmatic rocks from the western part of the Central Srednogorie and related ore deposits (in Russian). *Comptes rendus Acad. bulg. Sci.* **29**, 101–104.

Chipchakova, S., Karadjova, B., Andreev, A. and Stefanov, D. (1981): Rare alkalis in wall rock metasomatites of massive-pyrite deposits in Central Srednogorie, Bulgaria. *Geol. Balcanica* **11**, 89–102.

Ciobanu, C.L., Cook, N.J. and Stein, H. (2002): Regional setting and geochronology of the Late Cretaceous banatitic magmatic and metallogenic belt. *Mineral. Deposita* **37**, 541–567.

Cooke, D.R. and Simmons, S.F. (2000): Characteristics and genesis of epithermal gold deposits. In: Hagemann, S.G. and Brown, P.E. (eds): Gold in 2000, *Reviews in Economic Geology* **13**, 221–244.

Corbett, G.J. and Leach, T.M. (1998): Southwest Pacific Rim gold-copper systems: structure, alteration, and mineralization. *Soc. Econ. Geol. Spec. Publ. 6*, 237 pp.

Dabovski, C. (1988): Precambrian in the Srednogorie zone (Bulgaria). In: Cogne, J., Kozhoukharov, D. and Krautner, H.G. (eds.): Precambrian in younger fold belts, Essex, 841–847.

Dabovski, C., Zagorchev, I., Rouseva, M. and Chounev, D. (1972): Paleozoic granitoids in the Sushtinska Sredna Gora (in Bulgarian). *Annual UGP* **16**, 57–92.

Dabovski, C., Harkovska, A., Kamenov, B., Mavrudchiev, B., Stanisheva-Vassileva, G. and Yanev, Y. (1991): A geodynamic model of the Alpine magmatism in Bulgaria. *Geol. Balcanica* **21**, 3–15.

Dimitrov, C. (1960): Magmatismus und Erzbildung im Erzgebiet von Panagjuriste. *Freib. Forschungshefte:* **C. 79**, 67–81.

Dimitrov, C. (1983): Senonian initial volcanic rocks south of Panagjuriste and Strelca (in Bulgarian). *Rev. Bulg. Geol. Soc.* **44**, 95–128.

Dimitrov, C. (1985): On the genesis of the Elshitsa, Radka, Krassen and Bialata Prast ore deposits, Panagyurishte area (in Bulgarian). *Rev. Bulg. Geol. Soc.* **46**, 257–266.

Dobrev, T., Dimitrov, I., Pishtalov, S., Ivanova, V. and Radkov, R. (1967): Studies on the deep structure of east Bulgaria based on geophysical data (in Bulgarian). *Rev. Bulg. Geol. Soc.* **28**, 35–54.

Einaudi, M.T., Hedenquist, J.W. and Inan, E.E. (2003): Sulfidation state of fluids in active and extinct hy-

drothermal systems: Transitions from porphyry to epithermal environments. In: Simmons, S.F. and Graham, I. (eds.): Volcanic, geothermal, and ore-forming fluids: Rulers and witnesses of processes within the Earth. *Soc. Econ. Geol. Spec. Publ.* **10**, 285–313.

Georgieva, S., Velinova, N., Petrunov, R., Moritz, R. and Chambefort, I. (2002): Aluminium phosphate-sulphate minerals in the Chelopech Cu–Au deposit: Spatial development, chemistry and genetic significance. *Geochem. Mineral. Petrol.* **39**, 39–51.

Haydoutov, I. (2001): The Balkan island-arc association in West Bulgaria. *Geol. Balcanica* **31**, 109–110.

Heald, P., Foley, N. and Hayba, D. (1987): Comparative anatomy of volcanic-hosted epithermal deposits: acide-sulfate and adularia-sericite types. *Econ. Geol.* **82**, 1–26.

Hedenquist, J.W. and Henley, R.W. (1985): The importance of CO_2 on freezing point measurements of fluid inclusions: Evidence from active geothermal systems and implications for epithermal ore deposition. *Econ. Geol.* **80**, 1379–1406.

Hedenquist, J.W. and Lowenstern, J.B. (1994): The role of magma in the formation of hydrothermal ore deposits. *Nature* **370**, 519–527.

Hedenquist, J.W., Arribas, A. and Gonzalez-Urien, E. (2000): Exploration for epithermal gold deposits. In: Hagemann, S.G. and Brown, P.E. (eds): Gold in 2000, *Reviews in Economic Geology* **13**, 245–277.

Hedenquist, J.W., Claveria, R.J.R. and Villafuerte, G.P. (2001): Types of sulfide-rich epithermal deposits and their affiliation to porphyry systems: Lepanto-Victoria-Far Southeast deposits, Philippines, as examples. Pro Explo, CD with abstracts, Lima, Peru.

Heinrich, C.A. and Neubauer, F. (2002): Cu–Au–Pb–Zn–Ag metallogeny of the Alpine-Balkan-Carpathian-Dinaride geodynamic province. *Mineral. Deposita* **37**, 533–540.

Ivanov, Z. (1988): Aperçu général sur l'évolution géologique et structurale du massif des Rhodopes dans le cadre des Balkanides. *Bull. Soc. Géol. Fr.* **IV**, 227–240.

Ivanov, Z. (1998, in press.): Tectonics of Bulgaria (in Bulgarian).

Ivanov, Z., Henry, B., Dimov, D., Georgiev, N., Jordanova, D. and Jordanova, N. (2001): New model for Upper Cretaceous magma emplacement in the southwestern parts of Central Srednogorie – Petrostructural and AMS data. In: ABCD-GEODE 2001, Workshop, Vata Bai, Romania, Abstracts volume, 60–61.

Jacquat, S. (2003): Etude paragénétique et géochimique du gisement épithermal d'or et de cuivre de type "high-sulfidation" de Chelopech (Bulgarie). Unpublished M.Sc. thesis, Dept Mineralogy, Uni. Geneva, Switzerland, 171 pp.

Jelev, V., Antonov, M., Arizanov, A. and Arnaudova, R. (2003): On the genetic model of Chelopech volcanic structure (Bulgaria). 50 Years University of Mining and Geology "St Ivan Rilski", *Annual vol.* **46**, part I, 47–51.

Kamenov, B.K., von Quadt, A. and Peytcheva, I. (2002): New insight into petrology, geochemistry and dating of the Vejen pluton, Bulgaria. *Geochem. Mineral. Petrol.* **39**, 3–25.

Kamenov, B., Moritz, R., Nedialkov, R., Peytcheva, I., von Quadt, A., Stoykov, S., Yanev, Y. and Zartova, A. (2003a): Petrology of the Late Cretaceous ore-magmatic centers from the Central Srenogorie, Bulgaria: Magma evolution and sources. In: Neubauer, F. and Handler, R. (eds.): Programme and abstracts, Final ABCD-GEODE 2003 workshop, Seggauberg, Austria, 22–24 March 2003, p. 30.

Kamenov, B., Nedialkov, R., Yanev, Y. and Stoykov, S. (2003b): Petrology of the late Cretaceous ore-magmatic-centres in the Central Srednogorie, Bulgaria. In: Bogdanov, K. and Strashimirov, S. (eds.): Cretaceous porphyry-epithermal systems of the Srednogorie zone, Bulgaria, *Society of Economic Geologists Guidebook series* **36**, 27–46.

Kamenov, B., von Quadt, A. and Peytcheva, I., (2003c): New petrological, geochemical and isotopic data bearing on the genesis of Capitan-Dimitrievo pluton, Central Srednogorie, Bulgaria. In: Neubauer, F. and Handler, R. (eds.): Programme and abstracts, Final ABCD-GEODE 2003 workshop, Seggauberg, Austria, 22–24 March 2003, p. 31.

Katskov, N. and Iliev, K. (1993): Panagyurishte map sheet (in Bulgarian), In: Explanatory note to the Geological Map of Bulgaria in scale 1:100000, 53 pp.

Koepnick, R.B., Burke, W.H., Denison, R.E., Hetherington, E.A., Nelson, H.F., Otto, J.B. and Waite, L.E. (1985): Construction of the seawater $^{87}Sr/^{86}Sr$ curve for the Cenozoic and Cretaceous: supporting data. *Chem. Geol.* **58**, 55–81.

Kouzmanov, K. (2001): Genèse de la concentration en métaux de base et précieux de Radka et Elshitsa (zone de Sredna Gora, Bulgarie): une approche par l'étude minéralogique, isotopique et des inclusions fluides. Unpublished Ph.D. thesis, University of Orléans, France, 437 pp.

Kouzmanov, K., Bailly, L., Ramboz, C., Rouer, O. and Bény, J.-M. (2002): Morphology, origin and infrared microthermometry of fluid inclusions in pyrite from the Radka epithermal copper deposit, Srednogorie zone, Bulgaria. *Mineral. Deposita* **37**, 599–613.

Kouzmanov, K., Moritz, R., Chiaradia, M., Fontignie, D. and Ramboz, C. (2001): Sr and Pb isotope study of Au–Cu epithermal and porphyry-Cu deposits from the southern part of the Panagyurishte district, Sredna Gora zone, Bulgaria. In: Piestrzynski, A. et al. (eds.): Mineral deposits at the beginning of the 21st century, Proceedings 6th biennial SGA meeting, Krakow, Poland, 539–542.

Kouzmanov, K., Ramboz, C., Lerouge, C., Deloule, E., Beaufort, D. and Bogdanov, K. (2003): Stable isotopic constrains on the origin of epithermal Cu–Au and related porphyry copper mineralisations in the southern Panagyurishte district, Srednogorie zone, Bulgaria. In: Elioupoulos, D.G. et al. (eds.): Mineral exploration and sustainable development, Proceedings 7th biennial SGA meeting, Athens, Greece, 24–28 August 2003, Millpress Rotterdam, 1181–1184.

Kouzmanov, K., Ramboz, C., Bailly, L. and Bogdanov, K. (2004): Genesis of high-sulfidation vinciennite-bearing Cu–As–Sn (Au) assemblage from the Radka copper epithermal deposit, Bulgaria: Evidence from mineralogy and infrared microthermometry of enargite. *Can. Mineralogist* **42**, 1501–1521.

Lips, A.L.W. (2002): Correlating magmatic-hydrothermal ore deposit formation over time with geodynamic processes in SE Europe. In: Blundell, D.J., Neubauer, F. and von Quadt, A. (eds): The timing and location of major ore deposits in an evolving orogen. *Geol. Soc. London Spec. Publication* **204**, 69–79.

Moev, M. and Antonov, M. (1978): Stratigraphy of the Upper Cretaceous in the eastern part of the Sturguel-Chelopech strip (in Bulgarian). *Ann. de l'Ec. Sup. Min. Géol.* **23**, 7–30.

Moritz, R., Chambefort, I., Chiaradia, M., Fontignie, D., Petrunov, R., Simova, S., Arisanov, A. and Doychev, P. (2001): The Late Cretaceous high-sulfidation Au–Cu Chelopech deposit, Bulgaria: geological setting, paragenesis, fluid inclusion microthermometry of

enargite, and isotope study (Pb, Sr, S). In: Piestrzynski, A. et al. (eds.): Mineral deposits at the beginning of the 21st century, Proceedings 6th biennial SGA meeting, Krakow, Poland, 547–550.

Moritz, R., Jacquat, S., Chambefort, I., Fontignie, D., Petrunov, R., Georgieva, S. and von Quadt, A. (2003): Controls of ore formation at the high-sulphidation Au–Cu Chelopech deposit, Bulgaria: evidence from infrared fluid inclusion microthermometry of enargite and isotope systematics of barite. In: Elioupoulos, D.G. et al. (eds.): Mineral exploration and sustainable development, Proceedings 7th biennial SGA meeting, Athens, Greece, 24–28 August 2003, Millpress Rotterdam, 1209–1212.

Mutafchiev, I. and Petrunov, R. (1996): Geological genetic models of ore-deposit formation in the Panagyurishte-Etropole ore region. Unpublished report for Chelopech LTD, Sofia, 69 pp.

Nedialkov, R. and Zartova, A. (2002): Magmatism of the Assarel area and its ore generating capability. In: Moritz, R. and von Quadt, A. (eds.): GEODE workshop on the Srednogorie zone, April 2002, Sofia, Bulgaria, Abstract volume, p. 13

Neubauer, F. (2002): Contrasting Late Cretaceous with Neogene ore provinces in the Alpine-Balkan-Carpathian-Dinaride collision belt. In: Blundell, D.J., Neubauer, F. and von Quadt, A. (eds): The timing and location of major ore deposits in an evolving orogen. *Geol. Soc. London Spec. Publication* **204**, 81–102.

Petrunov, R. (1989): Hypogene sulphate-sulphide zoning in a copper-pyrite deposit. *Comptes rendus Bulg. Acad. Sci.* **42**, 71–74.

Petrunov, R. (1994): Mineral parageneses and physicochemical conditions of ore-formation in the Chelopech deposit (in Bulgarian). Unpublished Ph.D. thesis, Geological Institute–BAS, Sofia, Bulgaria, 178 pp.

Petrunov, R. (1995): Ore mineral parageneses and zoning in the deposit of Chelopech (in Bulgarian), *Geochem. Mineral. and Petrol.* **30**, 89–98.

Petrunov, R., Dragov, P. and Neykov, H. (1991): Polyelemental (with As, Sn, V, Bi, Ag, Te, Ge, Se etc.) mineralization in Assarel porphyry-copper deposit (in Bulgarian). *Rev. Bulg. Geol. Soc.* **52**, 1–7.

Peytcheva, I. and von Quadt, A. (2003): U–Pb-zircon isotope system in mingled and mixed magmas: an example from Central Srednogorie, Bulgaria. EGS-AGU-EUG joint assembly Nice, France, April 2003, Geophysical research abstracts, vol. 5, abstract EAE03-A-09177.

Peytcheva, I., von Quadt, A., Kamenov, B., Ivanov, Z. and Georgiev, N. (2001): New isotope data for Upper Cretaceous magma emplacement in the southern and south-western parts of Central Srednogorie. In: ABCD-GEODE 2001, Workshop, Vata Bai, Romania, Abstracts volume, 82–83.

Peytcheva, I., von Quadt, A., Kouzmanov, K. and Bogdanov, K. (2003): Elshitsa and Vlaykov Vruh epithermal and porphyry Cu(–Au) deposits of Central Srednogorie, Bulgaria: source and timing of magmatism and mineralisation. In: Elioupoulos, D.G. et al. (eds.): Mineral exploration and sustainable development, Proceedings 7th biennial SGA meeting, Athens, Greece, 24–28 August 2003, Millpress Rotterdam, 371–373.

Popov, K. (2001a): Geology of the southern part of the Panagyurishte ore region. *Annual Univ. Mining Geol. vol.* **43–44**, 51–63.

Popov, K. (2001b): Porphyry copper – massive sulphide system in the Radka ore district (Bulgaria). *Annual Univ. Mining Geol. vol.* **43–44**, 65–71.

Popov, P. (1987): Tectonics of the Banat-Srednogorie rift. *Tectonophysics* **143**, 209–216.

Popov, P. (2002): Alpine geotectonic evolution and metallogeny of the Eastern part of the Balkan peninsula. University of Mining and Geology "St Ivan Rilski", *Annual vol.* **45**, part I, 33–38.

Popov, P. and Kovachev, V. (1996): Geology, composition and genesis of the mineralizations in the Central and Southern part of the Elatsite-Chelopech ore field. In: Popov P. (ed.): Plate tectonic aspects of the Alpine metallogeny in the Carpatho-Balkan region, UNESCO- IGCP project 356, Proceedings annual meeting, Sofia, Bulgaria, 1996, **vol. 1**, 159–170.

Popov, P. and Popov, K. (1997): Metallogeny of Panagyurishte ore region. In: Romic, K. and Konzulovic, R. (eds.): Symposium «Ore Deposits Exploration», Proceedings, Belgrade, 2–4 April 1997, 327–338.

Popov, P., Tsonev, D. and Kanazirski, M. (2000a): Elshitsa ore field. In: Strashimirov S. and Popov, P. (eds.): Geology and metallogeny of the Panagyurishte ore region (Srednogorie zone, Bulgaria), ABCD-GEODE 2000 workshop, Guidebook to excursions, 40–46.

Popov, P., Petrunov, R., Kovachev, V., Strashimirov, S. and Kanazirski, M. (2000b): Elatsite-Chelopech ore field. In: Strashimirov S. and Popov, P. (eds.): Geology and metallogeny of the Panagyurishte ore region (Srednogorie zone, Bulgaria), ABCD-GEODE 2000 workshop, Guidebook to excursions, 8–18.

Popov, P., Radichev, R. and Dimovski, S. (2002): Geology and evolution of the Elatzite-Chelopech porphyry-copper-massive sulfide ore field (in Bulgarian). *Annual Univ. Mining Geol.* **43–44**, 31–44.

Popov, P., Strashimirov, S., Popov, K., Petrunov, R., Kanazirski, M. and Tzonev, D. (2003): Main features in geology and metallogeny of the Panagyurishte ore region. 50 Years University of Mining and Geology "St Ivan Rilski", *Annual vol.* **46**, part I, 119–125.

Radonova, T. (1962): Primary mineralization and wall-rock alterations in the area of Radka mine, in the vicinity of Panagyurishte (in Bulgarian), *Travaux sur la Géologie de Bulgarie, Série «Géochimie, Gîtes métallifères et non-métallifères»* **3**, 93–128.

Radonova, T. (1967): Dumortierite from the area of the Elshitsa ore deposit, district of Panagyurishte (in Bulgarian), *Rev. Bulg. Geol. Soc.* **28**, 191–195.

Radonova, T. (1970): Certain petrogenetic factors controlling copper pyritic mineralizations in the Central Srednogorie (in Bulgarian), *Rev. Bulg. Geol. Soc.* **31**, 323–328.

Radonova, T. and Velinov, I. (1974): Relationship between propylites, secondary quartzites and ore deposition in the Central and Western Srednogorie (Bulgaria), (in Russian). In: Metasomatism and ore deposition, Nauka, Moscow, 60–69.

Ricou, L.-E., Burg, J.-P., Godfriaux, I. and Ivanov, Z. (1998): Rhodope and Vardar: the metamorphic and the olistostromic paired belts related to the Cretaceous subduction under Europe. *Geodynamica Acta* **11**, 285–309.

Rye, R.O. (1993): The evolution of magmatic fluids in the epithermal environment: The stable isotope perspective. *Econ. Geol.* **88**, 733–753.

Sillitoe, R.H. (1991): Gold metallogeny of Chile – An introduction. *Econ. Geol.* **86**, 1187–1205.

Sillitoe, R.H. (1995): The influence of magmatic-hydrothermal models on exploration strategies for volcano-plutonic arcs. In: Thompson, J.F.H. (ed.): Magmas, fluids and ore deposits. *Mineral. Assoc. Canada*, Short Course Series, **23**, 511–525.

Sillitoe, R.H. (1997): Characteristics and controls of the largest porphyry copper-gold and epithermal gold

deposits in the circum-Pacific region. *Austral. J. Earth Sci.* **44**, 373–388.

Sillitoe, R.H. (1999): Styles of high-sulphidation gold, silver and copper mineralisation in porphyry and epithermal environments. In: Weber, G. (ed.): Austr. Inst. Min. Metal., PacRim'99, Bali, Indonesia, 10–13 October, Proceedings, 29–44.

Simova, S. (2000): Mineral composition and paragenetic sequences in the ore mineralization of 405 horizon in the Chelopech deposit (in Bulgarian). Unpublished M.Sc. thesis, Sofia University, Bulgaria, 68 pp.

Stanisheva-Vassileva, G. (1980): The Upper Cretaceous magmatism in Srednogorie zone, Bulgaria: a classification attempt and some implications. *Geol. Balcanica* **10**, 15–36.

Stoykov, S. and Pavlishina, P. (2003): New data for Turonian age of the sedimentary and volcanic succession in the southeastern part of Etropole Stara Planina mountain, Bulgaria. *Comptes rendus Acad. Bulg. Sci.* **56**, 55–60.

Stoykov, S., Yanev, Y., Moritz, R. and Katona, I. (2002): Geological structure and petrology of the Late Cretaceous Chelopech volcano, Srednogorie magmatic zone. *Geochem. Mineral. Petrol.* **39**, 27–38.

Stoykov, S., Yanev, Y., Moritz, R. and Fontignie, D. (2003): Petrology, Sr and Nd isotope signature of the Late Cretaceous magmatism in the south-eastern part of the Etropole Stara Planina, Srednogorie magmatic zone. 50 Years University of Mining and Geology "St Ivan Rilski", *Annual vol.* **46**, part I, 161–166.

Stoykov, S., Peytcheva, I., von Quadt, A., Moritz, R., Frank, M. and Fontignie, D. (2004): Timing and magma evolution of the Chelopech volcanic complex, Bulgaria. *Schweiz. Mineral. Petrogr. Mitt.* **84**, 101–117.

Strashimirov, S., Petrunov, R. and Kanazirski, M. (2002): Porphyry-copper mineralisation in the central Srednogorie zone, Bulgaria. *Mineral. Deposita* **37**, 587–598.

Tarkian, M., Hüken, U., Tokmakchieva, M. and Bogdanov, K. (2003): Precious-metal distribution and fluid-inclusion petrography of the Elatsite porphyry copper deposit, Bulgaria. *Mineral. Deposita* **38**, 261–281

Tosdal, R.M. and Richards, J.P. (2002): Tectonic setting: A critical link in the formation of porphyry-Cu and epithermal deposits. In: Vearncombe, S. (ed.): Applied structural geology for mineral exploration and mining, Abstract volume, 23–25 Sept. 2002, Kalgoorlie, Western Australia. Australian Inst. Geoscientists Bull. **36**, p. 209–211.

Tsonev, D., Popov, K. and Kanazirski, M. (2000a): Krasen-Petolovo ore field. In: Strashimirov S. and Popov, P. (eds.): Geology and metallogeny of the Panagyurishte ore region (Srednogorie zone, Bulgaria), ABCD-GEODE 2000 workshop, Guidebook to excursions, 26–31.

Tsonev, D., Popov, K., Kanazirski, M. and Strashimirov, S. (2000b): Radka ore field. In: Strashimirov S. and Popov, P. (eds.): Geology and metallogeny of the Panagyurishte ore region (Srednogorie zone, Bulgaria), ABCD-GEODE 2000 workshop, Guidebook to excursions, 32–39.

Tsvetkov, K. (1976): Some data of the geological-geophysical prospecting for the distribution of the copper-porphyry mineralizations in the Panagyurishte region (in Russian). In: Problemi Rudoobrasovania, *Publ. House Bulg. Acad. Sci.* **1**, 191–198.

Velinov, I.A., Loginov, V.P., Nossik, L.P., Radonova, T.G. and Russinov, V.L. (1978): Particularities of the genesis of massive pyrite deposits from the Srednogorie zone in Bulgaria and Jugoslavia (in Russian). In: Korjinskiy, D.S., Jarikov, V.A., Landa, E.A., Omelianenko, B.I., Percev, N.N. and Rass, I.T. (eds.): Metasomatism and ore formation, Moscow, 176–183.

von Quadt, A., Peytcheva, I., Kamenov, B., Fanger, L., Heinrich, C.A. and Frank, M. (2002): The Elatsite porphyry copper deposit in the Panagyurishte ore district, Srednogorie zone, Bulgaria: U–Pb zircon geochronology and isotope-geochemical investigations of magmatism and ore genesis. In: Blundell, D.J., Neubauer, F. and von Quadt, A. (eds.): The timing and location of major ore deposits in an evolving orogen. *Geol. Soc. London Spec. Publication* **204**, 81–102.

von Quadt, A., Peytcheva, I., Heinrich, C., Frank, M., Cvetkovic, V. and Banjesevic, M. (2003a): Evolution of the Cretaceous magmatism in the Apuseni-Timok-Srednogorie metallogenic belt and implications for the geodynamic reconstructions: new insight from geochronology, geochemistry and isotope studies. In: Neubauer, F. and Handler, R. (eds.): Programme and abstracts, Final ABCD-GEODE 2003 workshop, Seggauberg, Austria, 22–24 March 2003, p. 60.

von Quadt, A., Peytcheva, I. and Cvetkovic, V. (2003b): Geochronology, geochemistry and isotope tracing of the Cretaceous magmatism of east-Serbia and Panagyurishte district (Bulgaria) as part of the Apuseni-Timok-Srednogorie metallogenic belt in eastern Europe In: Elioupoulos, D.G. et al. (eds.): Mineral exploration and sustainable development, Proceedings 7th biennial SGA meeting, Athens, Greece, 24–28 August 2003, Millpress Rotterdam, 407–410.

White, N.C., Leake, M.J., McCaughey, S.N. and Parris, B.W. (1995): Epithermal gold deposits of the southwest Pacific. *J. Geochem. Explor.* **54**, 87–136.

Zimmerman, A., Stein, H., Markey, R., Fanger, L., Heinrich, C., von Quadt, A. and Peytcheva, I. (2003): Re–Os ages for the Elatsite Cu–Au deposit, Srednogorie zone, Bulgaria. In: Elioupoulos, D.G. et al. (eds.): Mineral exploration and sustainable development, Proceedings 7th biennial SGA meeting, Athens, Greece, 24–28 August 2003, Millpress Rotterdam, 1253–1256.

Received 21 November 2003
Accepted in revised form 12 July 2004
Editorial handling: A. von Quadt

Δελτίο της Ελληνικής Γεωλογικής Εταιρίας τομ. XXXVI, 2004
Πρακτικά 10ου Διεθνούς Συνεδρίου, Θεσ/νίκη Απρίλιος 2004

Bulletin of the Geological Society of Greece vol. XXXVI, 2004
Proceedings of the 10th International Congress, Thessaloniki, April 2004

MINERAL ASSEMBLAGES AND GENESIS OF THE CU-AU EPITHERMAL DEPOSITS IN THE SOUTHERN PART OF THE PANAGUYRISHTE ORE DISTRICT, BULGARIA

Bogdanov K.[1], Tsonev D.[1], and Popov K.[2]

[1] *Department of Mineralogy, Petrology and Economic Geology, Sofia University, 15 Tsar Osvoboditel Bd., 1504 Sofia, Bulgaria, kamen@gea.uni-sofia.bg, dtsonev@ gea.uni-sofia.bg*

[2] *University of Mining and Geology "St.I. Rilski",1700 Sofia, Bulgaria, kpopov@mgu.bg*

ABSTRACT

Epithermal Cu-Au deposits hosted within volcanic rocks (Radka, Elshitsa, Krassen) are related to Late Cretaceous andesite-dacite volcanic terrain in the Panagyurishte ore district. The Cu-Au ores are linked by a similar mineralogy and differ by the ratio of tennantite, bornite, enargite and discrete trace minerals of Ga, Ge, In and Bi (e.g., roquesite, germanite, betekhtinite, renierite, vinciennite, aikinite). Bi-Se-Te and Ga-Ge-In-Sn signature with pronounced Au-enrichment of the bornite rich ores is a characteristic feature underlying the increasing role of the fS_2/fO_2 control during the transition from IS to HS environment. Formation of the epithermal Cu-Au deposits appears to have occurred during a single broad event of contemporaneous formation of epithermal and porphyry systems.The close connection between the volcano-plutonic structures facilitates the multistage and polycyclic character of their hydrothermal systems, the similar character of the epithermal ores and the mineral succession in Elshitsa, Radka and Krassen deposits. The $\delta^{34}S$ ratios in the sulphide minerals range from –6.7 to 4.0, suggesting comparable magmatic sources for the epithermal mineralizing fluids and close link with porphyry environment.

1 INTRODUCTION

The Panagyurishte ore district is located in a 30 x 50 km belt trending N-NW to S-SE, including the town of Panagyurishte in Central Srednogorie, Bulgaria (Fig.1). The district belongs to the Late Cretaceous Banat-Srednogorie metallogenic zone, part of the Alpine-Balkan-Carpathian-Dinaride (ABCD) belt (Heinrich & Neubauer 2002). The Srednogorie part of the ABCD belt in Bulgaria, developed during the Mesozoic as a copper-rich, andesite-dominated island arc system (Fig. 1) that continues eastwards through Turkey to Iran (Jankovic 1977, Bogdanov 1987, Dabovski et al. 1991).

A series of volcanic rock-hosted sulphide ore deposits (e.g. Radka, Elshitsa and Krassen) related to Late Cretaceous andesite-dacite volcanic activity are located in the southern part of the Panagyurishte district (Fig.1). They are spatially associated with small porphyry copper ore deposits (Vlaikov Vruh, Tsar Assen, Petelovo) hosted by co-magmatic subvolcanic monzodiorite, granodiorite and quartz diorite porphyritic intrusions.

Two main types of ore bodies are characteristic of the volcanic rock-hosted sulphide deposits: early massive pyrite ore bodies and late Cu-Au sulphide ore bodies. The massive structures of the early pyrite ores and the presence of pyrite laminations in the host dacite tuffs at Radka, Elshitsa and Krassen have been interpreted as possibly due to syngenetic VMS deposition coeval with dacitic volcanism (Bogdanov 1984, 1987, Bogdanov et al. 1997). However the VMS-style massive sulphide and porphyry copper deposits have been considered as incompatible ore types, characteristic of discrete tectono-magmatic settings (Sillitoe 1999). At the same time, characteristic features such as adularia-sericite and advanced argillic alteration styles, the steep fault-controlled ore bodies (including the early massive pyrite ore bodies), the abundance of enargite, bornite and chalcocite in the late Cu-Au ores provide good reasons to regard these deposits as the analogues of enargite-bearing massive sulphide deposits, positioned high and/or late in porphyry copper systems (Sillitoe et al. 1996). Such mineralizations have more recently been described as high (alunite-kaolinite) and

low (adularia-sericite) sulphidation epithermal deposits (Hedenquist et al. 1996). This classification based on oxidation state of sulphur has more recently been expanded (Hedenquist et al. 2000) to include an intermediate sulphidation division that is affiliated with some high-sulphidation deposits in volcanic arcs, a distinctly different volcano tectonic setting from most low sulphidation deposits.

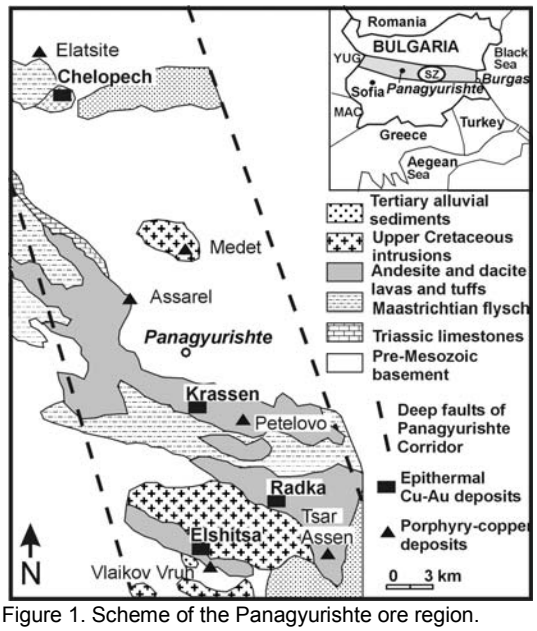

Figure 1. Scheme of the Panagyurishte ore region.

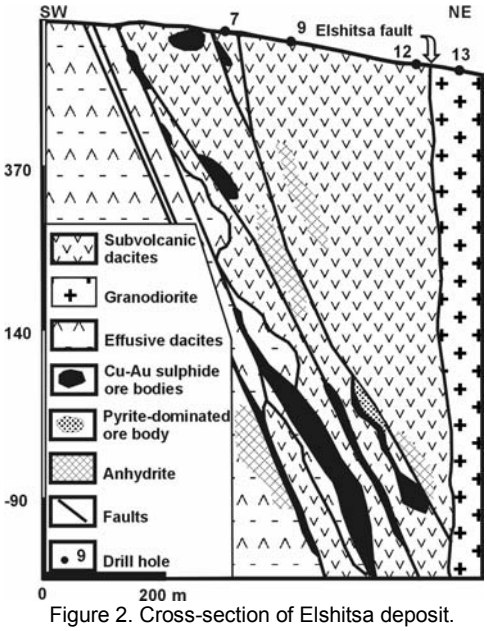

Figure 2. Cross-section of Elshitsa deposit.

2 GEOLOGICAL SETTING

The Panagyurishte ore district consists of pre- Upper Cretaceous metamorphic crystalline basement, Triassic sedimentary rocks, Turonian-Lower Senonian volcano-sedimentary rocks and Upper Senonian, Tertiary and Quaternary sedimentary rock complexes (Strashimirov & Popov 2000, Popov et al. 2003). The pre-Upper Cretaceous rocks comprise metamorphic basement of Balkanide type (two-mica gneisses, mica schists and orthoamphibolites), granites of Paleozoic age, and Triassic limestones, sandstones and dolomites (Fig. 1). The basement rocks are overlain by Upper Cretaceous rocks, subdivided into three distinct volcanic and sedimentary complexes of Turonian, Lower Senonian and Upper Senonian age. The Turonian terrigenous complex is 150 to 400 m thick and consists of breccia, conglomerates, coal-bearing slates and sandstones, lying discordantly above the older rocks.

The Upper Cretaceous (Lower Senonian) volcano-plutonic complex is composed of calc-alkaline to shoshonitic volcanic and rare sedimentary rocks and was formed in several extrusive centres. The volcano-plutonic complexes formation include: 1) volcanic; 2) plutonic; 3) sub-volcanic; and 4) dyke stages of magmatic activity. The Lower Senonian volcano-plutonic complex has a multistage and explosive character and hosts both porphyry and epithermal ores. The Upper Senonian postvolcanic sedimentary complex is represented by the Santonian-Campanian marlstones, sandstones and conglomerates as well as by the 500 to 700 m thick Campanian-Maastrichtian carbonaceous flysch. The Tertiary and Quaternary sediments consist of Paleogene conglomerates, Pliocene breccia and conglomerates, sandstones and clays; and Quaternary gravels, sands and clays covering part of the pre-Cenozoic sequence (Fig.1). Ages of the main magmatic stages using K/Ar dating are as follows: volcanic (92-87Ma), plutonic (88-82Ma), sub-volcanic (88-74Ma) and dyke (74-67Ma) (Bogdanov 1987, Lilov & Chipchakova 1999). Based on U-Pb zircon dating, Peytcheva et al. (2001, 2003) provided ages between 81.2 + 0.5/-0.7 and 86.62 ± 0.02 Ma for the Elshitsa granite and 86.11 ± 0.23 Ma for the Elshitsa subvolcanic dacites. $^{40}Ar/^{39}Ar$ amphibole age of 85.70 ± 0.35 Ma for the coarse-grained granodiorite of the Medet pluton was obtained by Handler et al.

(2002). These age dates span of about 25 m.y. suggesting that the magmatic activity was punctuated, changing character and relatively long lived.

3 THE EPITHERMAL ORE DEPOSITS

The Elshitsa ore deposit is situated close to the southern margin of the Elshitsa pluton (Fig. 1). The Elshitsa fault has a trend of 110 to 130^0, dips steeply to the NE at 75 to 85^0 (Figs. 1, 2A), and is the main ore-controlling structure where it intersects the N-NW strike-slip faults (Bogdanov, 1987). Quartz-sericite (illite±smectite) and propylitic (albite-chlorite-epidote ± calcite) styles of alteration are the most common in the andesites and dacites at Elshitsa. Adularia alterations are rarely observed, while the advanced argillic and quartz-diaspore alteration have been observed in the footwall of the massive pyrite ores (Radonova & Velinov, 1974; Strashimirov & Popov 2000). Two compositionally distinct types of ore can be recognized (Fig. 2): ores dominated by massive pyrite, and pyrite-chalcopyrite with minor galena, sphalerite and gold. The early massive pyrite ore bodies were formed in the eastern part, followed by later Cu-Au sulphide ore bodies in the central and western parts of the deposit (Fig. 2). Rare galena-sphalerite veinlets also occur, cutting the pyrite-chalcopyrite ore bodies. Lenticular and lens-like ore bodies are characteristic of the upper parts, while the sheet-like disseminated, vein and stringer ore bodies are commonly observed in the deeper parts of the deposit. The thickness of the ore bodies varies from several meters up to 50 m; the length from several meters up to 250-300 m horizontally and up to 500 m vertically. The sulphide mineralization in the inner parts of ore bodies is predominantly massive and changes gradationally from veinlet to disseminated on the periphery.

The Radka ore deposit is located within the northern part of the Elshitsa volcano-intrusive structure, 3 km S-SE of the village of Popintsi (Fig. 3A). The andesite and dacite lava flows, agglomerate and lapilli tuffs have an W-NW strike and dip 25-45^o N-NE. The effusive rocks are intersected by several sub-volcanic dacite dykes with varying thickness (Fig. 3A). The sub-vertical dyke-like granodiorite porphyry intrusion was found at depth by drilling and mining works (Fig. 3A). The E-NE, NW and NE faults played a considerable role in increasing of the permeability of the host andesite volcanic rocks. The ore bodies are distributed in a complicated V-shaped block, bordered by a group of conjugate faults (Fig. 3A).

Quartz-sericite (illite±smectite) and advanced argillic alteration affect the inner parts of the effusive rocks close to the ore bodies, while in the outer parts the propylitic alteration predominates (Radonova and Velinov, 1974). The pyrite and Cu-Au sulphide (copper-pyrite) ore bodies occur as columnar, lens-like, or pipe-like shapes. Mainly the fault zone with a W-NW direction and dip to the north controls their position. Ore shoots of massive pyrite-chalcopyrite and bornite ores with isometric or irregular shapes, diameters from 2 to 30 m and 10-50 m long in depth are characteristic for Radka. Low-grade typically veinlet-disseminated ores also occurred and were mined by open pit close to the surface. The ore bodies crosscut the bedding of the andesite and dacite tuffs and are rarely sub-parallel. According to the mineral composition, massive pyrite-dominant and Cu-Au-sulphide (pyrite-chalcopyrite, bornite-chalcopyrite-chalcocite-tennantite and galena-sphalerite-chalcopyrite) ore bodies can be recognized (Fig. 3A).

The Krassen ore deposit is located within an 80 to 100 m thick fault zone, limited by two sub-parallel fault arms trending 110 to 115^o and dipping 50 to 65^o to NE (Fig. 3B). The pyrite-enargite dominated mineralization is tectonically controlled by a series of sub-parallel zones of tectonic breccias that host the pyrite-enargite ore bodies (Fig. 3B).

The Krassen deposit represents a pipe-like tectonic breccia zone affected by intense quartz-sericite (illite±smectite) and advanced argillic quartz-kaolinite (dickite) alteration (Strashimirov & Popov 2000, Bogdanov and Popov 2003), in which individual lens-like and columnar ore bodies are located (Fig. 3B). This zone has an ellipse-like section, 300 to 100 m in length, a dip of about 50^o to NE and can be traced intermittently to a depth of 700 m. Most of the ore bodies are lenticular in shape (Fig. 3B). Pyrite, chalcopyrite, covellite and bornite are widespread, but the enargite is most abundant ore mineral in the Krassen deposit (Fig. 4D), placing the deposit firmly within the high sulphidation style of mineralization (Hedenquist et al. 1996, 2000). Enargite-chalcopyrite-bornite mineralization is dominant in the western part of the deposit. A series of massive pyrite-enargite

lenses, containing subordinate chalcopyrite and bornite, are characteristic of the central part of the deposit. Low-grade vein pyrite is common in the eastern part of Krassen deposit.

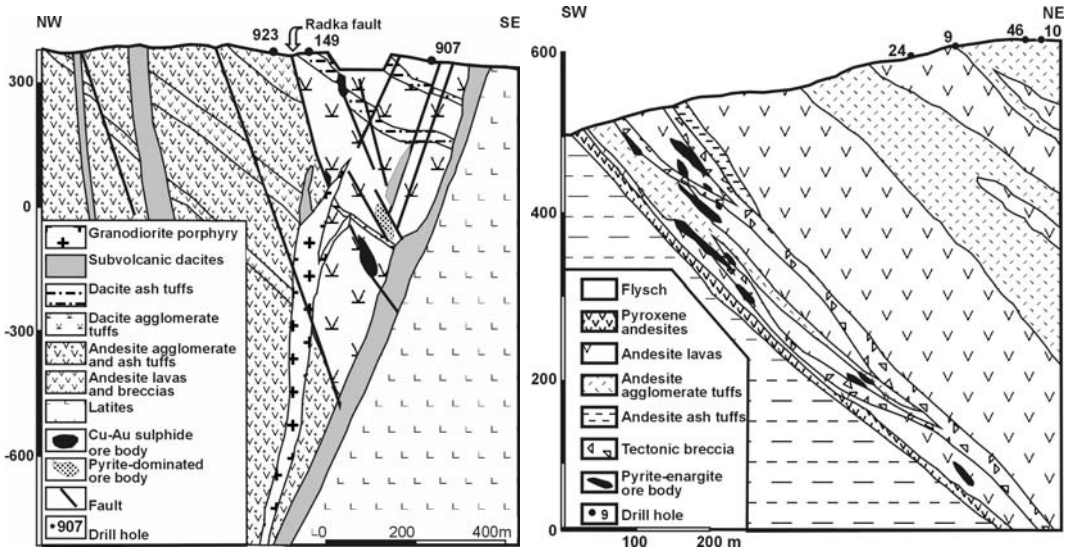

Figure 3. Cross-sections of Radka (A) and Krassen (B) Cu-Au epithermal deposits.

4 MINERAL ASSEMBLAGES

For the last 70 years the gold-bearing mineral assemblages and mineralization processes of these epithermal deposits now established in the subject of the paper have been studied by many researchers (Dimitrov 1960, Tsonev 1974, Bogdanov 1980, 1987, Bogdanov et al. 1997, Strashimirov & Popov 2000, Kouzmanov 2001, Bogdanov & Popov 2003 and many others).

The mineral assemblages of the ores at the Elshitsa, Radka and Krassen are similar and differ only by the amount of tennantite, bornite, enargite and trace minerals of Ga, Ge, In, Bi, Sn, Se and Te that are present. The ore mineralogy is dominated by pyrite and chalcopyrite (Elshitsa), pyrite, chalcopyrite and bornite (Radka) and pyrite and enargite (Krassen), which form more than 90% of the sulphide volume of the main ore bodies. The parageneses in the Elshitsa, Radka and Krassen deposits could be related to eight mineral assemblages: **Early** (1) Pyrite-quartz assemblage; **Main** (2) Chalcopyrite-pyrite; (3) Enargite-pyrite; (4) Bornite-tennantite and; (5) Galena-sphalerite-chalcopyrite; **Late** (6) Quartz-pyrite (7) Pyrite-marcasite and (8) Anhydrite-gypsum assemblages (Fig. 4, 5 and 6).

In **Elshitsa deposit** the early mineral assemblage is dominated mainly by pyrite with atoll-like, colloform and zonal textures (Fig. 4B) associated with quartz and rare 1-20μm relicts of rutile, cassiterite and titano-magnetite. The colloform pyrite contains 1 - 3 ppm Au and 0.24—1.67 wt% As (Todorov 1991, Bogdanov et al. 1997). Clastic deformation of pyrite is widespread with quartz, chalcopyrite (Fig. 4C), galena and sphalerite breccia fillings.

Except for pyrite, chalcopyrite is the dominant sulphide in the main mineral assemblages (Table 2) and occurs as massive lenses and veinlets. Tennantite-tetrahedrite mineral series, galena and sphalerite are subordinate. NAA data (Todorov 1991) indicate Au content at the range of 3.77-14.70 ppm in pyrite and 0.24-1.24 ppm in chalcopyrite. Enargite occurs as rare 5-50μm irregular shaped grains associated with pyrite, tennantite and sphalerite only in the upper horizons of Elshitsa suggesting only a local importance of the early HS fluids.

The galena-sphalerite-chalcopyrite mineral assemblage is characterized by the deposition of galena, sphalerite, pyrite, bornite, covellite and chalcopyrite, as well as tennantite-tetrahedrite series minerals. All these minerals are carriers of Au and Ag. Both tennantite and galena contains Te minerals observed as rare sub-5μm inclusions identified as stoichiometric altaite $Pb_{1.0}Te_{1.0}Se_{0.02}$ and hessite $Ag_{2.0}Te_{1.0}$. The bismuth minerals in Elshitsa are represented by Se-bearing aikinite with

composition $(Cu_{0.95}Fe_{0.01})_{0.96}Pb_{1.12}Bi_{0.90}(S_{2.91}Se_{0.10})_{3.01}$, native Bi and tetradymite, which are associated with the opaque minerals of the chalcopyrite-pyrite assemblage. There is a clear record of crosscutting and replacement relationships between the early pyrite-dominated ores and later copper-rich mineralization (Fig. 4C). Both are crosscut by the latest quartz-pyrite (Fig. 4F) and anhydrite veins.

The late mineral asssemblages consists of quartz-pyrite and anhydrite-gypsum veins crosscutting and replacing minerals assemblages from earlier stages. The widespread late quartz-pyrite assemblage is found as W-NW trending veins of milky quartz ranging from mere stringers up to 1-5 cm wide (Fig. 4F) and up to 50 m long, with {100} and {210} pyrite with up to 2-3 cm edge length. The late anhydrite-gypsum mineral assemblage is represented by anhydrite, gypsum and barite veins and lenses replacing the sulphide ore. Marcasite in assemblage with pyrite implies that the hydrothermal conditions were quite acid and lower temperature in the late mineral assemblages.

Native gold has been found in all eight mineral assemblages, but it is most abundant in galena-sphalerite-chalcopyrite assemblage, where it occurs as microscopic flattened, elongate, or irregular single grains that rare exceed 0.2 mm in size (Bogdanov et al. 1997).

The early pyrite assemblage in **Radka deposit** is represented mainly by colloform-textured pyrite, containing 0.80 - 4.17 ppm Au as indicated by NAA data (Todorov, 1991), due to dispersed particles of sub-microscopic gold. Chalcopyrite, bornite, covellite and tennantite-tetrahedrite are dominant minerals in the main assemblages and occur as intergrown massive aggregates, commonly containing 10-80 μm blebs of goldfieldite that seems to be the main Te carrier. As an important gold carrier bornite typically contains 8.10 - 41.80 ppm Au as indicated by NAA data of Todorov (1991). Enargite is rare and occurs only in the upper levels at Radka. Exotic rare Ga, Ge, In and Sn minerals occur as 1-10 μm inclusions within bornite, tennantite, galena and sphalerite, and as a rule accompany elevated Au concentrations in the HS-epithermal ores. Microanalytical data confirmed the following trace minerals: roquesite $(Cu_{1.11}Zn_{0.05}Fe_{0.01})_{1.17}In_{1.0}S_{2.08}$, gallite $Cu_{0.99}(Ga_{0.85}Fe_{0.09}Zn_{0.08})_{1.02}S_{2.00}$, germanite $(Cu_{22.32}Zn_{2.72}Fe_{1.52})_{26.56}(Ge_{4.64}As_{0.52})_{5.16}S_{31.64}$, briartite $Cu_{1.98}(Zn_{0.68}Fe_{0.38})_{1.06}(Ge_{1.01}As_{0.01})_{1.02}S_{3.96}$, renierite $Cu_{9.94}(Fe_{3.67}Zn_{0.40})_{4.07}(Ge_{1.87}As_{0.13})_{2.00}S_{15.99}$. Micron-sized inclusions of Sn minerals such as vinciennite $Cu_{10.16}Fe_{3.90}Sn_{1.00}As_{0.94}S_{15.98}$, stannite $Cu_{2.02}Fe_{1.05}Sn_{1.0}S_{4.11}$, kesterite $Cu_{2.05}(Zn_{0.74}Fe_{0.19})_{0.93}Sn_{0.93}S_{4.06}$, kiddcreekite $Cu_{6.01}Sn_{1.00}W_{1.00}S_{7.98}$, and buckhornite $Au_{0.77}Pb_{1.92}(Bi_{0.60}Fe_{0.47})_{1.07}Te_{1.92}S_{3.33}$ that have been identified in the bornite-tennantite and the galena–sphalerite-chalcopyrite assemblages, suggest a close link between epithermal and porphyry environment.

Bismuth minerals in Radka are represented by 5-10 μm lamellar inclusions of aikinite-bismuthinite series in addition to wittichenite (Bogdanov et al. 1997, Kouzmanov 2001, Bogdanov & Popov 2003) and the rare Bi-telluride, tsumoite $Bi_{1.0}Cu_{0.03}Te_{1.06}$, found in association with the minerals of the chalcopyrite-pyrite assemblage. Bi minerals are locally abundant and associated with gold and chalcopyrite, often indicating Au-enrichment.

The late assemblages consist of quartz-pyrite and anhydrite gypsum veins, which crosscut and replace minerals from the earlier mineralization stages. The anhydrite veins and lenses are abundant in the deeper horizons of Radka deposit while gypsum is more common at upper levels.

Native gold (Fig. 4E) is more abundant in the enargite-pyrite, bornite-tennantite and galena-sphalerite-chalcopyrite assemblages. The gold is 0.1-100 μm in size and commonly associated with bornite, tennantite, chalcopyrite, sphalerite and galena. Macroscopic (>100 μm) gold and electrum grains and aggregates of gold up to 5 mm are rarely found in the bornite-tennantite-chalcocite oresin Radka deposit (Fig. 4G). Electrum and gold occur as blebs or irregular particles in the sulphide minerals, or along grain boundaries. The elongate, isometric and ellipse-like gold grains are most commonly found in assemblages with enargite, bornite, tennantite, chalcopyrite, galena and chalcocite. Anhedral and sharp-edged gold grains, or short veinlets are also present in some cases. Native silver was found in wiry forms (Fig. 4H), as thin native silver veinlets, not exceeding 0.5 mm in width and up to 5 cm in length and as irregular inclusions in bornite. In Radka, the silver is Hg bearing. The gold grade in the primary ore is 1-3 g/t, rarely up to 8-10 g/t, and has been extracted as a by-product from both the pyrite and copper concentrates.

The ore mineralization in **Krassen deposit** is comparable to Radka, but enargite is much more abundant and characteristic (Fig. 4D) for individual orebodies at Krassen. The early assemblage is represented mainly by colloform-textured pyrite with up to 16.10 ppm Au (Todorov 1991), which

Early *assemblage Minerals*	*Pyrite-quartz*
Quartz	▬■■■---------
Cassiterite	-
Ti-magnetite	--
Rutile	-
Anatase	-
Pyrite	■■■■■--------
Gold	▬

Main *assem-blages Minerals*	*Chalcopyrite - pyrite*	*Enargite-pyrite*
Quartz	▬■■■■	▬▬▬---
Pyrite	■■■■■-------	■■■■▬
Gold	▬▬	▬▬▬
Electrum	▬	▬▬----
Chalcopyrite	■■■■■■■----	■■▬---
Enargite	-	--■-
Luzonite	-	▬
Wittichenite	-	
Emplectite	-	
Friedrichite	-	
Hammarite	-	
Aikinite	-	
Tetradymite	-	
Buckhornite	-	
Tsumoite	-	
Bismuth	-	
Micharaite	-	
Tennantite		-- ▬------

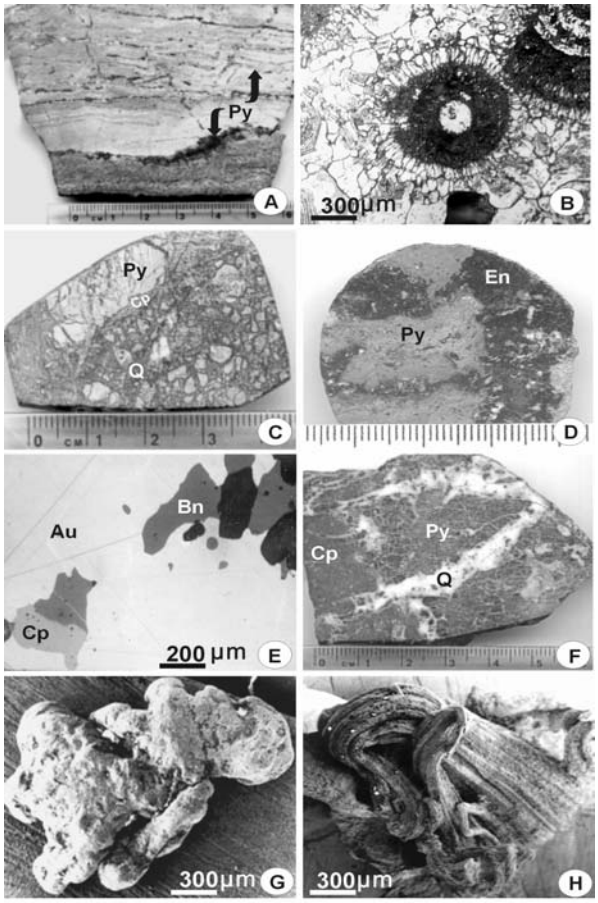

Figure 4. Early and main mineral assemblages: A- dacite tuff from Krassen with pyrite (Py) lamination (scale in cm); B- zonal texture of colloform pyrite (Early pyrite-quartz assemblage) from Elshitsa deposit; C -pyrite (Py) breccia replaced and crosscutted by chalcopyrite (Cp) and quartz (Q) from the chalcopyrite-pyrite assemblage; D- Early pyrite (Py) replaced by enargite (En) from Krassen deposit (scale in cm); E- gold (Au) in assemblage with bornite (Bn) and chalcopyrite (Cp), Radka deposit; F- early pyrite (Py) and (Cp) chalcopyrite chalcopyrite-pyrite assemblage) crosscutted and replaced by the late vein quartz (Q), (scale in cm); G -gold extracted from bornite-chalcopyrite ore, Radka deposit, SEM; H - native silver from Radka deposit, SEM.

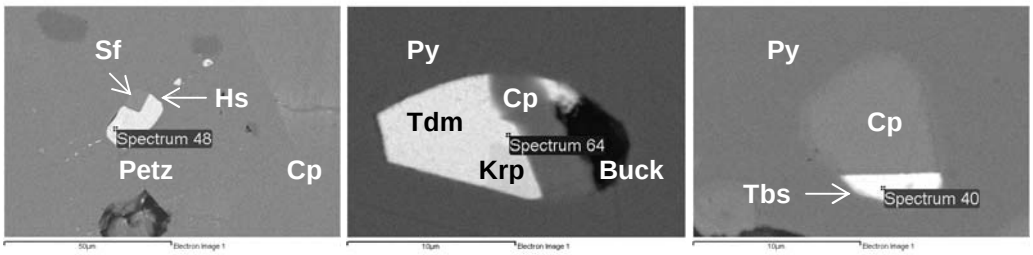

Figure 5. Trace minerals in Radka Cu-Au epithermal deposit (Hs-hessite; Petz-petzite; Tdm-tetradymite; Krp-krupkaite; Buck-buckhornite; Tbs-tellurobismutite).

occurs as anhedral disseminations and aggregates. Enargite $Cu_{3.14}(As_{1.0}Sb_{0.02})_{1.02}(S_{3.71}Se_{0.01})_{3.72}$ is very abundant and is observed replacing the early pyrite, or in association with chalcopyrite, bornite and chalcocite in the main mineral assemblages (Fig. 6). The enargite-rich ore bodies are also gold rich with grades up to 6-8 g/t. Aikinite with close to the stoichiometric composition

Main *assemblages Minerals*	*Bornite-tennantite*	*Galena-sphalerite-chalcopyrite*	***Late*** *assemblages Minerals*	*Quartz-pyrite*	*Pyrite-marcasite*	*Anhydrite-gypsum*
Quartz	▬▬▬	▬▬▬	Quartz	■■■■■	▬▬▬	-
Pyrite	▬■■■▬	▬■■■	Pyrite	■■■■■	▬■■■	----
Gold	▬■■■▬	▬▬■▬	Gold			
Electrum	▬▬▬	▬■■▬	Electrum	-	-	--
Chalcopyrite	▬■■■	----■■■▬	Chalcopyrite			---
Enargite			Sphalerite			--
Tennantite	■■■■■■	--	Galena			--
Bornite	■■■■■■		Silver			---
Idaite	-		Marcasite		■■▬	
Renierite	-		Calcite			▬
Germanite	-		Barite			■▬
Vinciennite	-		Anhydrite			■■■■■■
Stannite	-		Gypsum			■■■■■■
Briartite	-		Mordenite			--
Kesterite	-		Heulandite			--
Colusite	-		Laumontite			--
Digenite	-		Stilbite			--
Goldfieldite	----					
Chalcocite	-▬■■■----					
Tellurium	-					
Altaite	-					
Sulvanite	-					
As-sulvanite	-					
Tetrahedrite	-	-▬---				
Gallite		-				
Roquesite		--				
Sphalerite	----	--▬■■■▬				
Galena	----	▬■■■▬				
Silver	---	-▬-				
Betekhtinite		-				
Petzite		-				
Hessite		-				
Covellite		---■■▬				

Figure 6. Main and late mineral assemblages.

$Cu_{1.0}(Pb_{1.04}Ag_{0.01})_{1.05}(Bi_{1.04}As_{0.03})_{1.07}S_{3.08}$ was identified as sub 10 μm lamellar inclusions in chalcopyrite and seems to be the most common Bi phase in the all three deposits. Late quartz-pyrite vein assemblage in Krassen is not as abundant as compared to the Radka and Elshitsa deposits.

Gold in the early massive pyrite in Elshitsa, Radka and Krassen is sub-microscopic in size (< 0.1 μm) i.e., so-called “invisible” gold (Bogdanov et al. 1997). The deformation and recrystallization of the ore bodies and overprinting of the early sulphide assemblages by later stages caused Au and Ag migration to cracks and grain boundaries of the sulphide minerals. As a result of these processes, the native gold and electrum grain size increases from sub-microscopic (< 0.1 μm) in the early colloform pyrite to microscopic (0.1-100 μm) and macroscopic (>100 μm) in the late gold-sulphide assemblages (Bogdanov et al. 1997). The electrum fineness in individual grains varies between 764 and 998, as estimated by 126 microprobe analyses, characteristic for the epithermal class of mineral deposits (Morrison et al. 1991). Cu, Te, Sb and Bi are the most common trace elements in gold and electrum in Elshitsa, Radka and Krassen. Massive pyrite and pyrite- veinlet and disseminated ore bodies are poor in gold and other precious metals, as compared to the ore bodies with more complex mineral compositions. The latter are rich in enargite, chalcopyrite, chalcocite and bornite, and are also important Ga, Ge, Se and Te carriers.

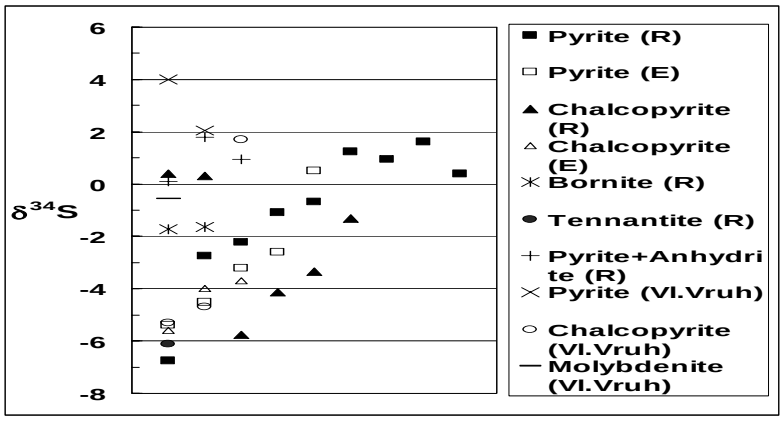

Figure 7. Sulphur isotope ratios in Radka (R) and Elshitsa (E) epithermal deposits and Vlaikov Vruh porphyry-copper deposit (data by Angelkov 1974, Velinov et al. 1978, Kouzmanov 2001).

5 ORE GENESIS

The Cu-Au sulphide ores are considered to be of hydrothermal and replacement origin (Dimitrov 1960, Tsonev 1974, Bogdanov 1984, 1987, Bogdanov et al. 1997, Kouzmanov 2001, Bogdanov and Popov 2003). They formed later than the pyrite bodies following intrusion of the sub-volcanic rhyodacites, replacing the volcanic dacites, andesites and the associated pyroclastites and rhyodacite dykes. The late quartz-pyrite vein (Fig. 4F) and anhydrite-gypsum mineral assemblages are characteristic for the Elshitsa, Radka and Krassen as well as for the closely associated porphyry copper deposits (Fig. 1) suggesting a common source and close link between the individual porphyry and epithermal systems.

Based on existing data, the formation of the Cu-Au epithermal deposits could be integrated into a single broad event of contemporaneous formation of epithermal and porphyry systems related to and surrounding magmatic centres, including: 1. Formation of early massive pyrite ores towards the end of the dacite volcanism. 2. Contemporaneous formation of the epithermal Cu-Au mineralization in the upper parts of the epithermal-porphyry systems. 3. Formation of the late quartz-pyrite and anhydrite veins characteristic of both epithermal (Elshitsa, Radka and Krassen) and porphyry-copper (Vlaikov Vruh, Tsar Assen, Petelovo) deposits (Fig. 1).

According to fluid inclusion studies (Bogdanov 1987, Strashimirov et al. 2002, Kouzmanov 2001, Tarkian et al. 2003) there is evidence for high salinity (28-64% NaCl eq) and low salinity (2-6% NaCl eq) fluids being present over the life of the hydrothermal systems. Hot (325-379 ^{o}C) and saline fluid (up to 64% NaCl eq) is characteristic of the porphyry environment in the Panagyurishte district. In contrast, liquid-rich, medium to high temperature (260-310^{o}C) and more dilute (4.7-5.9% NaCl eq) fluid that is typical of the Radka, Krassen and Elshitsa epithermal systems, transported considerable amounts of Cu, As, Fe and Au. The successive hydrothermal phases of the discrete evolving volcano-plutonic systems precipitated chalcopyrite and the high sulphidation ore assemblage consisting of enargite, chalcocite and gold minerals in the Krassen deposit. Rare remnants of enargite, indicative of localized high-sulphidation conditions are preserved in the Elshitsa intermediate-sulphidation epithermal system, whereas Radka represents a transitional epithermal system with an intermediate to local high sulphidation style of ore mineralization. Enargite in the leached residual quartz zones is more abundant here compared to Elshitsa. Anhydrite veins formed as temperature waned in the late stages of three systems.

Recrystallization of the sulphide minerals suggest tectonic and hydrothermal ore remobilisation during the evolution of epithermal and porphyry systems in accordance with the similar δ^{34}S values for the main sulphide minerals (Fig. 7) in Radka (δ^{34}S =-6.7 to -1.8) and Elshitsa (δ^{34}S =-5.6 to +0.5) epithermal deposits and for Vlaikov Vruh (δ^{34}S =-5.3 to +4.0) porphyry copper deposit, indicating a magmatic source for sulphur. Comparison of the Pb isotope values of the main sulphide minerals (^{206}Pb/^{204}Pb=18.49-18.76; ^{207}Pb/^{204}Pb=15.61-15.64; ^{208}Pb/^{204}Pb=38.53-38.80) from Elshitsa, Radka

and Vlaikov Vruh deposits with those of the Elshitsa granite ($^{206}Pb/^{204}Pb$=18.56-18.57; $^{207}Pb/^{204}Pb$=15.63-15.65; $^{208}Pb/^{204}Pb$=38.60-38.66) and the porphyry granodiorite of Vlaikov Vruh ($^{206}Pb/^{204}Pb$=18.61-18.77; $^{207}Pb/^{204}Pb$=15.62-15.66; $^{208}Pb/^{204}Pb$=38.61-38.82) suggest that the latter two were sources of the metals (Amov et al. 1974, Kouzmanov 2001). The $^{87}Sr/^{86}Sr$ ratios of anhydrite, gypsum, barite and calcite from Radka and Elshitsa epithermal deposits and Vlaikov Vruh porphyry copper deposit reported by Kouzmanov (2001) are between 0.7058 and 0.7072, suggesting some mixing of strontium from the dacitic host rocks ($^{87}Sr/^{86}Sr$=0.7058-0.7061) and ^{87}Sr enriched basement rocks ($^{87}Sr/^{86}Sr$=0.7085-0.7154).

Andesite-dominated magmatic activity in the Panagyurishte structural corridor (Fig. 1) has a life span from Turonian to Maastrichtian that is about 25 Ma, while the formation of the porphyry-epithermal systems of Elshitsa-Vlaikov Vruh, Radka-Tsar Assen, and Krassen-Petelovo (Fig. 1) appears limited to a narrower time interval of 1-5 m.y. (Lilov and Chipchakova 1999, Peytcheva et al. 2001, 2003). The recent Re-Os dating of molybdenite (82.1 ± 0.6 Ma) from Vlaikov Vruh (Kouzmanov 2001) and U-Pb zircon data (81.2 + 0.5/-0.7 Ma and 82.3 ±0.5 Ma) for the Elshitsa granite (Peytcheva et al. 2003) indicate a possible narrow interval of formation for the linked epithermal and porphyry deposits.

6 CONCLUSIONS

Epithermal deposits of intermediate (Elshitsa) and intermediate to local high (Radka, Krassen) sulphidation style of ores and porphyry copper deposits evolved in close proximity within three individual volcano-plutonic centers (Elshitsa-Vlaikov Vruh, Radka-Tsar Assen, and Krassen-Petelovo). The close connection between the andesite-granodiorite volcano-plutonic structures facilitates the multistage and polycyclic character of their hydrothermal systems. The similar character of the epithermal ores and the mineral assemblages in Elshitsa, Radka and Krassen deposits and their discrete trace mineralogy reflects the varying fS_2/fO_2 states in the individual epithermal deposits, depending on their depth of formation, level of erosion and the link to the porphyry environment.

The Bi-Se-Te and Ga-Ge-In signature with pronounced Au enrichment is a characteristic feature for IS and HS ore environment in the southern part of the Panagyurishte ore district suggesting a comparable sources for the epithermal mineralizing fluids.

Bi minerals often occur in close association with gold and chalcopyrite, giving the assemblage significance as potential guide to Au-rich environment. The aikinite derivates are most widespread and persistent minerals in the chalcopyrite-pyrite assemblage and also characteristic for the more deeply eroded hydrothermal systems (Elshitsa).

Se and Te enrichment is characteristic and most abundant in the main mineral assemblages and have greatest affinity to shallower transitional IS to HS type of epithermal systems (Radka, Krassen). The Bi dominant trace mineralogy is characteristic for the ABCD belt (Cook et al., 2002) and reflects, in particular in the southern part of the Panagyurishte ore district the, IS to HS type of epithermal environment, suggesting shared magma sources and convergence of the processes in the porphyry-epithermal systems.

As a result of the complex multistage and punctuated hydrothermal process the epithermal deposits of Elshitsa, Radka and Krassen contain Au and Ag in various proportions, but also rare Ge, Ga, In, Bi, Se, Te, Sn, V and W bearing minerals. The ore remobilization processes facilitate formation of a specific, narrow range of Se, Te, Ga, Ge and In minerals in the bornite-tennantite and galena-sphalerite-chalcopyrite assemblages in Radka and Krassen epithermal deposits, and corresponds to the increasing role of the fS_2/fO_2 control during the transition from IS to HS environment.

REFERENCES

Amov B., Bogdanov B. & Baldjieva T. 1974. Lead isotope composition and some features concerning the genesis and the age of the ore deposits in south Bulgaria. In: Problems of Ore Deposition, Proc 4th IAGOD Symp., vol. 2, 13-25 (in Russian).

Angelkov K. 1974. Ore formation and sulphur isotope composition of the deposits in Panagyurishte ore region (in Russian). In: Problems of Ore Deposition, Proc. 4th IAGOD Symp., 2, 26-33.

Bogdanov B. 1980. Massive sulphide and porphyry-copper deposits in the Panagyurishte district Bulgaria. In: European Copper Deposits. SGA Spec. Publ., 1, 50-58.

Bogdanov B. 1984. Hydrothermal systems of massive sulphide, porphyry-copper and vein copper deposits of Sredna Gora zone in Bulgaria. Proc. 6th IAGOD Symp., Stuttgart. 63-67.
Bogdanov B. 1987, The copper deposits in Bulgaria. Technika publ, Sofia. 388p. (in Bulgarian).
Bogdanov K., Tsonev D. & Kuzmanov K. 1997. Mineralogy of gold in the Elshitsa massive sulphide deposit, Sredna Gora zone, Bulgaria. Mineral. Deposita, 32. 219-229.
Bogdanov K. & Popov K. 2003. Cu-Au epithermal systems in the southern part of Panagyurishte ore region. Soc. Econ. Geol. Guidebook Series, Vol. 36, 91-114.
Cook N.J., Ciobanu C.L. & Bogdanov K. 2002. Trace mineralogy of the Upper Cretaceous Banatitic Magmatic and Metallogenic belt, S.E. Europe, 11th IAGOD Symp Geocongr 2002. CD vol. of ex. Abst., Geol. Surv. Namibia.
Dabovski C., Harkovska A., Kamenov B., Mavrudchiev B., Stanisheva-Vassileva G. & Yanev Y. 1991. A geodynamic model of Alpine magmatism in Bulgaria. Geol. Balc., 21, 4, 3-15.
Dimitrov C. 1960. Magmatismus und Erzbildung im Erzgebeit von Panagjuriste. Freib. Forschung. C79.
Handler R., Velichkova S., Neubauer F. & Ivanov Z. 2002. Late Cretaceous magmatic and tectonic processes in the Srednogorie zone, Bulgaria: constraints from $^{40}Ar/^{39}Ar$ age dating results. GEODE Workshop on Srednogorie. Sofia, April 2002, Abstr. 7.
Hedenquist J.W., Izawa E., Arribas A. & White N.C. 1996. Epithermal gold deposits: Styles, characteristics, and exploration. Resource Geol Spec Publ No 1, poster and booklet. 17p.
Hedenquist J.W, Arribas A.R. & Gonzalez-Urien E. 2000. Exploration for Epithermal Gold Deposits. In: Rev. in Econ. Geol., Hagemann S.G. & Brown P.E. eds, Vol. 13, Gold in 2000, 560p.
Heinrich C.A. & Neubauer F. 2002. Cu - Au - Pb - Zn - Ag metallogeny of the Alpine - Balkan - Carpathian - Dinaride geodynamic province. Mineral. Deposita, 37, 533-540.
Jankovic S. 1977. The copper deposits and geotectonic setting of the Tethyan-Eurasian metallogenic belt. Mineral. Deposita, 12, 37-47.
Kouzmanov K. 2001. Genese des concentrations et metaux de base et precieux de Radka et Elshitsa (zone de Sredna Gora, Bulgare): une approche par l'etude mineralogique, isotopique et des inclusions fluids. Ph.D. Thesis, Univ. of Orleans, 437p.
Lilov P. & Chipchakova S. 1999. K-Ar dating of the Upper Cretaceous magmatic rocks and hydrothermal metasomatic rocks from the Central Srednogorie. Geochem. Mineral. Petrol. 36, 71-91 (in Bulgarian).
Morrison G.W., Rose W.J. & Jaireth S. 1991. Geological and geochemical controls on the silver content (fineness) of gold in gold-silver deposits. Ore Geol. Rev., 6, 333-364.
Peycheva I., Von Quadt A., Kamenov B., Ivanov Zh. & Georgiev N. 2001. New isotope data for Upper Cretaceous magma emplacement in the southern and south-western parts of Central Srednogorie. ABCD-GEODE 2001 workshop, Vata Bai, Romania, Abs., Rom. J. Mineral. Depos. 79, Supl. 2, 82-83.
Peycheva I., Von Quadt A., Kouzmanov K. & Bogdanov K. 2003. Timing of magmatism and mineralisation in Elshitsa and Vlaykov Vrh Cu(Au) deposits of Central Srednogorie, Bulgaria: constraints from U-Pb zircon and rutile geochronology and Hf-zircon and Sr whole-rock tracing. ABCD-GEODE 2003 workshop, Seggauberg, Austria, Abs., 46.
Popov P., Strashimirov S. & Popov K. 2000. Geology and metallogeny of the Srednogorie zone and Panagyurishte ore region. Soc. Econ. Geol. Guidebook Series, Vol.36, 7-25
Radonova T. & Velinov I. 1974. Relationships between propylites and secondary quartzites with the ore mineralizations in the Central and Western Srednogorie (Bulgaria). In: Metasomatism and Ore Formation, Nauka, Moscow, 60-69. (in Russian).
Sillitoe R.H. 1999. VMS and porphyry copper deposits: Products of discrete tectono-magmatic settings. In: Mineral Deposits: Process to Processing, Stanley, C.J. et al. eds. Balkema, Rotterdam, 7-10.
Sillitoe R.H., Hannington M.D., Thompson J.F.H. 1996. High sulphidation deposits in the volcanogenic massive sulphide environment. Econ. Geol. 91, 204-212
Strashimirov. S. & Popov P. 2000. Geology and metallogeny of the Panagyurishte ore region (Srednogorie zone, Bulgaria). GEODE 2000 Workshop, Guide to excursions A and C, Sofia, 50p.
Strashimirov S., Petrunov R. & Kanazirski M. 2002. Porphyry-copper mineralisation in the central Srednogorie zone, Bulgaria. Mineral. Deposita, 37, 587-598.
Tarkian M., Hünken U., Tokmakchieva M. & Bogdanov K. 2003. Precious-metal distribution and fluid-inclusion petrography of the Elatsite porphyry copper deposit, Bulgaria. Minera. Deposita, 38, 261-281.
Todorov T. 1991. NAA analysis of gold in minerals from Upper Cretaceous massive copper deposits in Bulgaria. Terra Nova, 3, 311-316.
Tsonev D. 1974. Evolution of the mineral parageneses in the Radka and Elshitsa cupriferous-pyritic deposits, Panagyurishte ore district, Bulgaria. In: Bogdanov (ed) Problems of Ore Deposition, Proc. 4th IAGOD Symp, v. 2, 327-333.
Velinov I., Loginov V., Nosik L., Radonova T. & Rusinov V. 1978. Genetical features of the massive sulphide deposits from the Srednogorie zone of Bulgaria and Jugoslavia. In: Metasomatism and Ore Deposition. Nauka, Moscow, 176-183. (in Russian).

PLATE TECTONIC ASPECTS OF THE ALPINE METALLOGENY IN THE CARPATHO-BALKAN REGION
PROCEEDINGS OF THE ANNUAL MEETING - SOFIA, 1996
UNESCO - IGCP Project No 356
Volume 2, pp. 75-80

METALLOGENY OF THE SPAHIEVO ORE FIELD, SE BULGARIA

V.Georgiev, O.Malinov, P.Milovanov, L.Nikova

Geology & Geophysics Co, 23 Sitniakovo blv., 1505 Sofia

The Spahievo ore field is located in the NE part of the Rhodope massif. The Precambrian basement is overlain by Priabonian sediments, cross cutted or overlained by Eocene to Oligocene volcanic rocks.

The origin of the ore mineralizations in the Spahievo ore and their connection with the magmatism have been a subject of numerous investigations. Boyanov et al. (1960, unpublished data) proposed a genetic relationship between the Sumica monzonitoid intrusion and the base metal mineralisations.

According to Ivanov et al. (1971, unpublished data) the lead-zinc ores were deposited after the quartz-trachyrhyolite dike formation. Radonova (1973) and Maneva (1976) assumed, that the ore-forming folowed the "felsitic" rhyolites.

Dimitrov et al. (1987, unpublished data) identified two mineral types. Both quartz-base metal and carbonate-base metal types are related to the andesitic volcanism. Both quartz-gold-base metal and quartz-molibdenum types are in association with the latite volcanism.

Georgiev et al. (1993, unpublished data) suggested a relationship between the molybdenum mineralization and the monzonitoid intrusions, while the base metal-Bi-Au-Ag mineralisations are connected with the rhyolite-trachyrhyolite magmatism.

The opinions on the time of secondary formation of quartzites and their connection with the lead-zinc deposits are also contradictory. Radonova (1972) considered the secondary quartzites as a product of the fumarole-solfatara activity of the Priabonian andesitic volcanism. The wall-rock metasomatites of the lead-zinc mineralization was referred as later. Ivanov et al. (1971, unpublished data) connected the secondary quartzites with the lead-zinc ores.

Kounov (1994) regarded the lead-zinc manifestations as accompanying the andesitic and latitic volcanism but the overlapping continued after the rhyolite dyke formations.

During the Upper Eocene, the Koletz magmatic complex appeared. It mainly consists of potassic andesites, which built up the Koletz palaeo volcano. In the core of this volcano the Karaman diorite-monzodiorite body was intruded. We can observe the Ivorovo palaeo volcano in the SW part of the ore field. It consists of the products of the Voinovo magmatic complex, composed of latiandesites, shoshonites and absarokites.

At the end of the Upper Eocene and the beginning of the Lower Oligocene, the center of the magmatism was displased to the north. The Dragoinovo palaeo volcano appeared, built up of potassic andesites, latitandesites and shoshonites (the Bukovo and Dragoinovo complexes). At the end of this stage the Samitza monzonitoid body was intruded.

During the Lower and the Upper Eocene an intensive acid volcanic activity occured. First, the Borovitza complex (rhyolite tuffs) and Panichkovo complex (rhyolite tuffs, ignimbrites, rhyolites and trachyrhyolites) appeared. They built up the Borovitza volcano-tectonic depression (Ivanov,1972). Volcanic necks, bodies and dykes of these rocks can be also observed outside the depression. The Gradishte magmatic complex built up several extrusions of trachyrhyolites. The Tri mogili complex consisted of various volcanics and built up rhyolitic, rhyodacitic, shoshonitic and latitic dykes. The volcanic activity finished with the Bragovo magmatic complex (rhyolitic tuffs, bodies and flows. The sediments of the Dragoinovo (Oligocene-Miocene) and the Akhmatovo (Neogene) units overlay the volcanic rocks.

The important structures in the region are the E-NE Bukovo and Mechkovetz fault zones. They controll the location of the volcanic centres, the emplacement of the monzonitoid intrusion and the localisation of the ore mineralizations (fig.1).

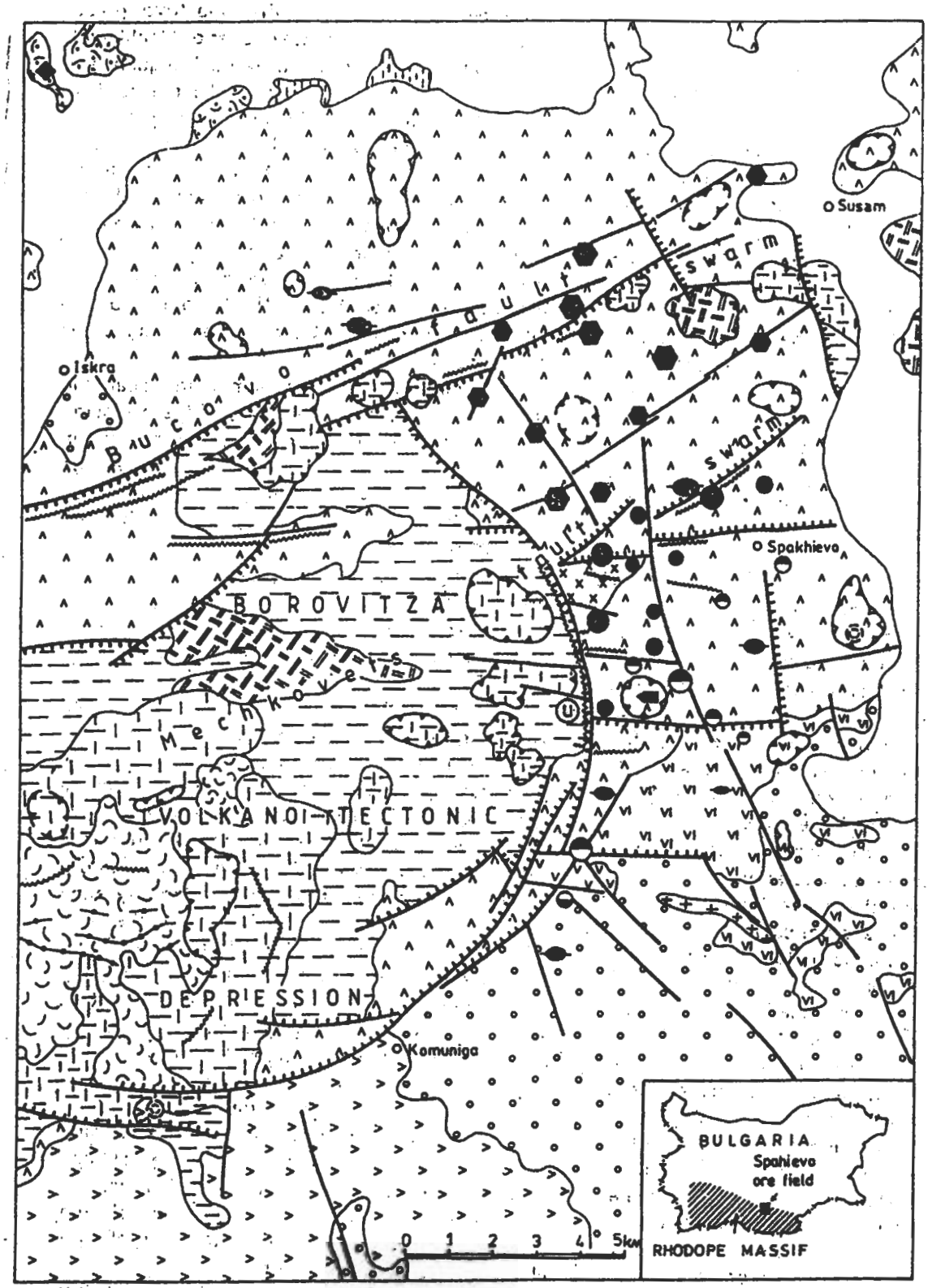

Fig. 1. Metallogenic map of the Spahievo ore field.

1. Akhmatovo unute (N_2-Q_1); 2. Dragoinovo unit (Pg_3^2- N_1); 3. Briagovo complex (Pg_3^1)- rhyolites and rhyolite tuffs. 4. Tri mogili complex (Pg_3^2)- dykes of rhyolites, rhyodacites, shoshonites and latites; 5. Gradishte complex (Pg_3^2)-extrusions and subvolcanic bodies of rhyodacites; 6. Panichkovo complex (Pg_3^2)- tuffs (a), flows and subvolcanic bodies (b) and dykes (c) of rhyolites and trachyrhyolites; 7. Borovitza complex (Pg_3^2)- rhyolite tuffs; 8. Bukovo and Dragoinovo complexes (Pg_3^2)- flows and subvolcanic bodies of latites (a) and monzonitoid intrusion (b); 9. Voinovo complex (Pg_3^2)- latite-andesites, shoshonites, absarokites; 10. Koletz complex (Pg2)- flows and subvolcanic bodies of potassic andesites (a) and monzodiorite intrusion (b); 11. Priabonian sediments; 12. faults (a) and normal faults; 13-14. Volcanic centres (necks, extrusions, diatremes) of acid (13) and intermediate (14) composition; 15-23. Deposits and occurrences of the corresponding mineral types: 15-silica-phosphatic, 16- uranium-base-metal, 17- quartz-adularia-gold-base-metal, 18-20- quartz-base-metal: 18-Q-lead- zinc subtype, 19- carbonate subtype, 20-molybdenum subtype, 21- molybdenum- base-metal type, 22- alunite type, 23- base-metal type.

According to the gravity data these structures also appeared as more regional intensive gravity gradients, interpreted as fault zones of vertical displacements of the metamorphic basement. Local magnetic maxima, aligned in NE to ENE direction outline the position of andesitic volcanic centres. High potassium and uranium airborne gamma-ray spectrometry anomalies trended to NE reflect the presence of a hydrothermal alteration, controlled by the faults (fig.2).

E-W and NW faults predominated in the southern part of the ore field. These faults characterized by linear local gravity maxima , are interpreted as related to the linear diorite-gabbro-diorite intrusions partly exposed on the surface.

The products of the Koletz palaeo volcano lack in known ore mineralizations.

The presence of quartz-sericite-pyrite alterations with a weak base-metal mineralization is observed, related to the rocks of the Iavorovo palaeo volcano (the Sokolite indications). The type of the mineralized zones and the level of erosion of the volcanic edifice, suggest the presence of a concealed hydrothermal ore bearing system.

The same mineralization is also observed in association with the early manifestations of the Dragoinovo palaeo volcano- the Bukovo complex (Hasara indication).

Intensive silicifications, argillic and propylitic alterations are associated with the final stage of the Dragoinovo palaeo volcano (Kunov,1994). These alterations are considered to be the element of the post volcanic fumarole-solfatara activity. Deposits of alunites are connected with them. The relationship between the silica bodies and the other ore mineralizations is not clear.

A molybdenum-base-metal ore-magmatic system is formed in connection with the monzonitoid intrusion, emplaced in the central parts of the Dragoinovo palaeo volcano. In the apical parts of the intrusion, a molybdenum stockwork type mineralization appeared. Above it a vein type of quartz-specularite-chalcopyrite-bismuth mineralization, followed by quartz-lead-zinc mineralization is observed. At the uppermost part of the system a quartz-carbonate mineralization occured (fig.3). The molybdenum-base metal ore-magmatic system is exclusively well presented in Briastovo ore deposit and partly in Dimitrova Chuka occurrence.

The monzonitoid intrusion is characterised by a large gravity minimum and a magnetic maximum (fig.2). A 2D inversion of the gravity data shows that the body can be extended to the north of the outcrop. Intensive thorium and uranium gamma-ray spectrometry , as well as IP and resistivity anomalies reflected the presence of a porphyry system under the outcropping latites (fig.2).

After the emplacement of the monzonitoid intrusion and the location of the molybdenum-base-metal mineralization, the Briastovo graben appeared between the Bukovo and Mechkovetz fault zones. Here, the entire vertical sequence of the ore-magmatic system exists. To the north of the Bukovo fault zone the system is preserved partly and to the south it is almost entirely eroded.

There is a connection between the quartz-base-metal type of mineralization and the Panichkovo rhyolite-trachyrhyolite magmatic complex . This mineralization has the basic economic importance in the ore field. We can find it such deposits as: Sazhe, North contact of the intrusion, Mezarlaka, Gabrovo and numerous occurrences.

The mineralization is predominantly located in the central and the southern part of the ore field . The quartz-lead-zinc mineral type is presented in the central parts. To the S-SE the role of the carbonate type is predominant. In the most southern part of the ore field a low temperature molybdenum mineral type appeared (the Kul dere occurrence). This horizontal zonality pattern is probably an element of a cupola zoning. In the central parts of the ore field the role of the copper mineralization increases with the depth (Ivanov et al.,1987)

A paragenetic association exists between the Gradishte trachyrhyodacite complex and the quartz-adularia-gold-base-metal ore formation. It is superimposed on the quartz-base-metal mineralization. This formation is a predominant at the periphery and at the upper part of the ore field. High potassium anomalies from the airborn gamma-ray spectrometry reflected the presence of the adularia alterations. The anomalies are aligned in the NE to ENE direction and are probably connected with the Bukovo and the Mechkovetz fault zones. In the southern part of the ore field the high potassium anomalies have a WNW direction and they coinside with the strike of the main ore veins. These anomalies can be used as an exploration guide for the near-surface quartz-adularia alterations. Some of the thorium anomalies in the northern part of the ore field can be used as the indication of adularia alterations in the greater depth. The linear trend of the anomalies suggest a tectonic control on alterations and mineralizations.

The Tri Mogili magmatic complex is probably connected with the uranium-base-metal ore formation.

The silica-phosphatic mineralization is associated with the Briagovo complex and it is located in the rhyolite tuffs and the reef limestones. In the Dragoinovo unit quartz-chalcedony veins are found. They are probably the final stage of the evolution of the magmatism. These mineralizations have been observed in the

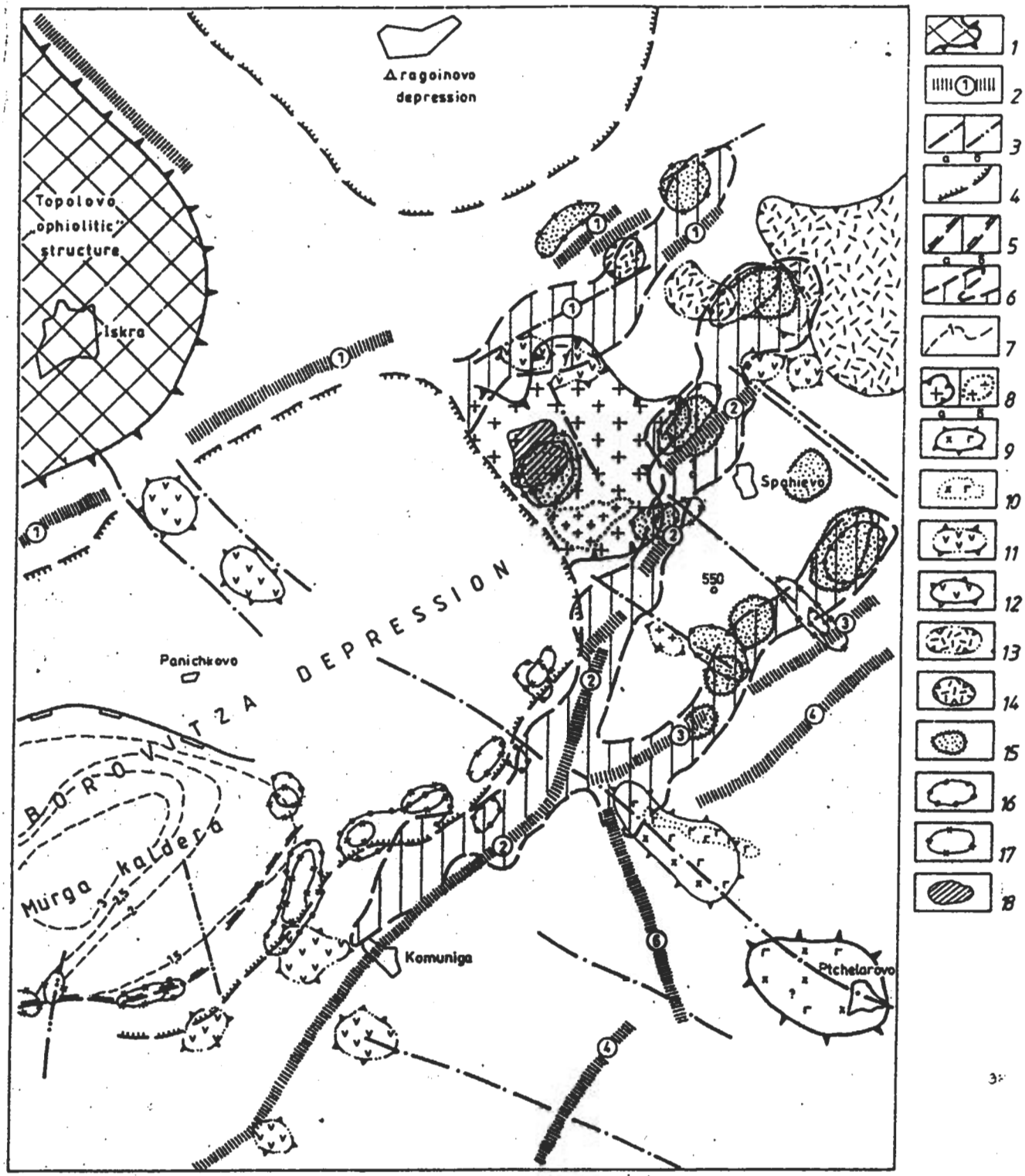

Fig. 2. Structure of the Spahievo ore field, according to the geophysical data interpretation.

1. High density "ophiolitic" structure, delineated according to the 2D gravity inversion; 2. Fault zone of vertical displacement of the metamorphic basement (high gravity gradients); 3. Faults, controlling the magmatic emplacement: a)- according to gravity, b)- according to magnetic data; 4- Concentric border fault of the Paleogene depression (concentric gravity gradients); 5- Subvolcanic dykes in the border faults of the Murga kaldera: axes of: a) negative magnetic anomalies, b) positive magnetic anomalies; 6. Fault zones, controlling the magmatism and ore mineralization location (UxK/Th ratio from the airborn gamma-ray spectrometry); 7. Isoline of the depth to the top of the metamorphic basement, according to the 2D gravity inversion; 8. Monzonitoid intrusion: a)-concealed (gravity minimum), b)- outcropped; 9. Gabbro-diorite intrusion (gravity maximum); 10. Outcropping gabbro-diorite intrusion; Volcanic center of intermediate volcanics: 11- magnetic maximum, 12- gravity maximum; Volcanic center of acid volcanics: 13- magnetic minimum, 14- gravity minimum; High values of the radioactive elements from the airborn gamma-ray spectrometry: 15-potassium (adularia alteration), 16- uranium, 17- thorium.

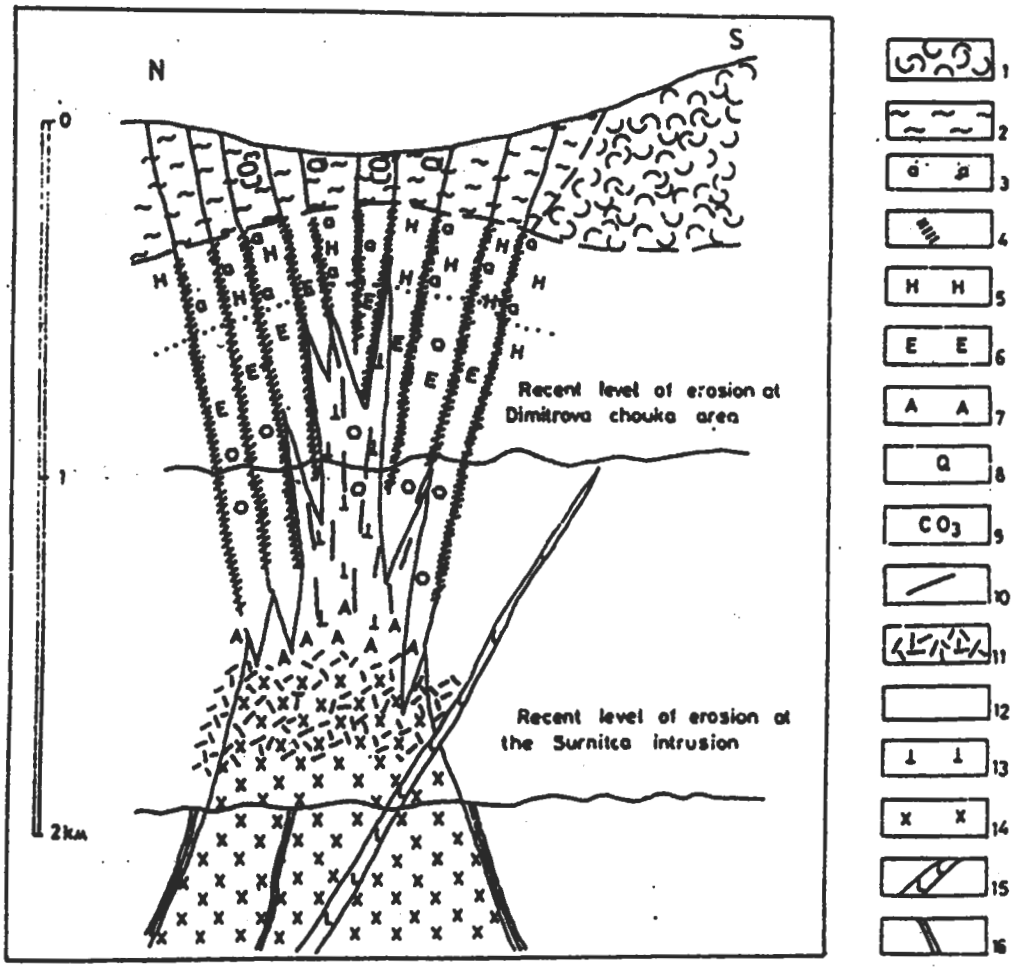

Fig. 3. Genetic model of the copper- molybdenum mineralization, related to the monzonitoid magmatism (Briastovo deposit example).

1. Kaolinite-dickite secondary quartzites; 2. Argyllizites; 3. Adularization; 4. Quartz-sericite alteration; 5. Albite-chlorite-calcite propylites; 6. Epidote-chlorite propylites; 7. Anhydrite zone; 8. Quartz veinlets; 9. Calcite veinlets; 10. Quartz- base-metal veins; 11. Stockwork Cu-Mo mineralization; 12. Disseminated molybdenite mineralization; 13. Quartz- latites; 14. Quartz- monzonite (Gradishte) intrusion; 15- Rhyolite and trachyrhyolite dykes; 16. Superimposed post-rhyolitic quartz- base-metal mineralization.

northern part of the ore field.

The Paleocene magmatism is established as collisional and of shoshonitic type. The evolution of the magmatism is represented by the gradual increase of the acidity in the final stages. It is accompanied by the potassic and the common alkalic raise. The magmatic development is accompanied by the evolution of the attendant mineralization: Mo (Pb,Zn)- Pb,Zn- Au (Pb,Zn)- U (Pb,Zn)- Si,P- Si.

Genetic links between the molybdenum-base-metal mineralization and the monzonitoid intrusion are well identified. There is a particular ore-magmatic system. The connections between the late and the low temperature mineralizations with the magmatism are not well defined. Therefore we accept it as a connection with deeper emplaced magmatic chamber but not as one with a particular intrusive body. The superimposing of different stages of mineralizations complicates the observed pattern and makes difficult the revealing of the genetic connection.

PLATE TECTONIC ASPECTS OF THE ALPINE METALLOGENY IN THE CARPATHO-BALKAN REGION
PROCEEDINGS OF THE ANNUAL MEETING - SOFIA, 1996
UNESCO - IGCP Project No 356
Volume 2, pp. 87-93

COMPARISON AND MODEL OF EPITHERMAL DEPOSITS IN THE EASTERN RHODOPES

Dimitar Dimitrov[1], Evgeni Pluschev[2], Kalinka Petrova[3]

[1]*Geoengineering Ltd.*
[2]*Dessica Co.*
[3]*Geology & Geophysics Corp.*

The most significant deposits and mineralisations known in the Eastern Rhodopes are the Madjarovo and Chala gold-polymetallic deposits, the Pcheloiad polymetallic (potentially gold-polymetallic) deposit, Sumak, Obichnik, and Rozino gold deposits, and Sedefche silver-gold deposit (fig. 1).

GEOLOGICAL SETTING

The Eastern Rhodope mountains are completely formed under the influence of Alpine collision processes. These processes produced regionally metamorphosed basement composed of two thrust sheets (Ivanov et al., 1989). The lower thrust sheet consist of predominantly metamorphosed granitic and granodioritic Paleozoic batholiths. The upper thrust sheet consists mainly of schists and amphibolites. Remnants of the pre-thrust cover of the upper sheet are preserved locally as metamorphic carbonate rocks and black shales.

The Alpine collision events also produced high-angle normal and strike-slip faults, mostly trending NNE, NNW and WNW, and large depressions filled in Paleocene and Eocene by continental and littoral terrigenous sediments and reef limestones. The collision continued in Late Eocene and Oligocene when several submarine volcanic domes appeared and acid to intermediate volcanic, volcano-sedimentary and sedimentary rocks deposited (Dabovski et al., 1991). As a final event of the volcano-tectonic evolution of the region, small gabbro-monzo-granodiorite intrusions, as well as subvolcanic bodies of rhyolite, rhyodacite, latite and andesite-basalt, cut the metamorphics and Paleogene volcano-sedimentary rocks (Atanasov et al., 1963).

CHARACTERISTICS OF THE DEPOSITS

The Madjarovo, Chala, Pcheloiad, Sumak, Obichnik, Rozino, and Sedefche deposits belong to the low sulfidation epithermal type, although some morphological subtypes may be distinguished.

Madjarovo (fig. 2b) and Chala (fig. 2c) are vein type gold-polymetallic deposits where the profitable gold tonnage is connected with the upper parts of the veins, mostly in oxide ores. The Pcheloiad deposit (fig. 2a) may probably be assigned to the same group and significant gold tonnage in abandoned oxide ores from the uppermost levels is possible. The Obichnik gold mineralisation (fig. 3a) represents the stockwork type. The Sumak (fig. 3d) and Rozino (fig. 3c) gold deposits belong to the disseminated flat lying type. The Sedefche silver-gold mineralisation (fig. 3b) represents the same type.

The major characteristics of these deposit are shown in the Table 1.

All vein and stockwork type deposits are hosted by Tertiary trachyandesite and andesite volcanics and volcaniclastics and in some cases they persist in metamorphics. The flat lying mineralisation is developed mostly in penetrable beds of volcaniclastics, epiclastics and terrigenous sediments as well as upper parts of the metamorphosed basement. The gabbro-monzo-syenite intrusions are determined near Chala, Pcheloiad, and Madjarovo deposits and they are supposed in the shallow depth for Rozino and Obichnik.

The positions of the mineralisations are commonly determined by NNW, NNE, and WNW faults and their intersections, volcanic and structural domes, overthrust structures, and collision grabens.

Usually the middle argillic alteration associates the ore mineralisation and the propylitic zones develop in their periphery. The advanced argillic alteration is fixed near Chala and Madjarovo deposits only.

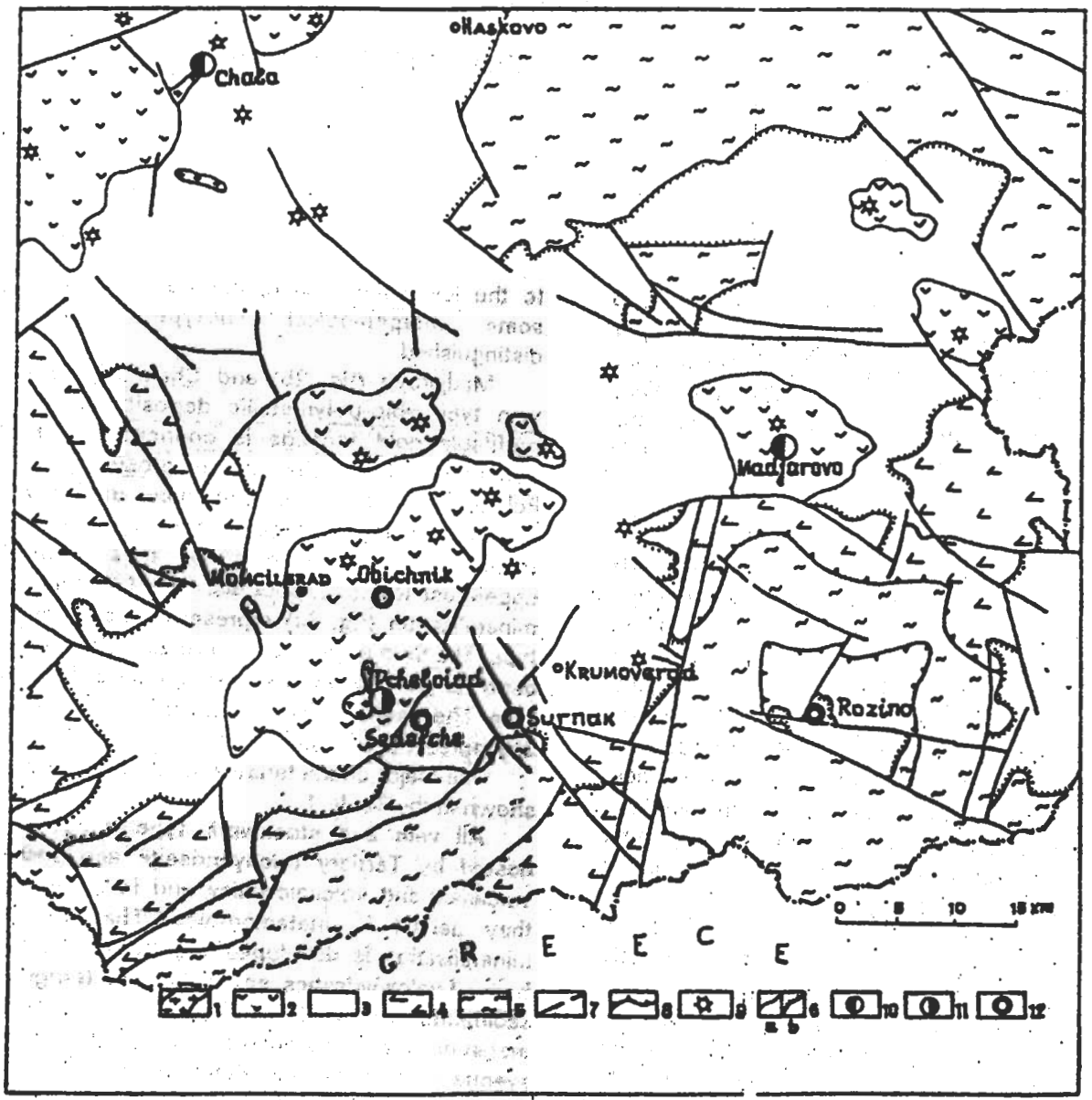

Fig. 1. Simplified geologic map.

Oligocene monzo-diorite, 2- Oligocene volcanics and volcaniclastics, 3- Eocene volcanics, volcaniclastics, and sediments, 4- allochthonous metamorphics, 5- autochthonous metamorphics, 6- normal (a) and transgressive (b) boundaries, 7- faults, 8- overthrusts, 9- central volcanoes, 10-12 - deposits: 10- gold-polymetallic, 11- polymetallic, 12- gold and silver-gold.

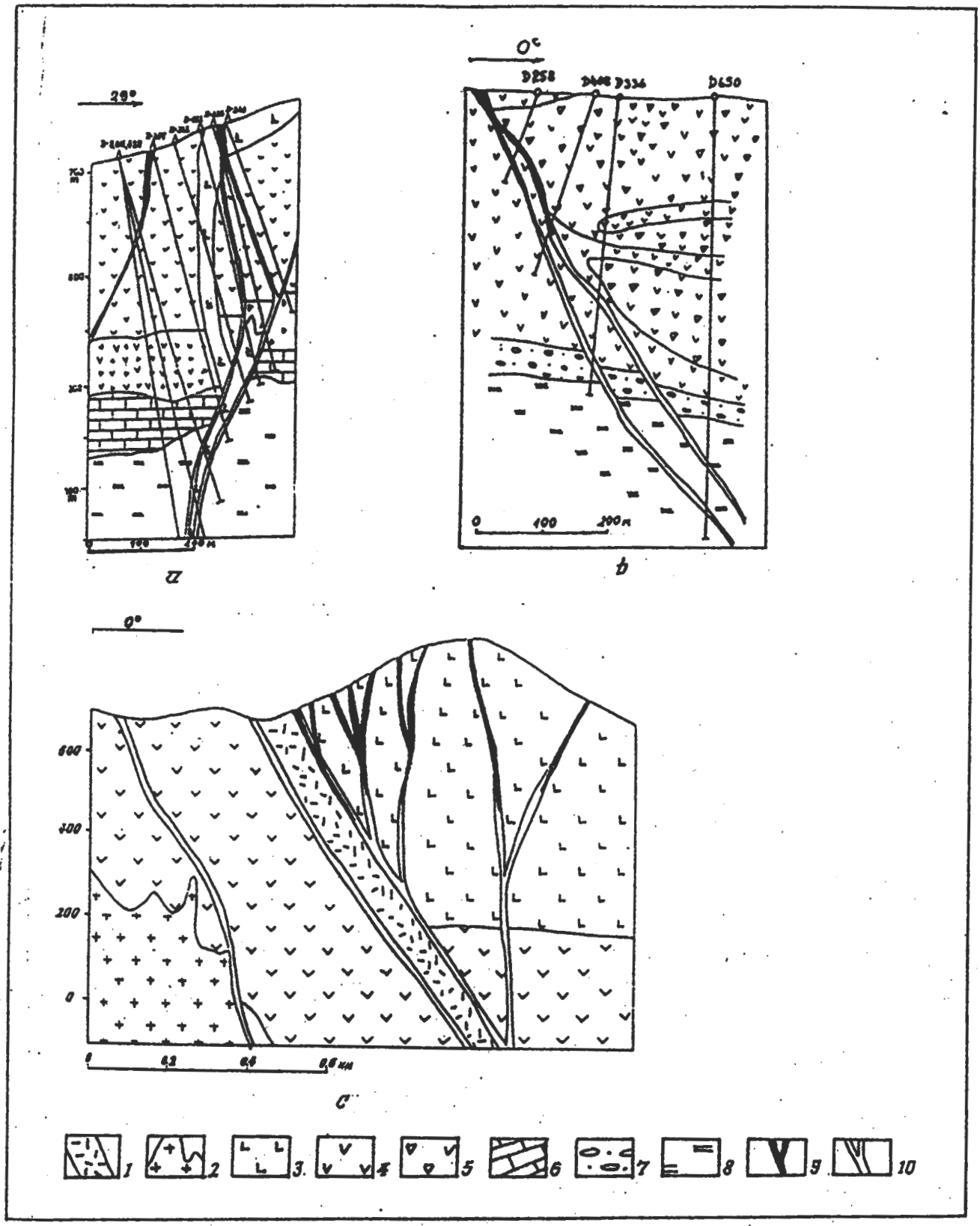

Fig. 2. Schematic cross sections of typical veins from the Pcheloiad (a), Madjarovo (b), and Chala (c) deposits.

1- rhyodacite, 2- monzo-diorite, 3- latite, 4- andesite, 5- andesite volcaniclastics and epiclastics, 6- limestones, 7- conglomerates and sandstones, 8- metamorphics, 9- gold veins, 10- polymetallic veins.

TABLE 1 CHARACTERISTICS OF EPITHERMAL DEPOSITS IN THE EASTERN RHODOPES

DEPOSIT	DEPOSIT TYPE		SHAPE	RESERVES / GRADE	HOST ROCKS	INTRUSIVE SEQUENCE	CONTROL	MAJOR ASSOCIATED ALTERATION	ORE MINERALIZATION*	GANGUE MINERALIZATION
PCHELOIAD	Pb-Zn-Cu-Ag	LS Epithermal	Fissure veins	7.2Mt @ 1.24% Pb, 2.12% Zn, 0.26% Cu, 32 g/t Ag	Tertiary intermediate volcanics, volcaniclastics & sediments; ?Paleozoic allochthonous metamorphics (metamorphosed basic volcanics, amphibol schists, marbles, gneiss)	Tertiary gabbro-monzo-granodiorite intrusion, latite & rhyolite dykes	Volcanic dome structure, WNW, NNW, NNE faults	Quartz + kaolinite, quartz + sericite, chlorite + sericite, epidote + chlorite + albite ± qartz ± carbonate, quartz + adularia	3) sphalerite, galena, pyrite, chalcopyrite; 4) (tenantite, tetrahedrite, native Au, Ag-Sb-sulfosalts, arsenopyrite)	Quartz, calcite, barite, chalcedony
MADJAROVO	Pb-Zn-Cu, Ag-Au	LS Epithermal	Fissure veins WNW or NNE trending	3.515Mt @ 0.2% Pb, 0.04% Zn, 0.003% Cu, 3.32g/t Au,	?Paleozoic metamorphics, Paleozoic-Mesozoic low metamorphosed schists, Tertiary trachyandesite volcs & volcaniclastics, andesite volcs	Tertiary monzo-syenite intrusion, intermediate dykes	E-W to WNW & NNE faults	Quartz + adularia ± carbonate; quartz + kaolinite, quartz + sericite, chlorite + sericite, epidote + chlorite + albite ± qartz ± carbonate, quartz + alunite ± diaspore	1) chalcopyrite, (sphalerite, galena); 2) specularite, native gold; 3) galena, sphalerite, wurtzite, (chalcopyrite, native gold, pyrite, tetrahedrite); 4) sulfosalts (enargite), native Au, Ag, Sb, electrum	1) quartz; 2) quartz, (chlorite); 3) quartz, (barite, amethyst); 4) quartz, chalcedony, amethyst, opal; 5) carbonates
CHALA	Au-(Pb-Zn-Cu)	LS Epithermal	Fissure veins & vein breccia zones	1.386 Mt @ 7.81g/t Au	Tertiary andesites, latites, & rhyolite dykes	Tertiary monzodiorite stock, rhyolite dykes	WNW& NE faults 3C3 - CH	Quartz + kaolinite, quartz + sericite, chlorite + sericite, epidote + chlorite + albite ± qartz ± carbonate, quartz + alunite ± diaspor	2) hematite, native Au & Ag; 3) native Au & Ag, tenantite, tetrahedrite, Ag-sulfosalts, (galena, sphalerite, pyrite, chalcopyrite, marcasite)	Quartz, adularia, carbonate, chlorite, kaolinite, gypsum, barite
OBICHNIK	Au	LS Epithermal	Stock-work	2.6 Mt @ 1.57g/t Au	Tertiary andesite volcanics & volcaniclastics	Probably intermediate intrusion in depth	NW, ENE, NNW, NE faults	Quartz + kaolinite, quartz + sericite, quartz + adularia ± carbonate ± barite	3) pyrite, sphalerite, galena, chalcopyrite, native Au, tenantite, tetrahedrite	Quartz, adularia, carbonate, barite
ROZINO	Au	LS Epithermal	Flat lying & incline bodies, veins & veinlets	2.180Mt @ 1.97g/t Au	Tertiary terrigenous sediments overlying ?Paleozoic allochthonous metamorphics	Probably intermediate intrusion in depth	Periphery of structural dome, N-NE & W-NW faults	Quartz + kaolinite, quartz + sericite, quartz + adularia ± carbonate ± barite	1) pyrite, chalcopyrite, arsenopyrite, native gold; 3) galena, chalcopyrite, sphalerite, (sulfosalts)	Quartz, carbonate, gypsum, barite
SEDEFCHE	Au-Ag	LS Epithermal	Flat lying bodies	1.8Mt @ 1.33g/t Au, 49g/t Ag	Tertiary intermediate volcaniclastics, epiclastics & sediments	Tertiary andesite-basalt & rhyodicite dykes & sills	periphery of volcanic dome, NNW, NNE, WNW faults	Quartz, quartz + kaolinite, quartz + sericite, quartz + adularia ± carbonate ± barite	4) pyrite, marcasite, sulfosalts, arsenopyrite	Quartz, chalcedony, barite
SURNAK	Au-(Ag)	LS Epithermal	Flat lying bodies	7.6 Mt @ 1.57g/t Au, 22 g/t Ag	Tertiary terrigenous sediments overlying ?Paleozoic allochthonous metamorphics		NW, NE, ENE faults	Quartz + kaolinite, quartz + sericite, quartz + adularia ± carbonate	4) pyrite, marcasite, arsenopyrite, (tenantite, native Ag)	Quartz

*Note: Stages of ore mineralisation: 1) - chalcopyrite, 2) - hematite, 3) - sulfides, 4) - sulfosalts.

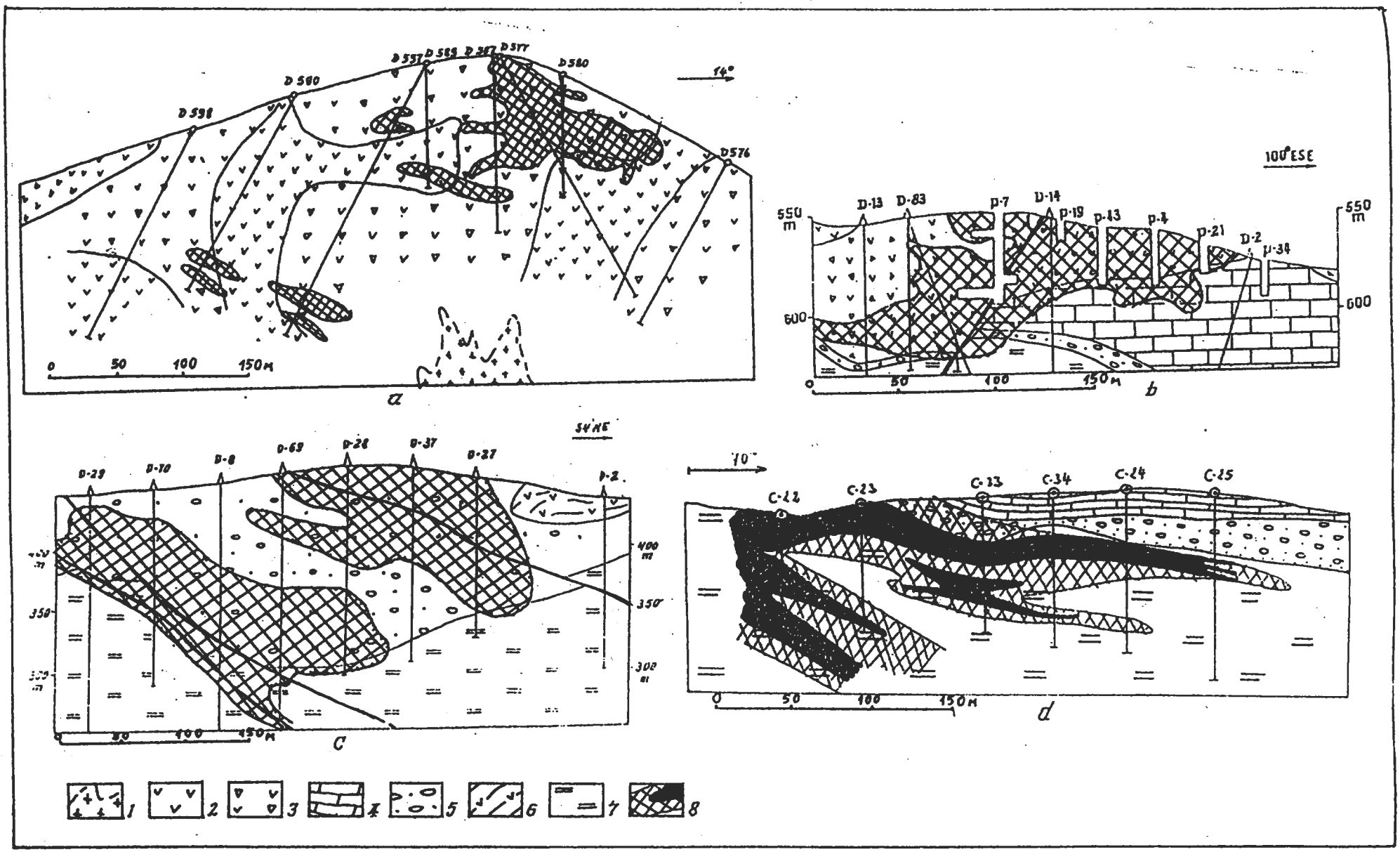

Fig. 3. Schematic cross sections of typical ore bodies from the Obichnic (a), Sedefche (b), Rozino (c), and Surnak (d) deposits.

1- probably intermediate intrusion, 2- andesite, 3- andesite volcaniclastics and epiclastics, 4- limestones, 5- conglomerates and sandstones, 6- black shales, 7- metamorphics, 8- ore bodies

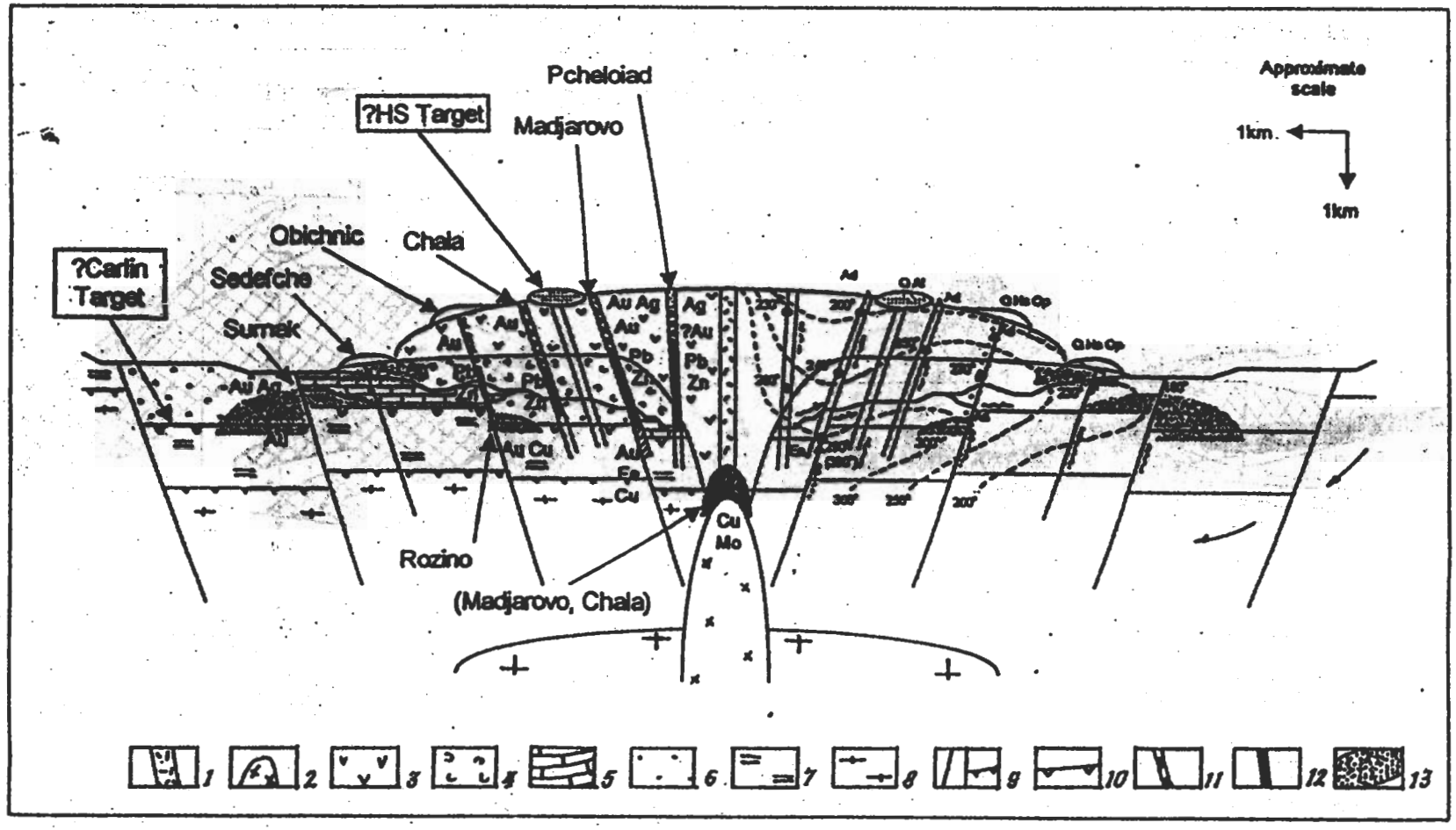

Fig. 4. Model of hydrothermal gold-polymetallic deposits in Eastern Rhodopes.

rhyodacite dykes, 2- monzo-diorite porphyry intrusion, 3- andesite dome, 4- permeable volcaniclastic horizon, 5- impervious limestone, 6- permeable conglomerate horizon, 7- allochthonous metamorphics, 8- autochthonous metamorphics, 9- high-angle faults and overthrusts, 10- tectonized border, 11- gold-polymetallic veins, 12- polymetallic veins, 13- disseminated mineralization.

Four basic stages of ore mineralisation are distinguished. They are named according to the major ore minerals - chalcopyrite, hematite, sulfides and sulfosalts, and their presence in the every deposit is shown in the table. Some manifestations of gangue minerals (carbonates, zeolites, barite, and gypsum) follow the deposition of ore minerals.

GENETIC MODEL

All significant epithermal gold and polymetallic deposits in the Eastern Rhodopes are situated close to the centres of Tertiary magmatic activity. Their spatial distribution in relation to volcanic domes and intrusions is approximately shown on the scheme. The additional components of the environment are:

- highly penetrable levels of Eocene sediments and Oligocene volcaniclastics and epiclastics, divided by impervious levels of carbonate rocks;
- tectonized border between the Tertiary cover and the basement;
- overthrust zones in the basement;
- high-angle faults.

It could be suggested that ore forming process occurred as follows:

- the overthrust zones that usually are about 1 km thick provided the inflow of meteoric water into the hydrothermal system;
- the intrusions (magmatic chambers) and their thermogradient fields were in charge of the convectional movement of the fluid;
- the faults, tectonized zones and penetrable levels acted as the channels for this movement.

In this way the hydrothermal solution leached the elements from the host rocks in the deeper part of the system and deposited them in the upper part. The shape of the channels determined the morphology of the mineralisation - fissure filling ore veins appeared in high-angle faults, and flat lying disseminated ores - in highly penetrable horizons. The ore minerals zonality, from the other hand was determined by the thermogradient fields. Their isothermal curves were reconstructed on the base of fluid inclusion data and characteristic mineralogy (Dimitrov (ed.) et al., 1988; Mladenova et al., 1992; Breskovska and Tarkian, 1993; Kunov et al., 1994). This zonality from the bottom to the top was as follows: Cu-Mo mineralization - Cu-Au - polymetallic - Au-pyrite sulfosalts with Au and Ag.

CONCLUSIONS

The comparison of this scheme with current models of epithermal deposits (for example of Hedenquist & Lowenstern, 1994) shows that they describe the Eastern Rhodopes environment very successfully. In this case the presence of High Sulfidation Epithermal deposits that have not been discovered yet in the Eastern Rhodopes could be suggested. The model of Hedenquist & Lowenstern shows that the approximate distance from the High Sulfidation target to the volcanic centre and intrusion is similar to that for Madjarovo and Chala deposits. It is known that near this deposits silica caps with quartz and alunite exist and they are not sufficiently investigated in depth. The discovery of bonanza gold ore under these caps is possible. In addition, the presence of the Carlin type gold mineralisation at the distance a little longer than the Surnak deposit is possible, too. The existence of metamorphic carbonate rocks and black shales under the Tertiary cover ore under the overthrust is favourable for its formation.

We hope that using this model in prospecting and investigation in the Eastern Rhodopes it is possible to discover new prospective deposit types and to change significantly the potential of the territory.

REFERENCES

Atanasov, A., Mavroudtchiev, B., Boyanov, I., Vapzarov, I. 1963. Little intrusions in the Eastern Rhodopes and their metallogenic significance. - Works on the Geology of Bulgaria. Ser. Geochemistry, mineralogy and petrography, 4, p. 27-44 (in Bulgarian).

Breskovska, V., Tarkian, M. 1993. Mineralogy and Fluid Inclusion. Study of Polymetallic Veins in the Madjarovo Ore Field, Eastern Rhodope, Bulgaria. - Mineralogy and Petrology, 49, p. 103-118.

Dabovski, Ch., Harcovska, A., Kamenov, B., Mavroudtchiev, B., Stanisheva-Vasileva, G., Yanev, Y. 1991. A geodynamic model of the Alpine magmatism in Bulgaria. - Geologica Balcanica, 21, 4, p. 3-15.

Dimitrov, R. (ed.). The Lead-Zinc Deposits in Bulgaria. 1988. Sofia, 257 p.(in Bulgarian)

Hedenquist, J. W., J. B. Lowenstern. 1994. The role of magmas in the formation of hydrothermal deposits. - Nature, 370, 6490, p. 519-527

Ivanov, Z. 1989. Setting and tectonic evolution of the central parts of the Rhodope massif. In: Setting and geodynamic evolution of the internal zones of the Balkanides. CBGA, XIV congress, Guidebook for excursions E-3, p. 53-91 (in Russian).

Kunov, A., I. Velinov, Y. Yanev, R. Nakov, N. Stephanov. 1994. Adularia-sericite type of wall-rock alteration of the epithermal Au-Ag mineral occurrence of Obichnik (Eastern Rhodopes, Bulgaria). - Comptes rendus de l'Academie bulgare des Sciences, 47, 8, p. 61-64.

Mladenova, V., Bogdanov, K., Breskovska, V. 1992. The gold and its paragenesses in the Rosino locality, Eastern Rhodopes.- Proceeding of the symposium Metallogeny of Bulgaria, Abstracts (in Bulgarian).

Schweizerische Mineralogische und Petrographische Mitteilungen 84, 59–78, 2004

The Ada Tepe deposit: a sediment-hosted, detachment fault-controlled, low-sulfidation gold deposit in the Eastern Rhodopes, SE Bulgaria

Peter Marchev[1], *Brad S. Singer*[2], *Danko Jelev*[3], *Sean Hasson*[3], *Robert Moritz*[4] and *Nikolay Bonev*[5]

Abstract

The Ada Tepe gold deposit, 230 km SE of Sofia, formed in the eastern part of the Rhodope Mountains that underwent extension and metamorphic core complex formation, followed by normal faulting, basin subsidence, and silicic to mafic magmatism during the Maastrichtian–Oligocene. The region comprises numerous volcanic-hosted epithermal and base-metal vein deposits spatially and temporally associated with the Oligocene magmatism. Ada Tepe is a typical low-sulfidation epithermal gold deposit, unusual in that it is older than adjacent magmatic-related deposits and is hosted in Maastrichtian–Paleocene sedimentary rocks above a detachment fault contact with underlying Paleozoic metamorphic rocks.

Gold mineralization is located in: (1) a massive, tabular ore body above the detachment fault; and (2) open space-filling ores along predominantly east–west oriented listric faults. The ores are zones of intensive silicification and brecciation synchronous with detachment faulting. Brittle deformation opened spaces in which bands of opaline silica and electrum, quartz, pyrite, massive and bladed carbonates were deposited. Mineralization is exclusively a Au system with Au/Ag ~3, trace As and no base metals. Alteration consists of quartz, adularia, chlorite, sericite, calcite, pyrite and clay minerals. Adularia and abundant bladed carbonates indicate boiling within the entire span of the deposit, whereas bands of opaline silica with dendritic gold suggest that silica and gold were transported as colloids. The physical setting of formation of the Ada Tepe deposit was very shallow and low temperature. The Sr and Pb isotope ratios of carbonates and pyrite reflect hydrothermal fluid signatures derived predominantly from the metamorphic rocks.

The age of mineralization and association with the detachment fault suggest that gold mineralization at Ada Tepe is more closely linked to the Kessebir metamorphic core complex rather than to local magmatism.

Keywords: detachment fault, sediment-hosted, low-sulfidation epithermal, Eastern Rhodopes, Bulgaria.

1. Introduction

The Rhodope metallogenic province (Stoyanov, 1979) comprises numerous volcanic-hosted epithermal (Madjarovo, Chala, Zvezdel, Losen, Perama Hill, Sappes) and base-metal vein (Madan, Luki, Popsko, Thermes) deposits hosted by metamorphic basement (Marchev et al., 2000). The spatial and temporal association of these deposits with Oligocene magmatic centers is documented by the radioisotopic dating of Singer and Marchev (2000), Marchev and Singer (2002), Rohrmeier et al. (2002) and Ovtcharova et al. (2003).

The Ada Tepe deposit is one of a newly discovered group of gold deposits in the Eastern Rhodopes. These share many features with the adularia class of epithermal deposits, but they are atypical in that they are hosted mostly in sedimentary rocks and do not show direct relationships to local magmatic activity. Three of them, including Ada Tepe, Rozino and Stremtsi (Fig. 1), are major targets for commercial exploration. Exploration carried out in the last 2 years shows that Ada Tepe is the major potential economic deposit in the region.

The Ada Tepe low-sulfidation epithermal gold deposit is located 4 km SE of Krumovgrad in the Eastern Rhodopes, 230 km SE of Sofia (Fig. 1). Balkan Minerals and Mining AD (BMM; owned by Dundee Precious Acquisitions Inc.) operates

[1] Geological Institute, Bulgarian Academy of Sciences, Acad. G. Bonchev St., 1113 Sofia, Bulgaria. <pmarchev@geology.bas.bg>
[2] Department of Geology and Geophysics, University of Wisconsin-Madison, 1215 West Dayton St., Madison, WI 53706, USA.
[3] Balkan Mineral and Mining AD, 24 Saedinenie St, Krumovgrad, Bulgaria.
[4] Section des Sciences de la Terre, Université de Genève, rue des Maraîchers 13, CH 1211 Genève, Switzerland.
[5] Department of Geology and Paleontology, Faculty of Geology and Geography, Sofia University "St. Kliment Ohridski", 15 Tzar Osvoboditel Bd., 1504 Sofia, Bulgaria.

0036-7699/04/0084/59

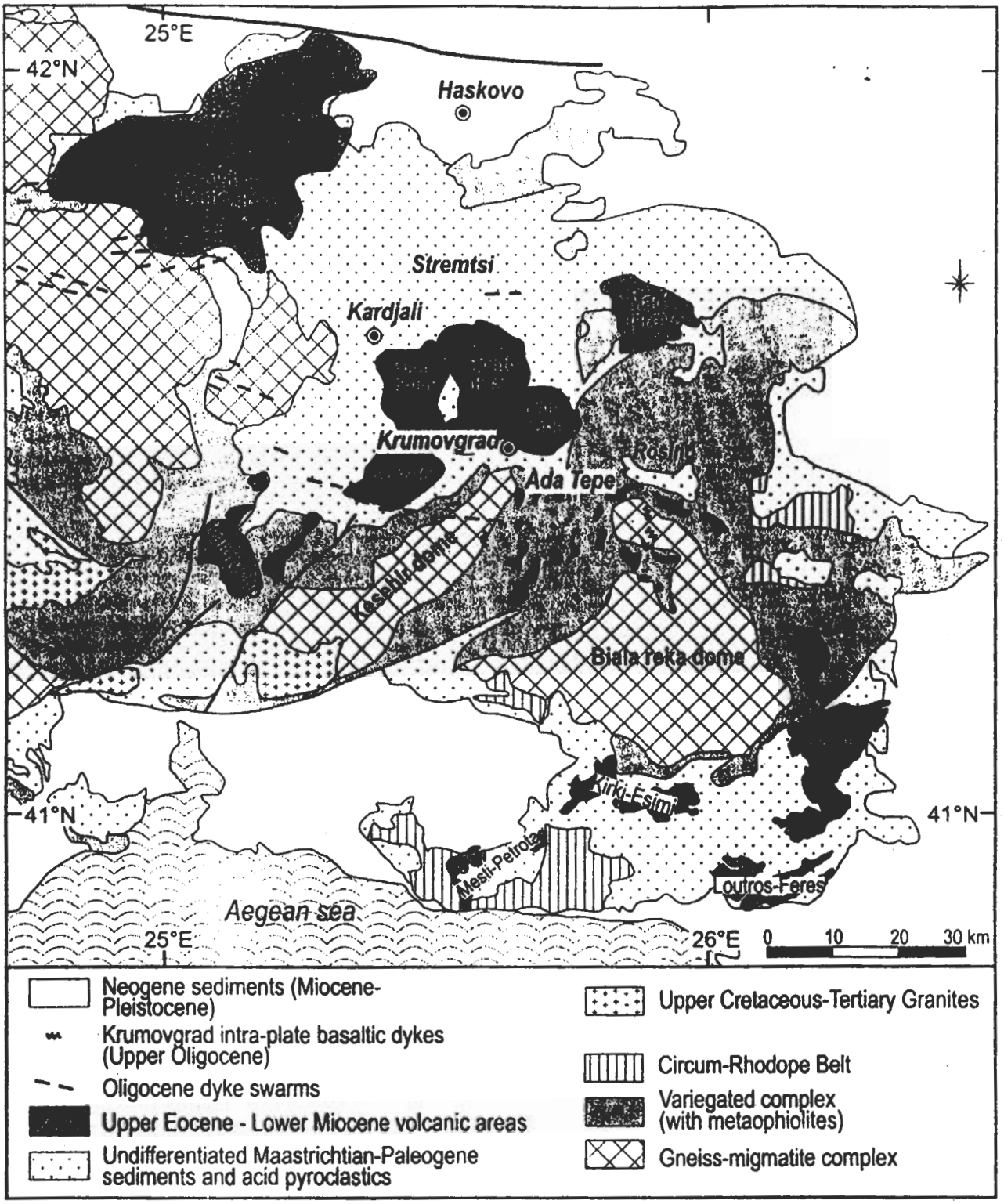

Fig. 1 Schematic geological map of the Eastern Rhodope showing metamorphic dome structures, major volcanic areas and dyke swarms. Compiled from Ricou et al. (1998), Yanev et al. (1998a) and Marchev et al. (2004). Inset shows location of Krumovgrad within Bulgaria.

this project. The deposit is unusual in that it is located along a regional detachment fault. Moreover, it is geochemically distinctive with respect to the adjacent deposits owing to high Au/Ag ratios and low base metal content (Marchev et al., 2003).

Here we summarize results from recent studies on the surface geology, structure, alteration types, and textural and mineralogical characteristics of the gold mineralization. The paper provides limited Sr and Pb isotope data for Ada Tepe and discusses the age relationships among gold mineralization, local igneous activity and thermal events in the nearby Kessebir metamorphic dome (Figs. 1, 2).

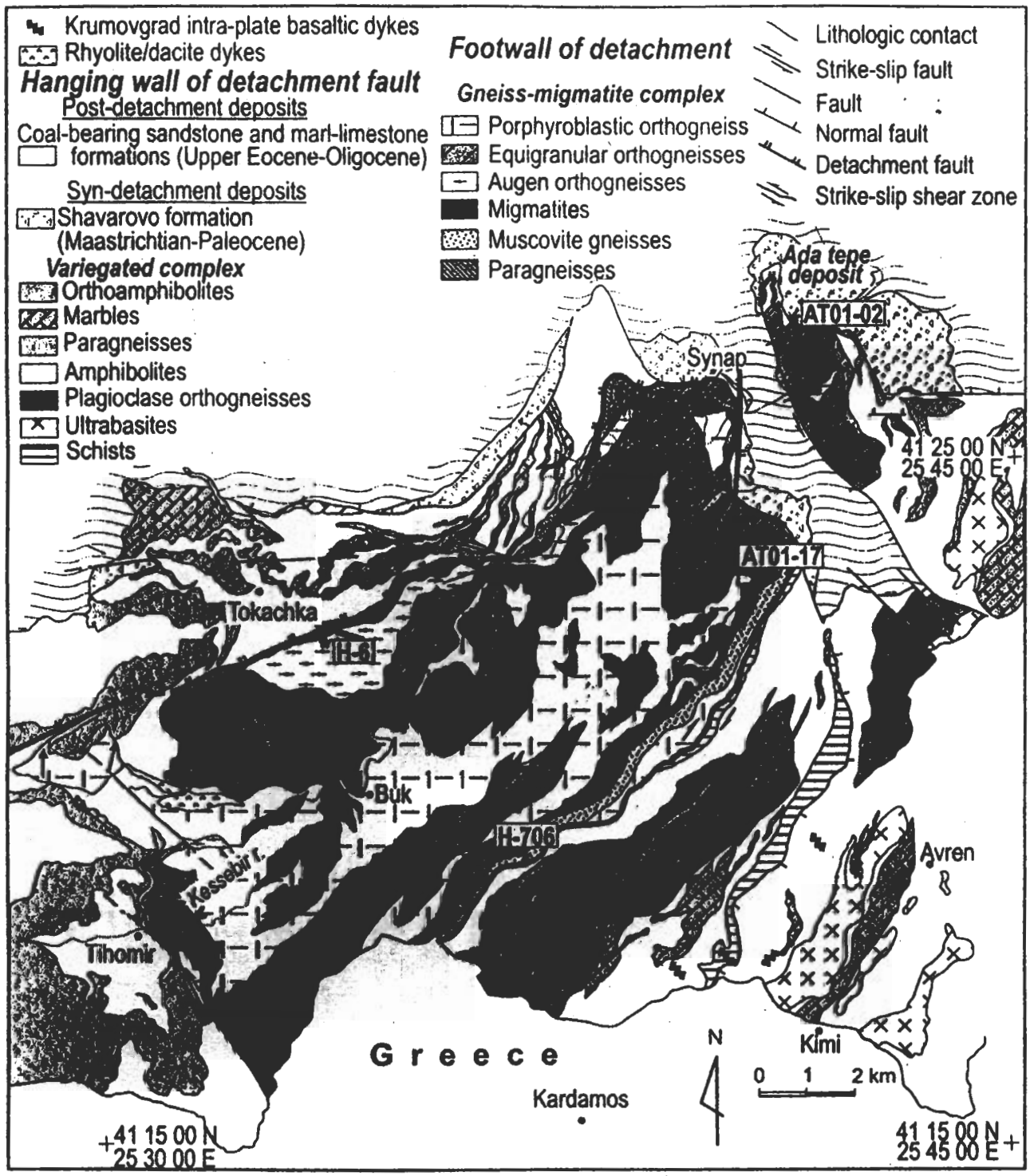

Fig. 2 Geological map of Kessebir dome (after Bonev, 2002) and location of Ada Tepe deposit and Synap prospect.

2. Historical background and previous studies

Small adits and large dumps at the eastern part of the Ada Tepe hill (Fig. 3a) provide tangible evidence for the historical mining activity, probably of Thracian and Roman times. Regional mapping of the Krumovgrad area was conducted in 1965 (Shabatov et al., 1965) and recently between 1995 and 1996 (Sarov et al., 1996) by the State exploration Company "Geology and Geophysics" at a 1:25 000 scale. Studies by Goranov and Atanassov (1992) and a Ph.D thesis by Bonev (2002) have clarified the stratigraphic and tectonic relationships of the Krumovgrad area. The latter work advocates a detachment-fault model for the formation of the Kessebir metamorphic dome. Limited exploration in the area of the Ada Tepe deposit was followed by the first description of its alteration and mineralization, and its classification as Au–Ag-polymetallic

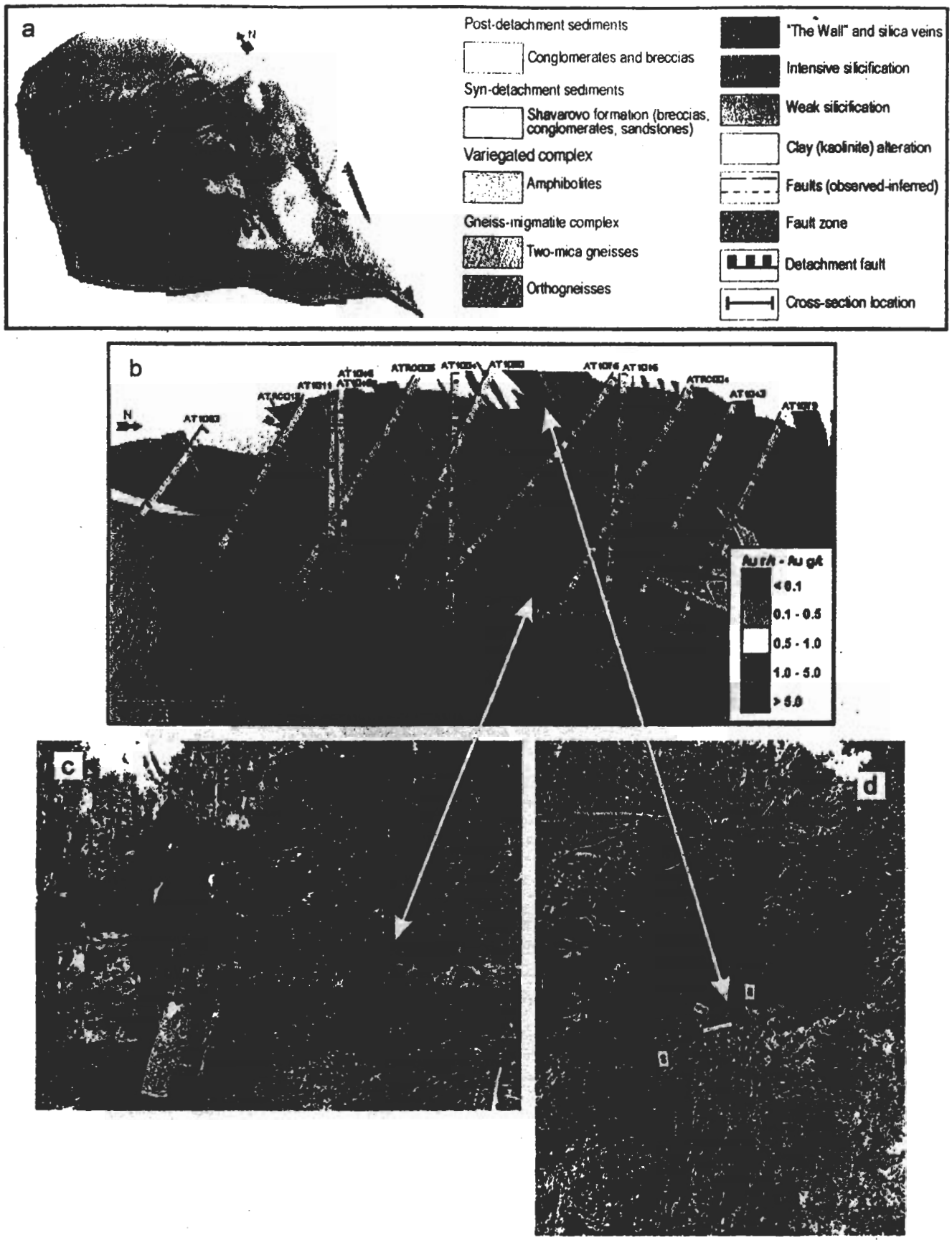

Fig. 3 (a) 3D view of Ada Tepe deposit. (b) Cross section of Ada Tepe deposit. Major ore bodies. (c) Massive, tabular ore body ("The Wall") above the detachment fault. (d) Open space-filling ores along predominantly E–W oriented listric faults

occurrence of the adularia-sericite type (Kunov et al., 2001).

Since June 2000, the Ada Tepe deposit has been included in the Krumovgrad license area, and is explored by Balkan Mineral and Mining AD. Based on the results of regional mapping and surface sampling, BMM conducted two drilling programs, with 145 drill holes, using both diamond and reverse circulation drilling techniques, for a total length of 12 440 m. A total of 10 218 m of surface channel samples were also collected during 2001–2002. Resource calculations by RSG Global of Perth, Australia, show that Ada Tepe is a high-grade Au–Ag deposit containing 6.15 Mt of ore at 4.6 g/t Au for 910 000 ounces of Au, using a 1.0 g/t cutoff grade.

On the basis of initial results from the exploration program and the geographical proximity of the Ada Tepe deposit to the base metal mineralization at the Oligocene Zvezdel volcano, Crummy (2002) suggested a direct genetic link between the base and precious metal districts. Marchev et al. (2003) favoured an Upper Eocene age based on precise $^{40}Ar/^{39}Ar$ data and a detachment faulting model for the origin of the Ada Tepe deposit.

3. Geologic setting

3.1. District geology

Basement metamorphic rocks in the Krumovgrad area build up the elongated Kessebir dome in N–NE direction (Kozhoukharov et al., 1988; Ricou et al., 1998; Bonev, 2002) (Figs. 1, 2). Two major tectonostratigraphic units (complexes) have been recognized on the basis of composition and tectonic setting of the metamorphic rocks: a Gneiss-migmatite complex, and a Variegated Complex (Kozhoukharov et al., 1988; Haydoutov et al., 2001), which correspond to the Continental and Mixed units of Ricou et al. (1998), respectively. The structurally lower Gneiss-migmatite complex crops out in the core of the Kessebir metamorphic dome. It is dominated by igneous protoliths including metagranites, migmatites and migmatized gneisses overlain by a series of pelitic gneisses, and rare amphibolites. Eclogites and eclogitic amphibolites have been described in the Greek part of the Kessebir dome (Mposkos and Krohe, 2000). Rb–Sr ages of 334.6 ± 3.4 Ma (Mposkos and Wawrzenitz, 1995) from metapegmatites in Greece and Rb–Sr (328 ± 25 Ma) and U–Pb zircon ages of 310 ± 5.5 Ma and 319 ± 9 Ma (Peytcheva et al., 1995, 1998) from metagranites of the Kessebir dome in Bulgaria indicate that the Gneiss-migmatite complex is formed of Variscan or older continental basement.

The overlaying Variegated complex consists of a heterogeneous assemblage of pelitic schists, paragneisses, amphibolites, marbles and ophiolite bodies (Kozhoukharova, 1984; Kolcheva and Eskenazi, 1998). Metamorphosed ophiolitic peridotites and amphibolitized eclogites are intruded by gabbros, gabbronorites, plagiogranites and diorites. U–Pb zircon dating of a gabbro from the neighbouring Biala Reka dome (Fig. 1) yields a Late Neoproterozoic age of 572 ± 5 Ma for the core and outer zone recording a Hercynian metamorphic event at ~300–350 Ma (Carrigan et al., 2003). Volumetrically minor plutonic bodies of presumably Upper Cretaceous age intrude the Variegated complex, and represent an important phase of igneous activity in the area (Belmustakova et al., 1995). The rocks are medium to fine-grained, light grey, two-mica granites of massive to slightly foliated structure.

The rocks of the Variegated complex in the Krumovgrad area are overlain by the Maastrichtian–Paleocene syndetachment Shavarovo Formation (Goranov and Atanasov, 1992; see below), which is in turn overlain by Upper Eocene–Lower Oligocene coal-bearing-sandstone and marl-limestone formations. Lava flows and domes of the ~35 Ma andesites (Lilov et al., 1987) of the Iran Tepe volcano are exposed northeast of Krumovgrad (Fig. 1). This magmatic activity was followed by scarce dykes of latitic to rhyolitic composition in the northern part of the Kessebir dome, dated at 31.82 ± 0.20 Ma and finally by 26–28 Ma old intra-plate basaltic magmatism in the southern part of the dome (Marchev et al., 1997, 1998).

3.2. Deposit geology

The Ada Tepe deposit is hosted by the syndetachment Maastrichtian–Paleocene Shavarovo Formation, overlaying the northeastern closure of the Kessebir metamorphic core complex (Fig. 2). The contact between poorly consolidated sedimentary rocks and underlying metamorphic rocks corresponds to the location of a regionally developed low-angle normal fault, named the Tockachka detachment fault (TDF) by Bonev (1996). The fault dips 10–15° to the north-northeast. It can be traced further southwest for more than 40 km from Krumovgrad to the Bulgarian-Greek frontier and is well exposed in the area southwest of Synap village, about 2 km west of Ada Tepe. In the latter area, the rocks in the hanging wall of the TDF consist of metamorphic blocks, breccia, conglomerates, sandstone, marls and argillaceous limestone. This unit was first recognized by Atanasov and Goranov (1984) in the

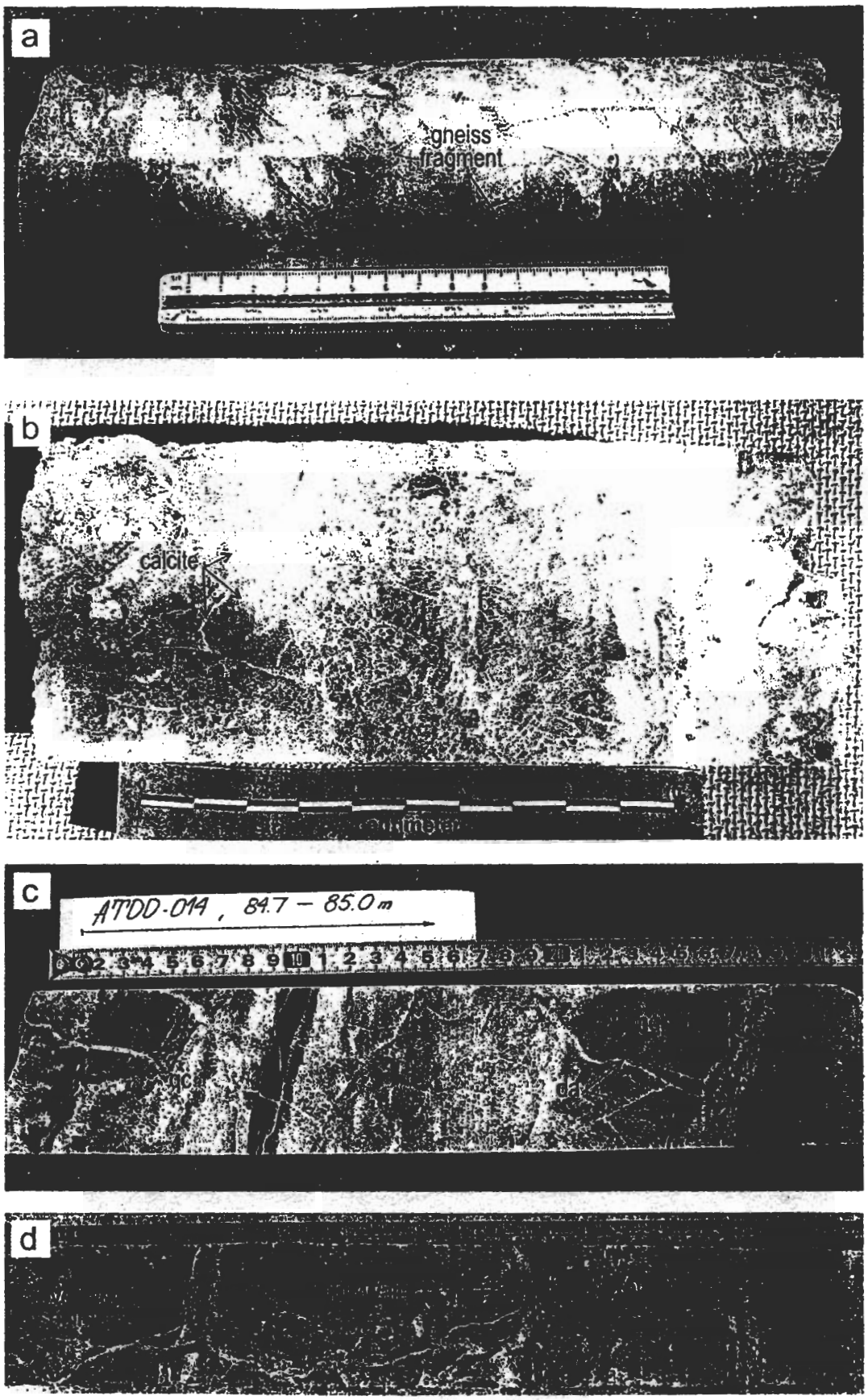

Fig. 4 **Mineralization of The Wall showing multiple periods of silicification and veining. (a) Brecciated early microcrystalline silica (early stage) with a single gneiss fragment. (b) Breccia of the microcrystalline silica (early stage) cemented by calcite (third stage). (c) Subvertical colloform finely banded vein. Early stage gray (g) microcrystalline silica on the margins of the veins followed by the massive microcrystalline (mq) cross cut by the third stage sugary quartz and massive and bladed calcite (qc). Late veinlets of dolomite ankerite (da) cut early vein mineralization. (d) Transition of subhorizontal opaline carbonate vein into subvertical step-like vein in the overlying sediments.**

Krumovgrad area and described as the Shavarovo Formation of the Krumovgrad Group in a later paper (Goranov and Atanasov, 1992). The total thickness of the type section of the Shavarovo Formation (~350 m) was measured along the Kaldjic river, near the Shavar village. Blocks and clasts of breccia and conglomerate are mixtures of gneiss, amphibolite and marble, derived primarily from the Variegated complex.

4. Structure

The dominant structure in the Ada Tepe prospect is the TDF. It is a mapable tectonic contact, best expressed along the western slope of Ada Tepe hill (Fig. 3a). In outcrop and drill cores, the fault is recognized as a contact between Paleozoic metamorphic rocks and Maastrichtian–Paleocene sedimentary rocks of the Shavarovo Formation. Immediately above the detachment fault there is a 0.5 to 20 m thick zone of massive silicification. In drill core, the lower limit of the structure is marked by a 10–20 cm-thick layer of tectonic clay. Gneiss, migmatite, marble and the amphibolite of the metamorphic basement beneath the detachment surface are transformed into a cataclastic rock over a thickness of several meters. The southwestern slope of the Ada Tepe hill is cut by a NW–SE-oriented high-angle fault (Fig. 2), which formed a small half graben fill by older Maastrichtian–Paleocene syndetachment sedimentary rocks overlain in the eastern part by younger Priabonian–Oligocene sedimentary rocks.

Major structures cutting the basement rocks of the Ada Tepe deposit are rare, although several E–W and N–S-oriented subvertical faults, marked by a zone of silicification, occur to the south, east and west of the Ada Tepe deposit. The longest N–S-striking zone has been traced for almost 200 m. The E–W and N–S faults coincide with the major directions of the mineralized veins in the sedimentary cover and can be interpreted as feeder structures for the mineralizing fluids.

5. Mineralization

5.1. Ore geometry and ore bodies

The Ada Tepe deposit is 600 m along strike and 300–350 m wide. Gold mineralization occurs as: (1) a massive, tabular body located immediately above the detachment fault (Figs. 3b, c), and (2) open space-filling within the breccia-conglomerate and sandstone along predominantly east-west oriented subvertical listric faults within the hanging wall (Figs. 3b, d). In cross section the tabular body dips (10–15°) to the north-northeast, which is consistent with the low angle TDF. The ore body is so strongly silicified; company geologists refer to it as "The Wall". Detailed observations on The Wall indicate a complicated sequence of events with multiple periods of silicification and veining. Silicification began with the deposition of massive white to light grey silica above the detachment fault partly or totally replacing the original rocks. Original rock textures were destroyed with the exception of ghosted gneiss fragments (Fig. 4a). The latter are rounded with veins of quartz or carbonate cutting or surrounding the clasts. Early microcrystalline silica was commonly veined by subvertical banded veins or brecciated by later fault movements and cemented by calcite; sugary quartz (Fig. 5b) or by pyrite.

In the less silicified parts The Wall consists of numerous differently oriented veins ranging in width from less than 1 cm up to 30 cm (Fig. 4c). Subvertical veins, which were formed by deposition of colloform silica layers in open space, can be traced from The Wall into the listric faults in the overlying sedimentary rocks (Fig. 4d). On the surface they form E–W-trending ridges, separated by argillic zones (Figs. 3a, b, d).

5.2. Ore and gangue mineralogy and stages of mineralization

The ore mineralogy of the Ada Tepe deposit is simple, consisting mainly of electrum and subordinate pyrite with traces of galena, and gold-silver tellurides. Gangue minerals consist of silica polymorphs (microcrystalline, fine-grained, sugary quartz and opaline silica), various carbonates (calcite, dolomite, ankerite and siderite), and adularia. Tellurides include hessite (Ag_2Te) and petzite (Ag_3AuTe_2). All samples with Au content higher than 1 g/t have almost constant Au/Ag ratios ~ 3, reflecting the composition of electrum (76–73 wt% Au).

Unlike the massive silicification of The Wall, banded veins in and above it provide an excellent framework for identifying the different stages of mineralization. Mineralization in Ada Tepe can be subdivided into 4 broad, generally overlapping stages of quartz and carbonate veins on the basis of cross-cutting relationships, changes in mineralogy, texture and gold grades.

The earliest stage is characterized by deposition of microcrystalline to fine-grained grayish to white massive or banded quartz with rare pyrite and adularia (Figs. 5a–d). In some veins silica deposition starts with a thin band of almost isotropic opaline (Fig. 4 c) followed by thin band of quartz with rare bladed calcite. Breccia texture is typical

for the massive silicification of The Wall. The products of the early stage form microfracture filling in the host rocks near the margins of the veins or rock fragments in The Wall, causing the silica-adularia-pyrite replacement in them. The gold grade of this stage is unknown.

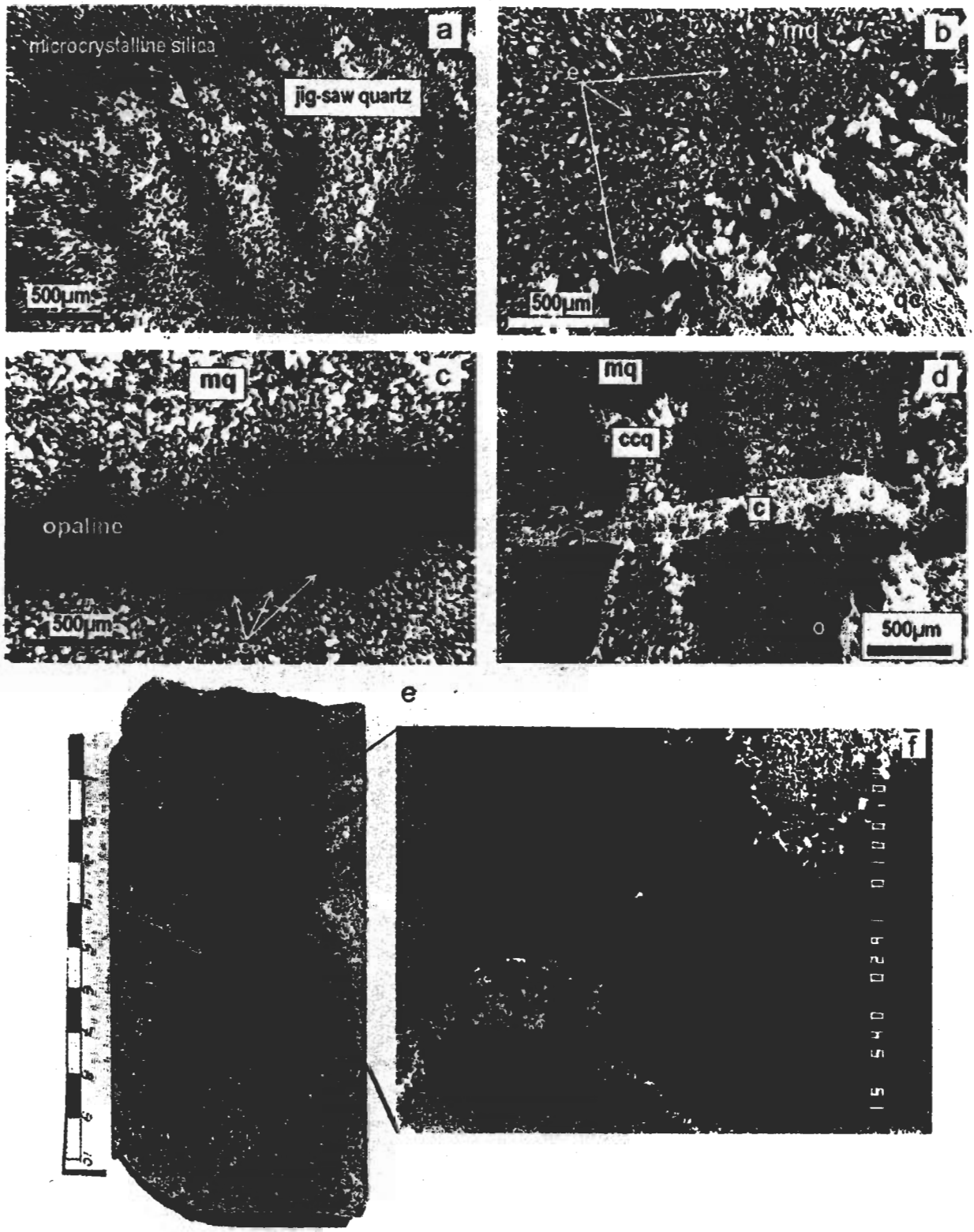

Fig. 5 Microphotographs and SEM images of silica and bonanza ore textures. (a) Bands of early stage microcrystalline (mq) and jigsaw quartz (jq). (b) Electrum band (e) deposited on the interface between early microcrystalline quartz (mq) and third stage sugary quartz and radiating bladed calcite (qc). (c) Band of electrum (e) and isotropic opaline. Electrum is located on the bottom of the band. (d) Third stage coarse crystalline quartz (ccq), cutting the opaline (o) and microcrystalline quartz (mq), which in turn is cut by calcite (c). (e) Subparallel bands of electrum (e) and microcrystalline adularia and silica separated by a calcite vein (c). The arrow shows the vertical direction. (f) SEM image of the outlined area.

The economic gold is related to the second stage of mineralization. It starts at the end of the microcrystalline quartz and the beginning of the coarser grained (sugary) quartz of the third stage below (Fig. 5b). Usually, it forms black millimeter-scale bands of opaline or microcrystalline chalcedony-adularia and electrum (Figs. 5c–f). Locally opaline silica crosscuts the microcrystalline quartz (Figs. 5c–d) of the early stage and in turn is cut by the coarser grained quartz and carbonates of the third and forth stages (Figs. 5d–e). Petrographic examination of the electrum-rich bands reveals that electrum commonly occurs towards the bottom of the opaline or microcrystalline bands (Figs. 5c, e). Where opaline bands are not present, electrum precipitates at the boundary of first and third stages (Fig. 5b). The electrum has irregular forms as the result of crystallization in the quartz interstices, being relatively well-shaped in the coarser-grained quartz crystals. The size of electrum grains ranges from less than 1 to 20 μm. However the single crystals form chains reaching up to 650 μm (Figs. 5b, 6a). Electrum in gold-rich bands etched with HF is characterized by botryoidal surfaces that appear to have formed by the aggregation of spherical electrum particles (Figs. 6a–b), as observed in the Sleeper deposit, Nevada (Saunders, 1990, 1994). Electrum in bonanza veins can occupy 50 vol% (Figs. 5f, 6c), accompanied by rare As-bearing pyrite. Occasionally, micron or submicron size electrum inclusions form zones within the As-bearing pyrite (Figs. 6d). Tiny Au–Ag tellurides have been observed at the contacts between electrum grains and small galena crystals (Fig. 6f).

The third stage starts with deposition of sugary quartz (up to 1.5 mm large; Figs. 5d, 7a) followed by bands of quartz and bladed calcite (Figs. 5b, 7b) and finally by massive calcite with small amount of quartz (Fig. 5d). Locally, calcite fills quartz geodes or forms small veins (Fig. 7a). Microscopically the late calcite corrodes and replaces quartz crystals. Small amount of adularia and pyrite are also typical for this stage.

The hydrothermal mineralization ended with the deposition of pinkish ankerite-dolomite and siderite, which was preceded by precipitation of massive pyrite in some parts of the deposit (Figs. 7c–d).

The mineralization of Ada Tepe exhibits several important spatial and textural features that provide insights to the physical environment of ore deposition. In its upper part, quartz becomes the predominant gangue mineral, whereas carbonates are subordinate. This is particularly obvious in the last stage, where in the surface samples dolomite and ankerite are absent in the geodes and bladed minerals consist of microcrystalline quartz only. Another spatial variation is the diminishing of banding textures with the decrease in grade of Au mineralization to the north. An important feature is the absence of bladed carbonates in the veinlets beneath The Wall, in contrast to the entire extent of the deposit above the detachment surface.

5.3. Oxidized zone

The uppermost part of the Ada Tepe deposit has been oxidized by supergene processes with the depth of oxidation being dependent upon intensity of faulting. Due to extensive silicification, The Wall itself is generally not oxidized; however, a 2 to 5 m thick zone of oxidation invariably occurs above The Wall. Narrow zones of oxidation occur down to this zone utilizing high angle listric faults. These faults and fractures most likely acted as conduits for the surface waters to reach the impermeable silicified zone, forming the oxidized zone above The Wall.

Most of the pyrite in the oxidized zones has been converted into limonite identified as goethite. Kaolinite is widely distributed in this zone, forming locally small veinlets. Electrum in the oxidized zone however, shows no evidence of Au enrichment.

6. Alteration

In the poorly mineralized zones hydrothermal alteration is weak with most of the detrital minerals (quartz, muscovite and feldspars) remaining unaltered. Alteration consists of chlorite, calcite, kaolinite and subordinate albite, pyrite and ankerite-dolomite. It seems that calcite and ankerite-dolomite are late; however, it is difficult to distinguish replacement calcite from vein calcite. Quartz, adularia, calcite, pyrite and dolomite-ankerite-siderite ± sericite and clay minerals in variable proportions occur in The Wall and immediate proximity to the subvertical quartz and carbonate veins in the strongly mineralized zones. They formed through replacement of the original metamorphic minerals included in the sandstone and conglomerate, and are associated with relict, detrital quartz and muscovite. This complex mineral assemblage is the result of the evolution of the hydrothermal activity.

Hydrothermal alteration of the basement metamorphic rocks is developed within a halo several meters in extent beneath The Wall, and is more pronounced around the subvertical veins. The alteration assemblage includes quartz, adu-

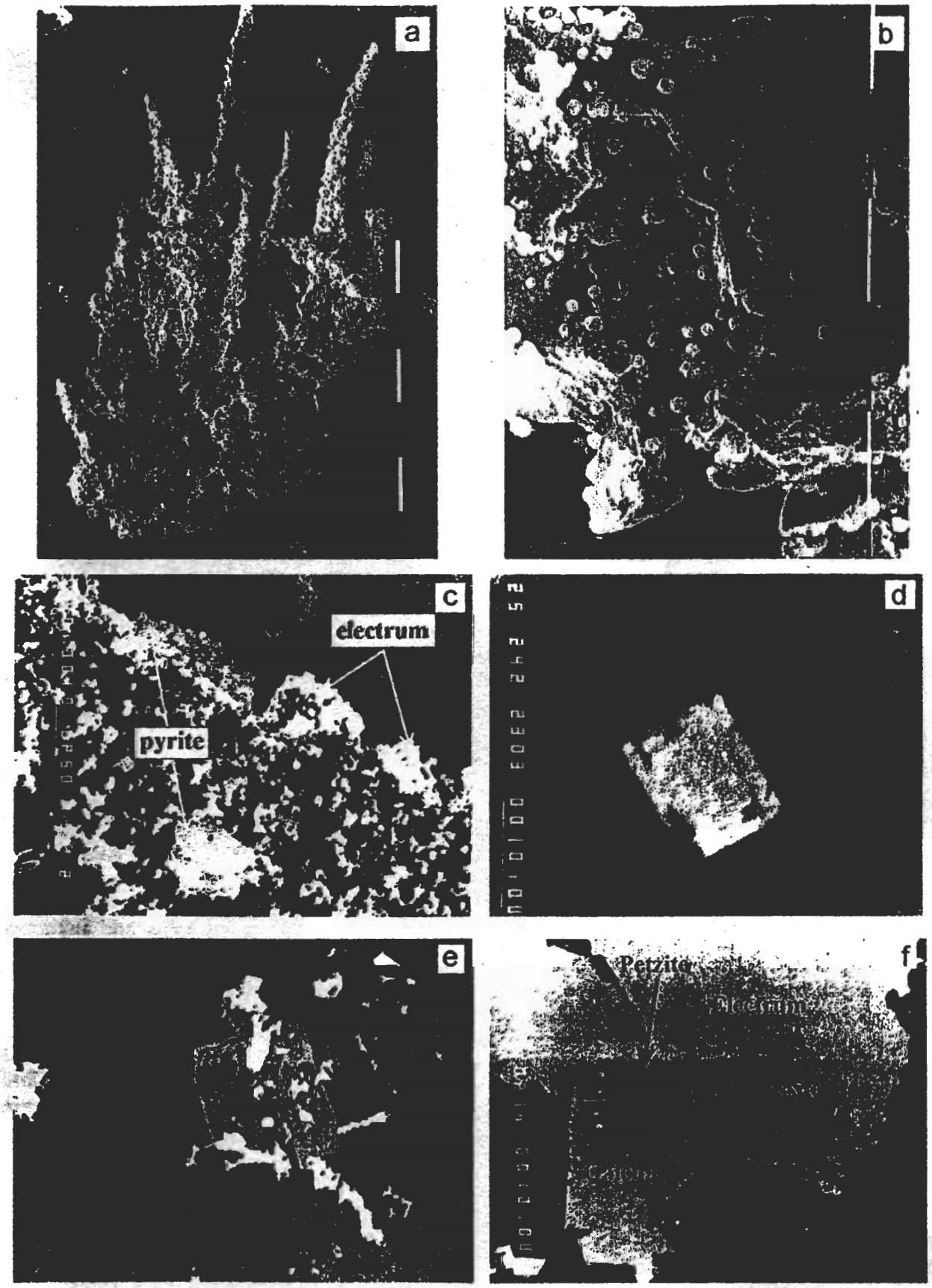

Fig. 6 (a) SEM images of electrum dendrite etched with HF. (b) Negative forms of quartz removed by HF and spherical colloidal particles. (c) Opal-electrum band, containing ~ 50% electrum and small amount of pyrite. Dark crystals between electrum are adularia and silica; (d) Pyrite with a zone of submicron-size electrum; (e) Former Py converted to goethite with inclusions of Au. (f) Au–Ag tellurides between larger electrum and galena crystals.

laria, illite or sericite, pyrite, kaolinite, and late stage ankerite-dolomite-siderite.

Clay minerals are more abundant and better developed in the alteration close to the surface where they form argillic zones between the E–W-oriented swarms of veins. Kaolinite and quartz predominate in the argillic zones, and illite, chlorite, adularia and carbonate are subordinate, accompanied locally by illite-montmorillonite. Part of the shallow-level kaolinite may be supergene, but its association with unoxidized pyrite beneath and within The Wall indicates that a hypogene origin is likely at least for the deeper kaolinite.

7. Geochronology

$^{40}Ar/^{39}Ar$ ages from adularia and sanidine samples were determined to constrain the timing of mineralization and volcanic activity in the Kessebir dome. Sample AT01-2, from which adularia was extracted for dating, is from a drill-hole at 72.5 m depth. It represents a quartz-adularia-carbonate banded vein filled with finely veined gneiss clasts. It is a mixture of completely replaced detrital K-feldspar and directly deposited adularia crystals. The rhyolite dyke (sample AT01-17) is emplaced within the core orthogneisses of the Kessebir dome located 4 km southwest from Ada Tepe (Fig. 2). It comprises 2 cm diameter sanidine phenocrysts that were separated for dating, plus plagioclase, biotite, and quartz.

$^{40}Ar/^{39}Ar$ experiments were conducted at UW-Madison Rare Gas Geochronology Laboratory. Minerals were separated from 100–250 micron sieve fractions using standard magnetic, density, and handpicking methods. Five milligrams of each mineral were irradiated at Oregon State University, U.S.A. for 12 hours, along with 28.34 Ma sanidine from the Taylor Creek rhyolite as the neutron fluence monitor. Analytical procedures, including mass spectrometry, procedural blanks, reactor corrections, and estimation of uncertainties are given in Singer and Brown (2002). Isotopic measurements were made of the gas extracted by incrementally heating of 2–3 mg multi-crystal aliquots using a defocused CO_2 laser beam. Results of incremental heating experiments along with the $^{40}Ar/^{39}Ar$ ages of muscovite and biotite from the lower plate of the metamorphic basement rocks taken from Bonev et al. (accepted) are in Table 1. Incremental heating experiments and age spectra of the sanidine and adularia are presented in Table 2 and Fig. 8. Uncertainties in the ages include analytical contributions only at $\pm 2\sigma$.

The plateau age of the adularia, based on 79.3% of the gas released, is 34.99 ± 0.23 Ma (Fig. 8) and is indistinguishable from the total fusion age of 35.05 ± 0.23 Ma. Sanidine from the rhyolite dyke yielded a plateau age of 31.82 ± 0.20 Ma based on 60 percent of the gas released, which is indistinguishable from the total fusion age of 31.88 ± 0.20 Ma. As is the case for the adularia, this indicates that argon loss due to weathering or alteration is negligible. Moreover, the inverse isochron ages of 35.11 ± 0.37 Ma for the adularaia and 31.91 ± 0.27 Ma for the sanidine are indistinguishable from the plateau ages and the $^{40}Ar/^{36}Ar$ intercept values indicate that there is virtually no excess argon present.

Lavas from the Iran Tepe volcano, four km northeast of Ada Tepe give K–Ar ages of ~35 Ma but their stratigraphic position above the Upper Priabonian–Lower Oligocene marl-limestone formation suggests that they are younger than 34 Ma.

$^{40}Ar/^{39}Ar$ measurements on muscovite and biotite (Bonev et al., accepted) from the Gneiss-migmatite complex, record ages of 38.13 ± 0.36 and 37.73 ± 0.23 Ma, respectively (Table 1). These ages are broadly in agreement with the published $^{40}Ar/^{39}Ar$ ages for muscovite (42.2 ± 5.0 and 36.1 ± 5.0 Ma; Lips et al., 2000) and muscovite and amphibole (39 ± 1 and 45 ± 2 Ma, respectively; Mukasa et al., 2003) from the Biala Reka metamorphic core complex. Similar ages (39–35 Ma) have been obtained by Peytcheva et al. (1992) for the closing of Sr isotope system in the metagranites from the Biala Reka dome.

The relative age of the mineralization was determined based on its relationship with the host Krumovgrad group and the overlying Upper

Table 1 Summary of $^{40}Ar/^{39}Ar$ incremental heating experiments on adularia, sanidine, biotite and muscovite from Ada Tepe deposit and Kessebir dome.

Sample	Mineral	Weighted Plateau age (Ma)	Total Fusion age (Ma)	Source
AT01-2	adularia	34.99 ± 0.23	35.05 ± 0.23	this study
AT01-17	sanidine	31.82 ± 0.20	31.88 ± 0.20	this study
H6	biotite	37.73 ± 0.25	37.56 ± 0.24	Bonev et al. (accepted)
H706	muscovite	38.13 ± 0.36	38.34 ± 0.31	Bonev et al. (accepted)

Table 2 $^{40}Ar/^{39}Ar$ incremental-heating analyses of adularia and sanidine from Ada Tepe.

Experiment number	Laser power (Watts)	^{36}Ar (Volts)	± 1σ	$^{37}Ar^a$ (Volts)	± 1σ	^{38}Ar (Volts)	± 1σ	$^{39}Ar^a$ (Volts)	± 1σ	^{40}Ar (Volts)	± 1σ	$^{40}Ar^*$ (%)	^{39}Ar (%)	K/Ca	Age (Ma)[b]	± 2σ
AT01-2 adularia; J = 0.002987 ± 0.000009; mass discrimination per amu: 1.0022 ± 0.0004.																
AB2121	0.04 W	0.012604	0.000030	0.000159	0.000005	0.002772	0.000021	0.029850	0.000077	3.871564	0.001557	4.7	0.4	6.1	32.72	± 3.84
AB2122	0.10 W	0.009696	0.000022	0.004566	0.000046	0.004738	0.000020	0.239380	0.000131	4.348793	0.003120	34.9	2.9	1.6	33.85	± 0.38
AB2123	0.16 W	0.008804	0.000015	0.005107	0.000032	0.006792	0.000030	0.427709	0.000337	5.368227	0.002780	52.2	5.3	2.6	34.93	± 0.18
AB2124	0.22 W	0.003814	0.000011	0.000564	0.000010	0.003949	0.000012	0.268571	0.000112	2.865288	0.000789	61.3	3.3	15.0	34.83	± 0.16
AB2126	0.30 W	0.008692	0.000011	0.000261	0.000002	0.009565	0.000020	0.650692	0.000347	6.809601	0.002755	62.7	8.0	79.9	35.01	± 0.11
AB2127	0.45 W	0.011765	0.000015	0.000226	0.000006	0.017464	0.000035	1.258986	0.000312	11.697117	0.006487	70.5	24.8	177.0	35.00	± 0.09
AB2128	0.69 W	0.013209	0.000022	0.000199	0.000003	0.017401	0.000014	1.230663	0.001217	11.960795	0.012113	67.6	37.9	195.9	35.11	± 0.15
AB2129	1.25 W	0.012274	0.000021	0.000249	0.000003	0.017405	0.000037	1.255200	0.000803	11.896055	0.004493	69.8	17.3	161.1	35.32	± 0.10
											Plateau age				34.99	± 0.23
											MSWD (n = 5 of 8)				1.86	
											Total Fusion Age				35.05	± 0.23
AT01-17a sanidine; J = 0.002976 ± 0.000009; mass discrimination per amu: 1.0022 ± 0.0004.																
AB2132	0.04 W	0.000551	0.000005	0.000014	0.000006	0.000175	0.000005	0.003621	0.000024	0.182522	0.000076	11.8	0.0	45.6	31.31	± 4.56
AB2133	0.06 W	0.000193	0.000004	0.000026	0.000003	0.000343	0.000006	0.025791	0.000046	0.214316	0.000110	74.5	0.3	44.7	32.60	± 0.51
AB2134	0.12 W	0.000188	0.000004	0.000116	0.000007	0.002511	0.000023	0.204688	0.000253	1.288211	0.000967	95.9	2.0	56.8	32.08	± 0.12
AB2136	0.18 W	0.000503	0.000004	0.000568	0.000012	0.015207	0.000032	1.251793	0.000404	7.625113	0.002510	98.0	12.4	67.8	31.81	± 0.04
AB2137	0.24 W	0.000560	0.000005	0.000843	0.000018	0.023512	0.000025	1.921939	0.000651	11.637885	0.004597	98.5	19.0	70.0	31.79	± 0.04
AB2138	0.27 W	0.000361	0.000008	0.000707	0.000010	0.019152	0.000024	1.578728	0.000654	9.556079	0.004091	98.8	15.6	68.6	31.87	± 0.05
AB2139	0.31 W	0.000363	0.000001	0.000522	0.000008	0.014727	0.000035	1.202936	0.000478	7.300394	0.003784	98.5	11.9	70.9	31.84	± 0.05
AB2141	0.35 W	0.000311	0.000007	0.000377	0.000008	0.010541	0.000029	0.878996	0.000319	5.353642	0.002077	98.3	8.7	71.6	31.88	± 0.05
AB2142	0.45 W	0.000328	0.000004	0.000553	0.000015	0.015927	0.000034	1.307859	0.000548	7.947037	0.003239	98.7	12.9	72.6	31.96	± 0.05
AB2143	0.59 W	0.000285	0.000005	0.000394	0.000012	0.010851	0.000045	0.891613	0.000557	5.430367	0.002402	98.4	8.8	69.6	31.93	± 0.06
AB2145	0.84 W	0.000160	0.000004	0.000196	0.000007	0.005603	0.000028	0.451835	0.000332	2.760099	0.001984	98.3	4.5	70.6	31.97	± 0.08
AB2146	1.35 W	0.000166	0.000005	0.000183	0.000004	0.004620	0.000018	0.382947	0.000252	2.353853	0.001397	98.0	3.8	64.7	32.05	± 0.08
											Plateau age			31.82	± 0.20	
											MSWD (4 of 12)				2.79	
											Total Fusion Age				31.88	± 0.20

[a] Corrected for ^{37}Ar and ^{39}Ar decay

[b] Ages calculated relative to 28.34 Ma Taylor Creek Rhyolite standard; italics indicate steps omitted from the plateau age calculation, see text for details.

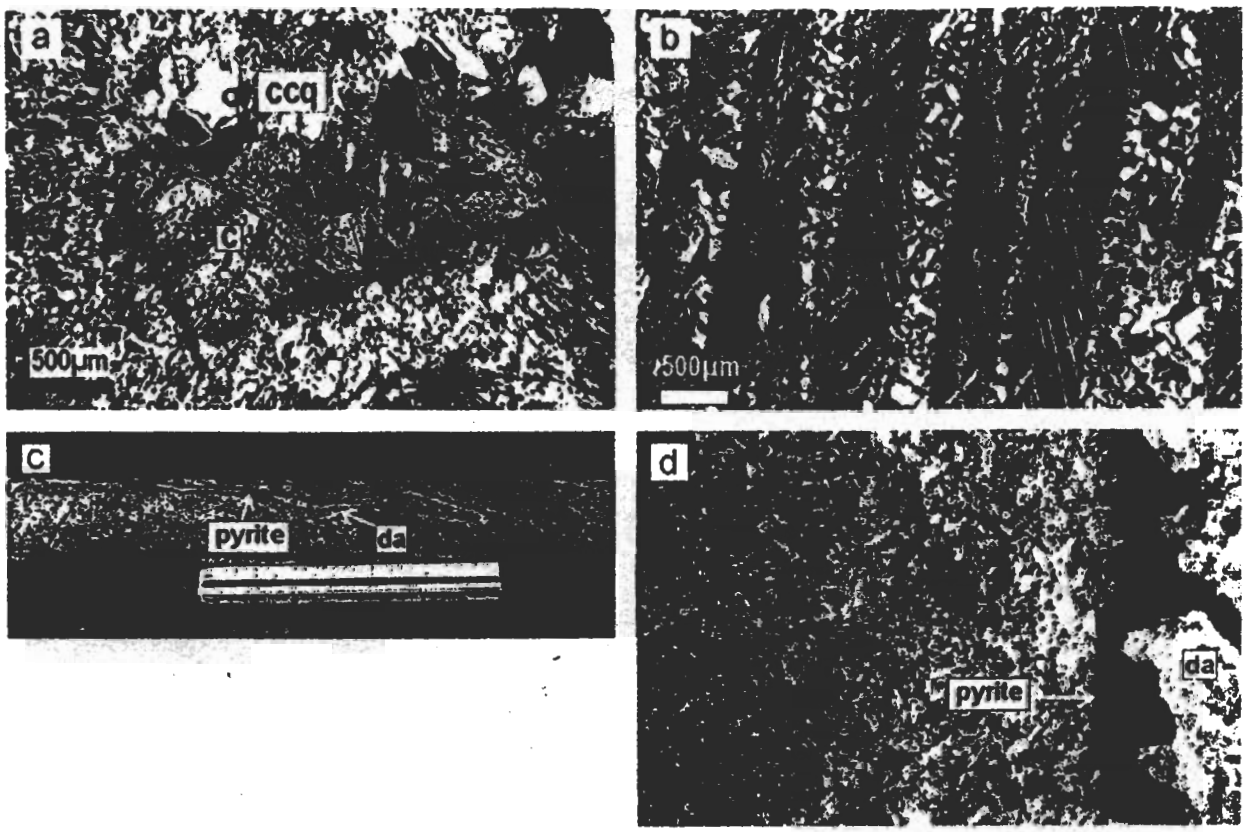

Fig. 7 (a) Geode of coarse-crystalline quartz with carbonate infill (third stage). (b) Third stage coarse-crystalline quartz (ccq) and bladed parallel type calcite (c). (c) Late vein (forth stage) composed by pyrite on its margins followed by dolomite-ankerite (da). (d) Same fracture. Dolomite-ankerite forms a halo overlapping quartz-adularia-pyrite alteration

Eocene–Oligocene sedimentary rocks. The latter is represented by sandstones unaffected by hydrothermal alteration, which cover the northern part of the deposit.

8. Sr and Pb isotope compositions of carbonates and pyrite

Sr and Pb isotopes were measured by standard TIMS procedures at the University of Geneva, Switzerland, following the methods of Valenza et al. (2000) and Chiaradia and Fontboté (2002). Sr isotope ratios on carbonate and Pb isotope ratios from pyrite at Ada Tepe along with whole rock Sr and Pb isotope ratios of the leachate fraction of a sample from Synap prospect, 2 km west of Ada Tepe, are presented in Table 3 and Figs. 9 and 10. The Ada Tepe carbonate is from a late stage ankerite-dolomite vein, taken from a drill-core sample (AT01-22) at 99.6 m depth. The bulk rock (sample Sin2000-28) from Synap is from sericite-adularia alteration from the surface. Pyrite from Ada Tepe is from a strongly silicified sample (Km2000-6). Pyrite from Synap is from the same hand sample Sin2000-28 on which the Sr was measured. Both samples belong to the early alteration. The initial $^{87}Sr/^{86}Sr$ ratio of the whole rock, corrected for 35 Ma, is 0.70809. The pyrite sample and whole rock leachate show identical $^{207}Pb/^{204}Pb$ (15.68) and $^{208}Pb/^{204}Pb$ (38.85) ratios and slightly different $^{206}Pb/^{204}Pb$ ratios (18.71 in Ada Tepe and 18.66 in Synap). The Sr and Pb isotope data are compared with those of local Paleogene volcanic rocks and dykes and the Rhodope metamorphic rocks in Figs. 9 and 10.

9. Discussion

9.1. Physical environment

Epithermal quartz from the Ada Tepe deposit is poor in fluid inclusions, particularly the early microcrystalline quartz and opal. Euhedral late sugary quartz is the only phase which contains larger fluid inclusions, but with no reliable characteristics that may allow to classify them as primary inclusions. For the similar Sleeper deposit, U.S.A., Saunders (1994) suggested that quartz formed by transformation of poorly ordered silica may exclude trapped fluids, thus precluding the use of microthermometry to constrain the physicochemical conditions of silica and gold deposition.

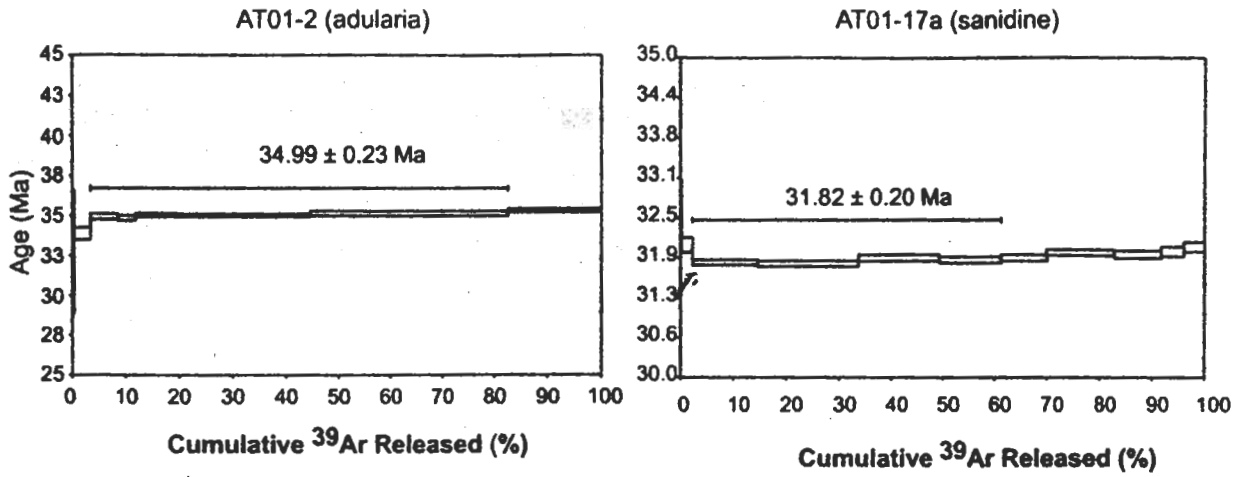

Fig. 8 $^{40}Ar/^{39}Ar$ incremental-heating age spectra for adularia from Ada Tepe and sanidine from rhyolite dyke from Kessebir dome.

The presence of adularia that spans the time of hydrothermal mineralization from the early microcrystalline stage to deposition of bonanza electrum bands accompanied by early bladed calcite and followed by late bladed Ca–Mg–Fe carbonates is consistent with boiling during most of the hydrothermal process (Izava et al., 1990; Simmons and Christenson, 1994). Evidence for boiling occurs throughout the Ada Tepe deposit from the present-day surface down to the detachment surface. The absence of bladed calcite in the veinlets beneath the detachment, however, suggests that boiling started as the fluid reached the sedimentary sequence. Boiling cools the fluid and concentrates dissolved silica, leading to precipitation of silica colloids (Saunders, 1994). Thus, much of the mineralization in The Wall appears to coincide with the onset of boiling.

Thermal conditions can be roughly evaluated on the basis of the distribution of temperature-sensitive minerals. The absence of epidote in the host-rock alteration can be interpreted in favor of a low-temperature (<240 °C) for the initial fluids (Bird et al., 1984; Rayes, 1990). This is confirmed by the large distribution of kaolinite, crystallizing at temperatures <200 °C (Simmons and Browne, 2000) and deposition of microcrystalline silica (chalcedony) or its transformation to jigsaw quartz in the stage of massive silicification, which occurs at temperature of >180 °C (Fournier, 1985). Thus, the temperature of the early fluid seems to have been 200–180 °C. Deposition of bonanza opal-electrum bands, however, requires considerably lower temperatures (100–150 °C; Hedenquist et al., 2000), suggesting a significant drop of temperature (see also Saunders, 1994). Such cooling can be attributed to simple boiling, causing cooling during decompression and increase in pH and fO_2 which accompanies the loss of dissolved gasses. Alternatively, it can be the result of mixing with cooler meteoric groundwater, in a manner similar to that described for the Hishikari low-sulfidation deposit (Izawa et al., 1990). Mixing of cool oxidized meteoric water with a hot, reduced deep crustal fluid has been proposed for low-angle faults bounding several metamorphic core complexes (Kerrich and Rehring, 1987; Kerrich and Hyndman, 1987; Spencer and Welty, 1986; Beaudoin et al., 1991).

9.2. Paleodepth

Mineralogical and textural characteristics, such as bladed carbonates and crustiform and colloform banded chalcedony and opaline silica plus adularia (Izawa et al., 1990; Cook and Simmons, 2000) suggest that the depth for the formation of mineralization at Ada Tepe deposit was shallow. In the absence of precise temperature and salinity data from fluid inclusion studies, the paleodepth of the Ada Tepe deposit cannot be precisely constrained. A minimum depth can be roughly estimated assuming boiling of low salinity solutions (<1 wt% NaCl equivalent) at a temperature of 200 °C. The depth of boiling of such a fluid below the water table is about 160–170 m (Haas, 1971).

Table 3 Sr and Pb isotope compositions of carbonate, pyrite and whole rock from Ada Tepe deposit and Synap mineralization.

Sample	AT 01-22 carbonate	Sin2000-28 bulk rock	KM 2000-6 pyrite
Rb		218	
Sr		82	
$^{87}Rb/^{86}Sr$		7.6950	
$^{87}Sr/^{86}Sr$	0.709270±14	0.711911±10	
$(^{87}Sr/^{86}Sr)_i$		0.70809	
$^{206}Pb/^{204}Pb$		18.663	18.707
$^{207}Pb/^{204}Pb$		15.682	15.684
$^{208}Pb/^{204}Pb$		38.849	38.843

For fluids under a hydrodynamic gradient and containing dissolved CO_2, the depth of boiling would be somewhat deeper (Hedenquist and Henley, 1985). This is consistent with the 350 m thickness of the host Shavarovo Formation (Goranov and Atanasov, 1992), which implies that the overlying coal-bearing-sandstone and marl-limestone formations had not yet been deposited when the ore formed.

9.3. Sources and relationships among mineralization, extension and magmatism

The new $^{40}Ar/^{39}Ar$ ages from adularia and sanidine have been compared with those from muscovite and biotite in the Kessebir dome (Bonev et al., accepted), K–Ar ages of nearby Iran Tepe volcano (Lilov et al., 1987) and intra-plate alkaline basalts (Marchev et al., 1997, 1998) to clarify relationships between volcanism, thermal events in the Kessebir dome and mineralization in the Ada Tepe deposit. As discussed above, the $^{40}Ar/^{39}Ar$ total fusion age of adularia (Marchev et al., 2003) shows that the mineralization at Ada Tepe formed at 35 Ma. Mineralization may have been coeval with 35 Ma lavas of the Iran Tepe paleovolcano (Lilov et al., 1987; Pecskay, pers. comm.), however, the uncertainties of the dating methods do not rule out differences in age on the order of several 100 kyr. Notwithstanding, field relationships indicate that volcanic activity of the Iran Tepe volcano is younger than the Krumovgrad group.

Another possible source of fluids and metals is the magmatism of the Kessebir dome itself. Comparison of the timing of Ada Tepe mineralization (35 Ma), the Kessebir rhyolite dyke (31.82 ± 0.20 Ma) and K–Ar ages of intra-plate alkaline basalts (28–26 Ma) show that mineralization preceded by at least 3 Ma the rhyolitic magmatism and at least 6 Ma the intra-plate basalts. Thus, it is highly unlikely that this younger igneous activity was the source of Ada Tepe mineralizing fluids or heat.

Mineralization at Ada Tepe is ca. 3 Ma younger than the $^{40}Ar/^{39}Ar$ ages of the muscovite (38.13 ± 0.36) and biotite (37.73 ± 0.25 Ma) from the lower plate of the Kessebir dome. Recently obtained older $^{40}Ar/^{39}Ar$ age for amphibole (45 ± 2 Ma) and similar age for the muscovite (39 ± 1 Ma) in the Biala Reka dome (Mukasa et al., 2003) have been interpreted as cooling ages for the upper plate. Therefore, muscovite and biotite ages from Kessebir can be interpreted as cooling of the lower plate rocks to below 350–300 °C following the Maastrichtian–Paleocene metamorphism (Marchev et al., 2004). The latter ages are generally consistent with a 42–35 Ma range of ages, obtained earlier by Peytcheva (1997) for the closing of Rb–Sr system in the granitoids in Biala Reka and Kessebir, after a presumable amphibolite facies metamorphism. Ore deposit formation at ~35 Ma in the hanging wall of the Tokachka detachment coincides with late stage brittle extension after cooling of the basement rocks at temperatures < 200 °C (Bonev et al., accepted). The highest grade portion of the ore mineralization (The Wall) is dominated by multiple phases of veining and brecciation suggesting a syndetachment evolution of the hydrothermal process. The presence of several unconformities in the overlying Upper Eocene–Lower Oligocene coal-bearing-sandstone and marl-limestone formations (Goranov and Atanassov, 1992; Boyanov and Goranov, 1994, 2001), suggests a continuation of the uplift and exhumation of the Kessebir dome even several million years after the formation of the Ada Tepe deposit.

Probable source rocks for the Sr (Ca) and Pb can be constrained by comparison of the Sr and Pb isotope ratios of carbonates and pyrites from Ada Tepe with the major source rocks (Figs. 9 and

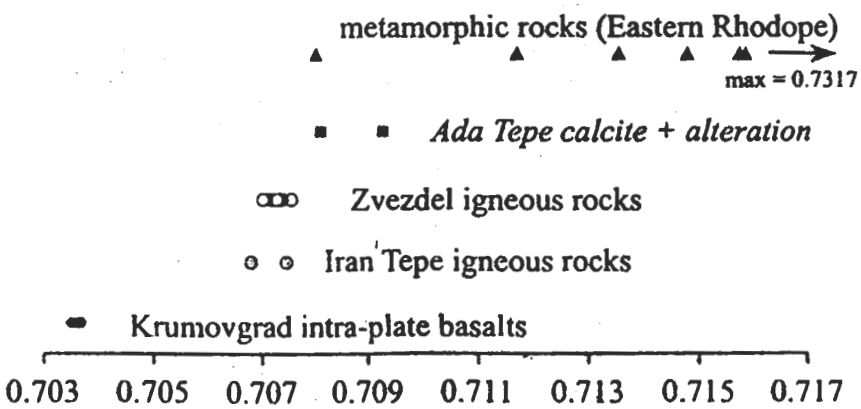

Fig. 9 Sr isotope composition of calcite from Ada Tepe and whole rock sample from Synap compared with Krumovgrad area igneous and metamorphic rocks. Data for the intra-plate basalts – Marchev et al., 1998; for the Zvezdel and Iran Tepe lavas – Marchev, unpublished data; for the metamorphic rocks – Peytcheva et al., 1992 and Pljusnin et al., 1988).

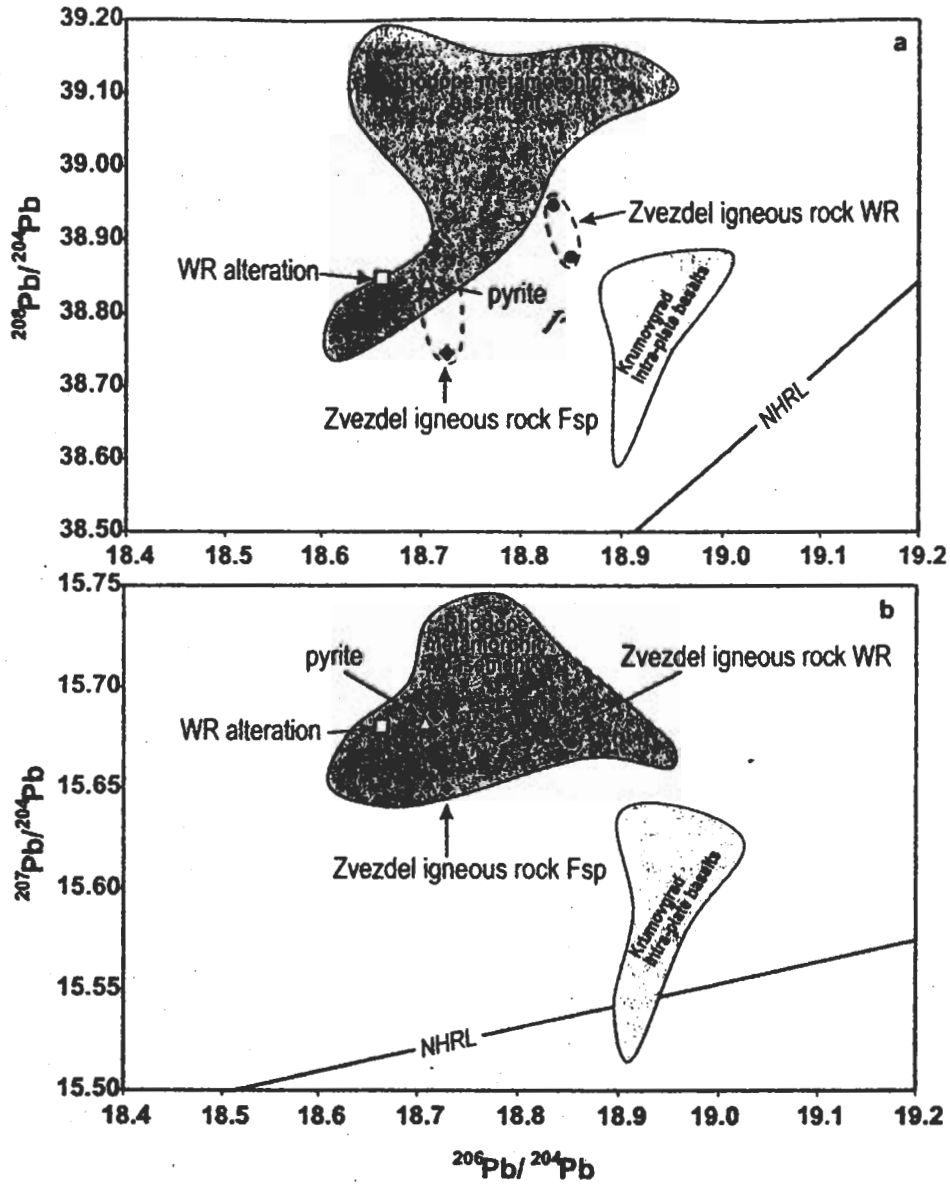

Fig. 10 Pb isotope composition of pyrite (Ada Tepe) and whole rock alteration (Synap), compared with feldspars and whole rocks from Zvezdel Oligocene volcano (Marchev et al., unpubl. data) and whole rocks from Krumovgrad intra-plate basalts (Marchev et al. (1998) and Rhodope metamorphic rocks from Frei (1995).

10). Bulk rock and carbonate Sr isotope data (0.70809–0.70927), lie within the lower range of present-day $^{87}Sr/^{86}Sr$ isotopic ratios between 0.708–0.737 for the prevailing gneissic metamorphic rock within the Eastern Rhodopes (Peytcheva et al., 1992) and are higher than the Sr isotopic values of the nearby younger igneous rocks from Iran Tepe and Zvezdel volcanoes (0.70641–0.70741; Marchev et al., unpubl. data). It appears likely that the hydrothermal Sr and, by inference Ca, is mostly of metamorphic origin or represent a mixture of metamorphic and small amount of old magmatic source isotopically similar to Iran Tepe and Zvezdel magmas (see below).

Pyrite Pb isotope ratios overlap with the field of feldspars from Zvezdel igneous rocks, however, the leachate fraction of the whole rock sample from Synap has a slightly lower $^{206}Pb/^{204}Pb$ ratio than the feldspars. Collectively, the two samples plot in the fields of the Rhodope metamorphic rocks. From these data, it is not possible to discriminate between a metamorphic and an igneous origin of Pb in the hydrothermal fluid. This is not surprising as orogenic igneous rocks of the Eastern Rhodopes were strongly contaminated with crustal Pb (Marchev et al. 1998 and 2004) and differ isotopically from the asthenospheric-derived Krumovgrad intra-plate basalts (Fig. 10). Therefore, isotopic homogenization of the orogenic igneous and metamorphic rocks in the region limits the possibility to discriminate between these two sources. Nevertheless, it may be suggested that fluid circulation through the metamorphic basement rocks and metamorphic-derived sediments

would cause a large contribution from metamorphic lead.

Thus, the simplest genetic model to explain the geology, geochronology, and Sr and Pb isotopes involves hydrothermal convection through the Paleozoic metamorphic basement. The close temporal association of mineralization at Ada Tepe with the exhumation processes and formation of the Kessebir dome favours a genetic link between them. We propose that the metamorphic basement rocks provided the heat to drive the hydrothermal system. During exhumation, however, the lower plate of the Kessebir metamorphic core complex experienced cooling and decompression since the Upper Cretaceous (Marchev et al., 2004). This has been used in other metamorphic complexes (Smith et al., 1991) to argue that prograde metamorphic devolatilization of the lower plate is unlikely to generate fluid responsible for mineralization during extension. These authors suggested that igneous rather than metamorphic fluid source is more likely for the metamorphic core complex-related mineralization. This apparent contradiction can be explained by asthenospheric upwelling that was operating in the Eastern Rhodope area (Marchev et al., 2004) causing retrograde metamorphism at shallow levels and at the same time resulting in prograde metamorphism at deeper levels observed by the high heat flow in the region. Although magmatic activity seems to be younger than the ore mineralization, the first erupted lavas of Iran Tepe were close in time. The beginning of this volcanism was probably preceded by accumulation of magma at greater depths. Under such conditions, fluids liberated by deep prograde devolatilization reactions and/or mantle degassing could ascend to form low temperature fluids.

9.4. Gold deposits associated with detachment faults

Different types of mineralization in low-angle detachment faults associated with metamorphic core complexes are described mostly in the southwestern United States. These include Picacho, (Drobeck et al., 1986; Liebler, 1988) and Bullard Peak (Roddy et al., 1988), Southwestern Arizona; and Riverside Pass (Wilkinson et al., 1988) and Whipple-Buckskin-Rawhide (Spencer and Welty, 1986), Southeastern California. Another example is in the Kokanee Range, Southern British Columbia, Canada (Beaudoin et al., 1991).

These kinds of deposits are divided by Eng et al. (1988) into two categories: base-metal enriched (Whipple-Buckskin-Rawhide and Kokanee deposits) and base-metal poor (Picacho and Riverside Pass). In the base-metal poor deposits gold is typically associated with silicification and hematite (Picacho), or hematite and chrisocolla (Riverside Pass). Pyrite, which is entirely oxidized in Riverside Pass, is the principal sulfide mineral. Quartz and lesser calcite are the main gangue minerals

Mineralization at Ada Tepe deposit shares many characteristics with Picacho and Riverside Pass, including association of gold with multiple episodes of silicification and veining within shallowly dipping detachment faults, and a low content of base-metals and As. However, comparison of the characteristics of Ada Tepe to other base-metal poor detachment-related mineralizations reveals several notable differences. These include lack of copper and specular hematite, a relatively high content of adularia and various silica polymorphs and carbonates. These features may reflect differences in crustal compositions and history, the nature of the ore-forming hydrothermal fluids, and physico-chemical conditions at the focus of ore deposition.

10. Conclusions

(1) Based on alteration, mineralization and textures, we classify Ada Tepe as a low-sulfidation epithermal gold deposit, hosted in sedimentary rocks.

(2) The Tokachka low-angle detachment fault and the steep listric faults in the Maastrichtian-Paleocene sedimentary sequence were the major sites of gold mineralization. There are many indicators, including breccias, that synmineralization movement took place along the detachment surface.

(3) The deposit formed at shallow depth, less than 200–250 m below the paleosurface. Microcrystalline quartz and opal, which are the main silica polymorphs crystallizing with the electrum bands, preclude the use of fluid inclusion to constrain the conditions of gold deposition. From other alteration minerals temperature of formation is evaluated to <200 °C. The mineralogy suggests that the fluid boiled throughout the deposit.

(4) Mineralization is an exclusively Au system with traces of As and with no base metals. The majority of the gold occurs as electrum with 73–76% Au, which is reflected in the average Au/Ag ratio (~3) of the deposit.

(5) The $^{40}Ar/^{39}Ar$ age of adularia indicates that the ore was deposited at Ada Tepe at 35.0 ± 0.2 Ma. This age is ~3 Ma younger than the closure of metamorphic muscovite and biotite at ~350 °C in the underlying basement, and 3 Ma older than sa-

nidine in the nearest rhyolite, thereby precluding local magmatism as a source of fluids or heat.

(6) Sr and Pb isotope ratios are consistent with the idea that metals and carbonates were probably derived from the metamorphic basement rocks with a possible contribution from an igneous source.

(7) Collectively, these data suggest an intimate association of Ada Tepe Au mineralization to the metamorphic core-complex formation rather than to the local magmatism.

Acknowledgments

This is a contribution to the ABCD-GEODE program of the European Science Foundation. Supported by the Swiss National Science Foundation Joint Research Project 7BUPJ062276 and grants 21-59041.99 and 200020-101853. $^{40}Ar/^{39}Ar$ analyses at UW-Madison supported by US NSF grants EAR-10114055 and EAR-0337667 to Singer. BMM gave permission to publish these results and provided financial support. The authors appreciate the comments and helpful reviews of the journal reviewers D. Altherton, N. Skarpelis and Albrecht von Quadt. Denis Fontignie and Massimo Chiaradia (Universities of Geneva, Switzerland and Leeds, U.K.) are thanked for the Sr and Pb isotope analyses. Thanks are owed to Albrecht von Quadt and Ivan Bonev for etching of gold samples and the SEM pictures of the etched samples, respectively.

References

Atanasov, G. and Goranov, A. (1984): On the Palaeogeography of the East Rhodopes. *C. R. Acad. bulg. Sci.*, **37(6)**, 783–784.

Beaudoin, G., Taylor, B.E. and Sangster, D.F. (1991): Silver-lead-zinc veins, metamorphic core complexes, and hydraulic regimes during crustal extension. *Geology*, **19**, 1217–1220.

Belmustakova, H., Boyanov, I., Ivanov, I. and Lilov, P. (1995): Granitoid bodies in the Byala Reka dome. *C. R. Acad. bulg. Sci.*, **48 (4)**, 37–40 (in Russian).

Bird, D.K., Schiffman, P., Elders, W.A., Williams, A.E. and McDowell, S.D. (1984): Calc-silicate mineralization in active geothermal systems. *Econ. Geol.*, **79**, 671–695.

Bonev, N. (1996): Tokachka shear zone southwest of Krumovgrad in Eastern Rhodopes, Bulgaria: an extensional detachment. *Ann. Univ. Sofia*, **89**, 97–106.

Bonev, N. (2002): Structure and evolution of the Kessebir gneiss dome, Eastern Rodopes. PhD. thesis, Univ. of Sofia, unpubl., 282 pp. (in Bulgarian).

Bonev, N., Marchev, P. and Singer, B. (accepted): Interference between tectonic, ore-forming and magmatic processes during the Tertiary extensional exhumation in the Eastern Rhodope (Bulgaria): $^{40}Ar/^{39}Ar$ geochronology constraints. *Geodin. Acta*.

Boyanov, I. and Goranov, A. (1994): Paleocene–Eocene sediments from the Northern periphery of the Borovica depression and their correlation with similar sediments in the East Rhodopean Paleogene depression. *Rev. Bulg. Geol. Soc.*, **55(1)**, 83–102 (in Bulgarian with English abstract).

Boyanov, I. and Goranov, A. (2001): Late Alpine (Paleogene) superimposed depressions in parts of Southeast Bulgaria. *Geol. Balc.*, **34(3–4)**, 3–36.

Carrigan, C., Mukasa, S., Haydoutov, I. and Kolcheva, K. (2003): Ion microprobe U–Pb zircon ages of pre-Alpine rocks in the Balkan, Sredna Gora, and Rhodope terranes of Bulgaria: Constraints on Neoproterozoic and Variscan tectonic evolution. *J. Czech Geol. Soc.* Abstract volume **48/1–2**, 32–33.

Chiaradia, M. and Fontboté, L. (2002): Separate lead isotope analyses of leachate and residue rock fractions: implications for metal source tracing in ore deposit studies. *Mineral. Deposita*, **38**, 185–195.

Cook, D.R and Simmons, S.F. (2000): Characteristics and genesis of epithermal gold deposits. *Reviews Econ. Geol.*, **13**, 221–224.

Crummy, J. (2002): A speculative genetic model for the location of gold mineralization on the Krumovgrad license, SE Rhodope, Bulgaria. *Geol. Mineral. Res.*, **1**, 20–24.

Duffield, W. and Dalrymple, G.B. (1990): The Taylor Creek Rhyolite of New Mexico: a rapidly emplaced field of lava domes and flows. *Bull. Volcanol.*, **52**, 475–487.

Drobeck, P.A., Hillemeyer, J.L., Frost, E.G and Liebler, G.S. (1986): The Picacho Mine: a gold mineralized detachment in southeastern California. In: Beatty, B. and Wilkinson, P.A.K. (eds): Frontiers in geology and ore deposits of Arizona and the Southwest. *Arizona Geol. Soc. Digest.* **XVI**, Tucson, 187–221.

Eng, T., Boden D.R., Reischman, M.R. and Biggs, J.O. (1995): Geology and mineralization of the Bullfrog Mine and vicinity, Nye County, Nevada. In: Coyner, A.R. and Fahey, P.L. (eds.): Geology and ore deposits of the American Cordillera. Symposium Proceedings, Geol. Soc. Nevada, Reno/Sparks, Nevada. **Vol.1**, 353–400.

Fournier, R.O. (1985): Silica minerals as indicators of conditions during gold deposition: *U.S. Geol. Survey Bull.* **1646**, 15–26.

Frei, R. (1995): Evolution of mineralizing fluid in the porphyry copper system of the Scouries deposit, Northeast Chalkidiki (Greece): Evidence from combined Pb–Sr and stable isotope data. *Econ. Geol.*, **90**, 746–762.

Goranov, A. and Atanasov, G. (1992): Lithostratigraphy and formation conditions of Maastrichtian-Paleocene deposit in Krumovgrad District. *Geol. Balc.*, **22(3)**, 71–82.

Haas, J.L. Jr. (1971): The effect of salinity on the maximum thermal gradient of a hydrothermal system at hydrostatic pressure. *Econ. Geol.*, **66**, 940–946.

Hedenquist, J.W. and Henley, R.W. (1985): The importance of CO_2 on freezing point measurment of fluid inclusions: evidence from active geothermal systems and implications for epithermal ore deposition. *Econ. Geol.*, **80**, 1379–1399.

Hedenquist, J.W. Arribas, A.R. and Gonzales-Urien, E. (2000): Exploration for epithermal gold deposits. *Soc. Econ. Geol. Reviews*, **13**, 245–277.

Izawa, E., Urashima, Y., Ibaraki, K., Suzuki, R., Yokoyama, T., Kawasaki, K., Koga, A. and Taguchi, S. (1990): The Hishikari gold deposit: High grade epithermal veins in Quaternary volcanics of southern Kyushu, Japan. *J. Geochem. Explor.*, **36**, 1–56.

Kerrich, R. and Rehring, W. (1987): Fluid motion associated with Tertiary mylonitization and detachment faulting: $^{18}O/^{16}O$ evidence from the Picacho metamorphic core complex, Arizona. *Geology*, **15**, 58–62.

Kerrich, R. and Hyndman, D. (1987): Thermal and fluid regimes in the Bitteroot lobe-Sapphire block detachment zone, Montana: Evidence from $^{18}O/^{16}O$ and geologic relations. *Geol. Soc. Am. Bull.*, **97**, 147–155.

Kolcheva, K. and Eskenazy, G. (1988): Geochemistry of metaeclogites from the Central and Eastern Rhodope Mts (Bulgaria). *Geol. Balc.*, **18**, 61–78.

Kozhoukharov, D., Kozhoukharova, E. and Papanikolaou, D. (1988): Precambrian in the Rhodope massif. In: Zoubek, V. (ed.): Precambrian in Younger Fold Belts, Chichester, 723–778.

Kozhoukharova, E. (1984): Origin and structural position of the serpentinized ultrabasic rocks of the Precambrian ophiolitic association in the Rhodope Massif. I: Geologic position and composition of ophiolite association. *Geol. Balc.*, **14**, 9–36 (in Russian).

Kunov, A., Stamatova, V., Atanasova, R. and Petrova, P. (2001): The Ada Tepe Au-Ag-polymetallic occurrence of low-sulfidation (adularia-sericite) type in Krumovgrad district. *Mining and Geol.*, **2001(4)**, 16–20 (in Bulgarian).

Liebler, G.S. (1988): Geology and gold mineralization at the Picacho mine, Imperial County, California. In: Schafer, R.W., Cooper, J.J. and Vikre P.G. (eds): Bulk mineable precious metal deposits of the Western United States, Symposium Proceedings, Geol. Soc. Nevada, Reno/Sparks, Nevada. Part IV, Gold-silver deposits associated with detachment faults. 453–504.

Lilov, P., Yanev, Y. and Marchev, P. (1987): K/Ar dating of the Eastern Rhodopes Paleogene magmatism. *Geol. Balc.*, **17(6)**, 49–58.

Lips, A.L.W., White, S.H. and Wijbrans, J.R. (2000): Middle-Late Alpine thermotectonic evolution of the southern Rhodope Massif, Greece. *Geodin. Acta*, **13**, 281–292.

Marchev, P., Harkovska, A., Pecskay, Z., Vaselli, O. and Downes, H. (1997): Nature and age of the alkaline basaltic magmatism south-east of Krumovgrad, SE-Bulgaria. *C. R. Acad. bulg. Sci.*, **50(4)**, 77–80.

Marchev, P., Vaselli, O., Downes, H., Pinarelli, L., Ingram, G., Rogers, G. and Raicheva, R. (1998): Petrology and geochemistry of alkaline basalts and lamprophyres: implications for the chemical composition of the upper mantle beneath the Eastern Rhodopes (Bulgaria). In: Christofides, G., Marchev, P. and Serri, G. (eds.): Tertiary magmatism of the Rhodopian region. *Acta Vulcanologica*, **10/2**, 233–242.

Marchev, P. and Singer, B. (2002): $^{40}Ar/^{39}Ar$ geochronology of magmatism and hydrothermal activity of the Madjarovo base-precious metal ore district, eastern Rhodopes, Bulgaria. In: Blundell, D., Neubauer, F. and von Quadt, A. (eds.): The timing and location of major ore deposits in an evolving orogen. *Geol. Soc. London Spec. Publ.*, **204**, 137–150.

Marchev, P., Singer, B., Andrew, C., Hasson, A., Moritz, R. and Bonev, N. (2003): Characteristics and preliminary $^{40}Ar/^{39}Ar$ and $^{87}Sr/^{86}Sr$ data of the Upper Eocene sedimentary-hosted low-sulfidation gold deposits Ada Tepe and Rosino, SE Bulgaria: possible relation with core complex formation. In: Eliopoulos et al. (eds.): Mineral Exploration and Sustainable Development. Millpress, Rotterdam, 1193–1196.

Marchev, P., Raicheva, R., Downes, H., Vaselli, O., Massimo, C. and Moritz, R. (2004): Compositional diversity of Eocene-Oligocene basaltic magmatism in the Eastern Rhodopes, SE Bulgaria: implications for its genesis and geological setting. *Tectonophysics*, **393**, 301–328.

Marchev, P., Raicheva, R., Singer, B., Downes, H., Amov, B. and Moritz, R. (2000): Isotopic evidence for the origin of Paleogene magmatism and epithermal ore deposits of the Rhodope Massif. In: Geodynamics and Ore Deposit Evolution of the Alpine-Balkan-Carpathian-Dinaride-Province. Borovets, Abstracts ABCD-GEODE 2000 workshop Borovets, Bulgaria, p. 47.

Mposkos, E. and Krohe, A. (2000): Petrological and structural evolution of continental high pressure (HP) metamorphic rocks in the Alpine Rhodope Domain (N. Greece). In: Panayides, I., Xenopontos, C. and Malpas, J. (eds.): Proceedings of the 3rd International Conf. on the Geology of the Eastern Mediterranean (Nicosia, Cyprus). Geol. Survey, Nicosia, Cyprus, 221–232.

Mposkos, E. and Wawrzenitz, N. (1995): Metapegmatites and pegmatites bracketing the time of high P metamorphism in polymetamorphic rocks of the E-Rhodope, N. Greece: Petrological and geochronological constraints. *Geol. Soc. Greece Spec. Publ.*, **4(2)**, 602–608.

Mukasa, S., Haydoutov, I., Carrigan, C. and Kolcheva, K. (2003): Thermobarometry and $^{40}Ar/^{39}Ar$ ages of eclogitic and gneissic rocks in the Sredna Gora and Rhodope terranes of Bulgaria. *J. Czech Geol. Soc.* Abstract volume **48/1–2**, 94–95.

Ovtcharova, M., Quadt, A. von, Heinrich, C.A., Frank, M. and Kaiser-Rohrmeier, M. (2003). Triggering of hydrothermal ore mineralization in the Central Rhodopean Core Complex (Bulgaria) – Insight from isotope and geochronological studies on Tertiary magmatism and migmatization. In: Eliopoulos et al. (eds.): Mineral Exploration and Sustainable Development. Millpress, Rotterdam, 367–370

Peytcheva, I. (1997): The Alpine metamorphism in Eastern Rhodopes – Rb–Sr isotope data. *Rev. Bulg. Geol. Soc.*, **58(3)**, 157–165 (in Bulgarian with English abstract).

Peytcheva, I., Kostitsin, Y., Salnikova, E., Ovtcharova, M. and von Quadt, A. (1999): The Variscan orogen in Bulgaria – new isotope-geochemical data. *Rom. Jour. tectonics and regional geology*, **77**, Abstract volume, p. 72.

Peytcheva, I., Kostitsin, J.A. and Shukolyukov, J.A. (1992): Rb–Sr isotope system of gneisses in the South-Eastern Rhodopes (Bulgaria). *C. R. Acad. bulg. Sci.*, **45(10)**, 65–68 (in Russian).

Peytcheva, I., Ovcharova, M., Sarov, S. and Kostitsin, Y. (1998): Age and metamorphic evolution of metagranites from Kessebir reka region, Eastern Rhodopes – Rb–Sr isotope data. Abstracts XVI Congress CBGA, Austria, Vienna.

Peytcheva, I. and von Quadt, A. (1995): U–Pb dating of metagranites from Byala-Reka region in the East Rhodopes, Bulgaria. *Geol. Soc. Greece Spec. Publ.*, **4(2)**, 637–642.

Plyusnin, G.S., Marchev, P.G. and Antipin, V.S. (1988): Rubidium-Strontium age and genesis of the shoshonite-latite series in the Eastern-Rhodope, Bulgaria. *Dokl. Akad. Nauk SSSR*, **303(3)**, 719–724.

Reyes, A.G. (1990): Petrology of Philippine geothermal systems and the application of alteration mineralogy to their assessment. *J. Volcanol. Geotherm. Res.*, **43**, 279–309.

Ricou, L.E., Burg, J.P., Godfriaux, I. and Ivanov, Z. (1998): Rhodope and Vardar: the metamorphic and the olistostromic paired belts related to the Cretaceous subduction under Europe. *Geodin. Acta*, **11**, 285–309.

Roddy, M.S., Reynolds, S.J., Smith, B.M. and Ruiz, J. (1988): K metasomatism and detachment-related mineralization, Harcuvar Mountains, Arizona. *Geol. Soc. Am. Bull.*, **100**, 1627–1639.

Rohrmeier, M., Quadt, A.von, Handler, R., Ovtcharova, M., Ivanov, Z. and Heinrich, C. (2002): The geodynamic evolution of hydrothermal vein deposits in the Madan metamorphic core complex, Bulgaria. *Geochim. Cosmochim. Acta*, Special Supplement,

Abstracts of the 12th Ann. Goldschmidt Conference, Davos, Switzerland, 66, S1, A645.

Sarov, S. and twelve others (1996): Report for the results of execution of the geological task "Geological mapping in scale 1:25 000 and geomorphologic mapping in scale 1:50 000 with complex prognostic evaluation of the mineral resources in the area of Krumovgrad and villages Gornoseltsi, Popsko, Djanka and Nanovitsa (Eastern Rhodopes), on area of 485 km² National geofond, IV-438.

Saunders, J.A. (1990): Colloidal transport of gold and silica in epithermal precious-metal systems: Evidence from the Sleeper deposit, Nevada. *Geology*, **18**, 757–760.

Shabatov, Y. and eight others (1965): Report for the geological mapping, accompanied with prospecting for ore mineralizations in scale 1:25 000 in 1963–1964 in part of the SE Rhodopes. Geofond of Committee of Geology, IV-217.

Saunders, J.A. (1994): Silica and gold texture in bonanza ores of the Sleeper deposit, Humbolt county, Nevada: Evidence for colloids and implications for epithermal ore-forming processes. *Econ. Geol.*, **89**, 628–638.

Simmons, S.F. and Browne, P.R.L. (2000): Hydrothermal minerals and precious metals in the Broadlands-Ohaaki geothermal system: Implications for understanding low-sulfidation epithermal environments. *Econ. Geol.*, **95**, 971–999.

Simmons, S.F. and Christenson, B.W. (1994): Origins of calcite in a boiling geothermal system. *Am. J. Sci.*, **294**, 361–400.

Singer, B. and Brown, L.L. (2002): The Santa Rosa Event: $^{40}Ar/^{39}Ar$ and paleomagnetic results from the Vales rhyolite near Jaramillo Creek, Jemez Mountains, New Mexico. *Earth Planet. Sci. Lett.*, **197**, 51–64.

Singer, B. and Marchev, P. (2000): Temporal evolution of arc magmatism and hydrothermal activity, including epithermal gold veins, Borovitsa caldera, southern Bulgaria. *Econ. Geol.*, **95**, 1155–1164.

Smith, B.M., Reynolds, S.J., Day, H.W. and Bodnar, R.J. (1991): Deep-seated fluid involvement in ductile-brittle deformation and mineralization, South Mountain metamorphic core complex, Arizona. *Geol. Soc. Am. Bull.*, **103**, 559–569.

Spencer, J.E. and Welty, J.W. (1986): Possible controls of base- and precious-metal mineralization associated with Tertiary detachment faults in the lower Colorado River trough, Arizona and California. *Geology*, **14**, 195–198.

Stoyanov, R. (1979): Metallogeny of the Rhodope Central Massif. Nedra, Moscow, 180 pp. (in Russian).

Valenza, K., Moritz, R., Mouttaqi, A., Fontignie, D. and Sharp, Z. (2000): Vein and karstic barite deposits in the Western Jebilet of Morocco: Fluid inclusion and isotope (S,O,Sr) evidence for regional fluid mixing related to Central Atlantic rifting. *Econ. Geol.*, **95**, 587–605.

Wilkinson, W.H., Wendt, C.J. and Dennis, M.D. (1988): Gold mineralization along Riverside Mountains Detachment Fault, Riverside County, California. In: Schafer, R.W., Cooper, J.J. and Vikre P.G. (eds.): Bulk mineable precious metal deposits of the Western United States, Symposium Proceedings, Geol. Soc. Nevada, Reno/Sparks, Nevada. Part IV, Gold-silver deposits associated with detachment faults, 487–504.

Received 24 March 2003
Accepted in revised form 23 July 2004
Editorial handling: A. von Quadt

N. Jb. Miner. Abh.	168	3	283–298	Stuttgart, März 1995

Mineralogy and fluid inclusion study of the Zidarovo copper polymetallic deposit, eastern Bulgaria

By

M. Tarkian, Hamburg, and **V. Breskovska**, Sofia

With 5 figures and 5 tables in the text

TARKIAN, M. & BRESKOVSKA, V.: Mineralogy and fluid inclusion study of the Zidarovo copper polymetallic deposit, eastern Bulgaria. – N. Jb. Miner. Abh. 168: 283–298; Stuttgart 1995.

Abstract: The Zidarovo polymetallic deposit is genetically related to trachyandesites and trachybasalts of Upper Cretaceous age. Four stages of vein type ore mineralization have been established; they carry the following mineral assemblages: 1. quartz–pyrite; 2. chalcopyrite–bismuthinite (including first generation gold and electrum); 3. hematite–chlorite; 4. galena–sphalerite (including a second generation of gold and electrum). Specific to Zidarovo are Bi-bearing (Bi up to 11.22 wt.%) zincian tetrahedrite and tennantite, which were deposited in the second and fourth stage of mineralization. Mineralogical data suggest that silver was enriched in hydrothermal fluids during the last stage of mineralization.

Fluid inclusions in quartz show gradually decreasing formation temperatures from early (371–310 °C) to late (292–197 °C) stage of mineralization. The lowest temperatures (150–120 °C) were obtained for sphalerites of stage four. The overall low salinities of the fluids (on average: 4.0 eq. wt.% NaCl) suggest that meteoric water was involved in mineralization. The possibility of interactions between ascending hydrothermal fluids and dilute meteoric waters is supported by geological features and mineralogical data which indicate a shallow depth of mineralization.

Key words: Zidarovo polymetallic deposit, subvolcanic–volcanic environment, Bi-bearing tetrahedrite–tennantite (cell size), gold-electrum, fluid inclusion data.

Introduction

The Zidarovo ore field represents a vein type deposit with multistage mineralization. In the last twenty years many papers have been dedicated to different geological, petrological and mineralogical problems in the Zidarovo ore field (e.g. STANISCHEVA 1971, KOVATCHEV 1976, 1983; KOVATCHEV & STRASHIMIROV 1979, MARINOV 1980, POPOV 1981, TZVETANOV 1986, TODOROV 1986). However, no comprehensive studies of ore mineral composition and of source and evolution of ore forming fluids have been carried out so far. We present here results of a detailed investigation of the composition of the ore minerals and their associations as well as a new scheme of evolutionary stages of mineraliza-

tion. The two main occurrences, Kanarata and Yurta, comprise all stages of mineralization; textural and compositional features of the ore minerals, as well as fluid inclusions in quartz and sphalerite have been studied. Ore genesis is discussed in the light of new mineralogical and fluid inclusion data.

Techniques

Microprobe analyses were carried out using a Camebax Microbeam wavelength-dispersive electron microprobe at the Department of Mineralogy and Petrology, University of Hamburg (20 kV, 20 nA, computer program PAP), and a JXA-5 Microanalyzer (25 kV, 11–18 nA, computer program NR-1) at Moscow State University, respectively. Pure elements as well as pyrite, arsenopyrite, chalcopyrite, covellite and galena were used as standards. Trace elements in chalcopyrite, galena, sphalerite, and pyrite were determined on a Perkin Elmer 3035 AAS at the Department of Mineralogy, Petrology and Ore Deposits, University of Sofia. Microthermometric measurements were carried out in 300–500 μm-thick doubly polished plates at the Department of Mineralogy and Petrology, University of Hamburg, using a Chaixmeca heating-freezing stage. The equipment is suitable for temperature measurements between −180 and 600 °C. Calibration was performed using the following melting point standards: CO_2-inclusions (M.P. −56.6 °C), destilled H_2O (M.P. 0 °C), Merck SK 70 (M.P. 70 °C), naphtalene (M.P. 80 °C), Merck 100 (M.P. 100 °C), O-toluidine (M.P. 130 °C), Na nitrite (M.P. 271 °C), and K-dichromate (M.P. 398 °C). Nitrogen gas and liquid nitrogen were used for cooling and freezing experiments.

Geological setting

The Zidarovo ore deposit is situated southwest of Burgas in the Burgas synclinorium, easternmost part of the Banato–Srednogorian metallogenic zone (Bogdanov 1987). The ore deposit is connected with a caldera structure of Upper Cretaceous age. U–Pb and Th–Pb model ages of the deposit are 153 ± 30 and 120 ± 25 Ma, respectively (Amov et al. 1985). Intensive tectono-magmatic processes during Upper Cretaceous time led to the emplacement of volcanic rocks, a ring-shaped dyke complex and intrusive rocks in the Zidarovo region (Fig. 1). The volcanogenic sequence (2000–2500 m thick) consists of trachyandesites, trachybasalts, pyroclastics and tuffs covered, in some places, by Pliocene sediments. Dyke formation took place after the effusive activity. Its ring-shaped structure is determined by intensive radial-concentric faulting. The composition of the dykes is analogous to the volcanic rocks. Intrusive rocks are emplaced in the central part of the caldera structure and penetrate the rocks of the effusive and dyke complex. The Zidarovo intrusion is elongated to the north-west. It consists of essexite, monzodiorites and alkaline quartz syenites (Marinov 1980, Marinov & Bajraktarov 1981, Popov 1981). Post-

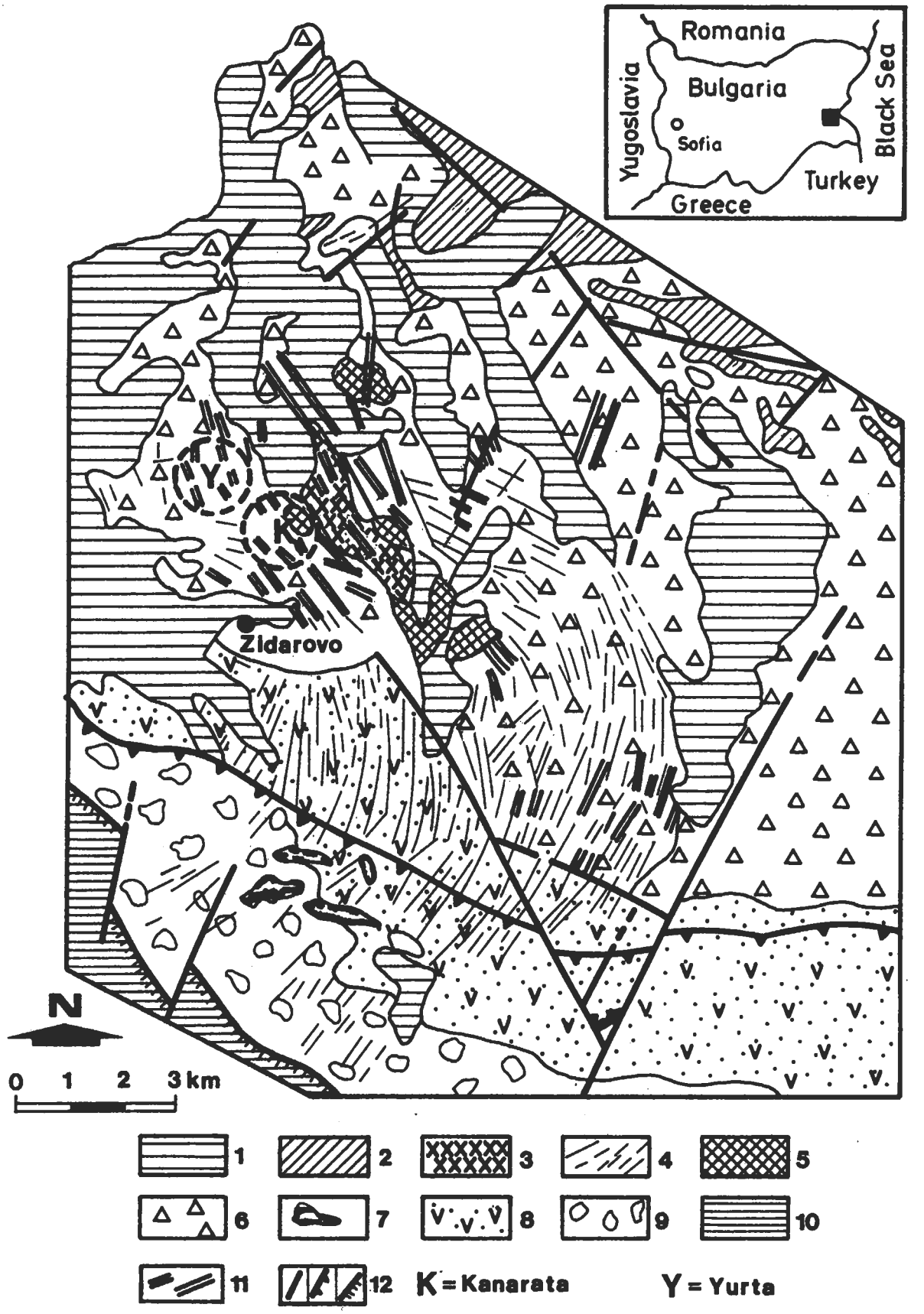

Fig. 1. Schematic geological map of Zidarovo ore field (after Popov 1981): 1 – Tertiary and Quaternary sediments; 2 – rocks of the Rossen volcano; 3 – Zidarovo intrusion; 4 – subvolcanic dykes; 5 – subvolcanic rocks (trachyandesites, trachybasalts); 6 – trachyandesite–trachybasalt lavas and pyroclastics; 7 – syenodiorite intrusion; 8 – effusive rocks of Papia volcano; 9 – olistostrome suite; 10 – Turonian sediments; 11 – ore veins; 12 – faults: a-strike-slip f., b-reverse-slip f, c-thrust f.

magmatic hydrothermal activity was responsible for the formation of polymetallic ore veins in the volcanic rocks.

Characteristics of ore veins

The ore veins have preferentially been emplaced in trachyandesites, trachybasalts and related pyroclastics. They are controlled by three groups of faults striking NW, NE and ESE. Near the contact with the Zidarovo intrusion, the ore veins display a fan-shaped structure striking between 290° and 320° (Fig. 1). The length of the ore bodies varies from several tens of meters to 1.5 km. Their width is in the range of 10 cm to 3 m. The depth of ore mineralization in Zidarovo is supposed to extend up to 900 m below the present surface.

Stages of mineralization

The host rocks of the ore veins in Zidarovo show intensive hydrothermal alteration: propylitization, silicification, argillic and potassic alteration (Tzvetanov 1986). The stages of mineralization in Zidarovo were investigated by Kovatchev (1983) and by Atanasov (1990). In the present study a new scheme of stages of mineralization is presented on the basis of textural interrelations and chemical composition of the ore minerals, and their paragenetic sequences.

In general four stages of ore mineralization were distinguished (Fig. 2). *The first stage* of mineralization can be observed both in Kanarata and Yurta (Fig. 1). Fine-grained pyrite and quartz brecciating the previously altered host rocks are typical for this stage. In most cases pyrite precipitated on the selvage of the veins. Mineral assemblages of the *second stage* were formed mainly in Kanarata. They carry the major quantity of copper, gold and bismuth, and occur as massive or nest-like aggregates in quartz veins and veinlets replacing pyrite of the first stage. The *third stage* comprises small veinlets (5–10 cm in width) of hematite and chlorite. Preferentially at Kanarata, some of them intersect the mineral parageneses of the second stage. Galena-Sphalerite assemblages with Ag-minerals are typical for the *fourth stage* of mineralization which is best represented at Yurta (Fig. 2). Specularite is the last mineral deposited in this stage.

Characteristics of the ore minerals

Chalcopyrite

Chalcopyrite is the major mineral in stage II mineralization. A second generation of chalcopyrite occurs in association with galena and sphalerite of stage IV. AAS analyses show Ag contents of 1–29 ppm and 23–325 ppm in the first and second generation of chalcopyrite, respectively. Bi (4–450 ppm) was detected only in the "early" (stage II) and Sb (12–207 ppm) only in the "late" (stage IV) chalcopyrite.

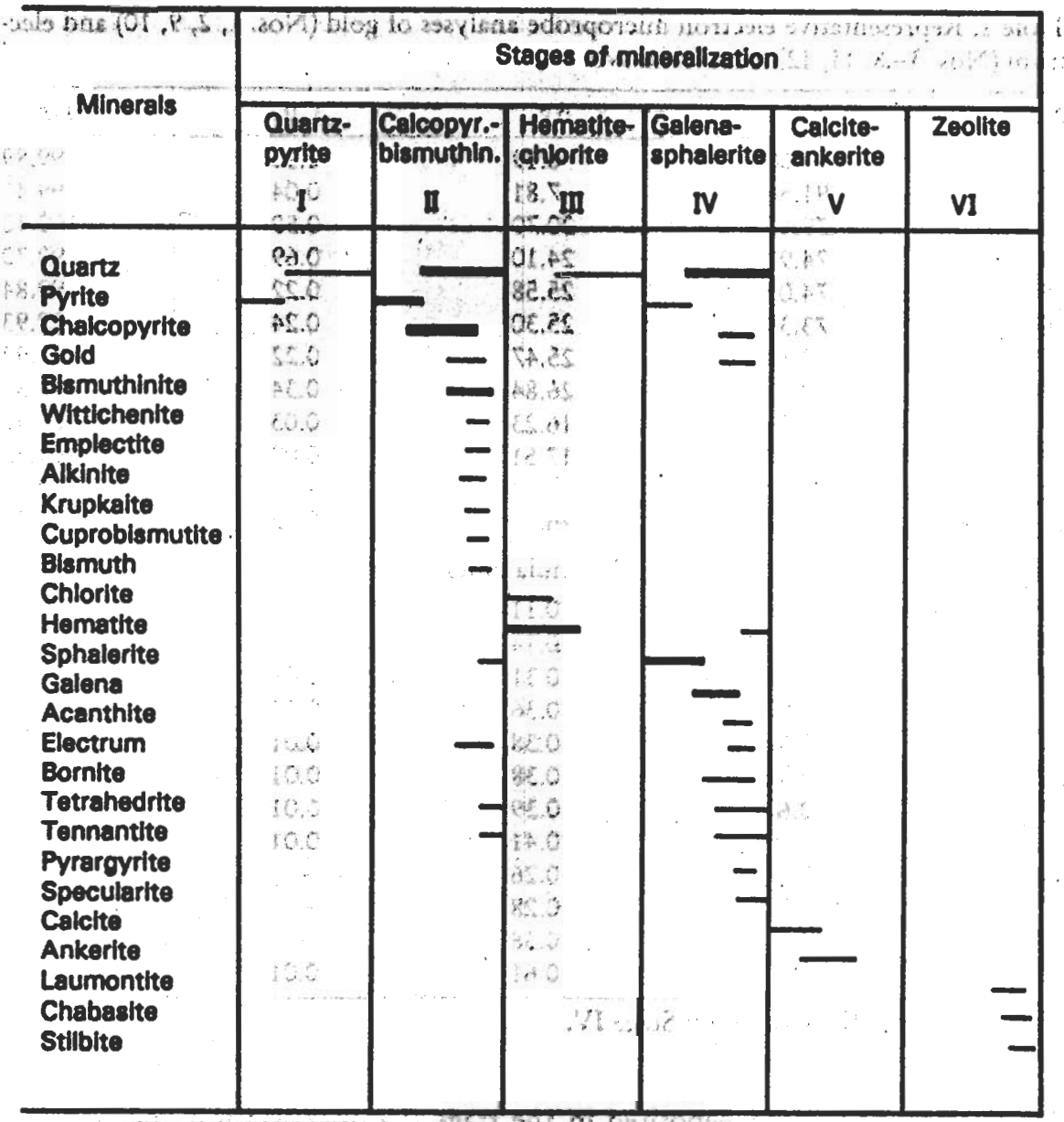

Fig. 2. Paragenetic diagram illustrating stages of mineralization in the Zidarovo ore deposit.

Gold and electrum

The deposition of gold and electrum took place during stages II and IV, in both stages in two generations. In the chalcopyrite–bismuthinite assemblage (stage II), the first generation of gold occurs in quartz. It is Ag-poor (Table 1, anal. 1+2), while the second one, always found intergrown with bismuthinite, is Ag-rich (Table 1, anal. 3–8). In the galena–sphalerite assemblage (stage IV), both generations of gold, "early" (as inclusions in quartz) and "late" one (as inclusions in galena) are Ag-rich (Table 1, anal. 9–12).

Bismuth minerals

Chemical composition of bismuth minerals is given in Table 2. They comprise native Bi, bismuthinite, aikinite, wittichenite, krupkaite and cuprobismutite.

Table 1. Representative electron microprobe analyses of gold (Nos. 1, 2, 9, 10) and electrum (Nos. 3–8, 11, 12) from Zidarovo.

No.	Au	Ag	Cu	Total
1	93.60	6.19	0.10	99.89
2	91.56	7.81	0.04	99.41
3	79.44	20.70	0.50	100.10
4	74.91	24.10	0.69	99.70
5	74.03	25.58	0.22	99.84
6	73.38	25.30	0.24	98.93
7	72.18	25.47	0.22	97.92
8	70.65	26.84	0.34	97.83
9	84.16	16.23	0.03	100.42
10	83.79	17.51	0.02	101.32
11	74.81	25.08	–	99.89
12	53.02	46.03	0.22	99.27
		Formula units		
1	0.89	0.11	–	
2	0.86	0.14	–	
3	0.67	0.31	0.01	
4	0.62	0.36	0.02	
5	0.61	0.38	0.01	
6	0.61	0.38	0.01	
7	0.60	0.39	0.01	
8	0.59	0.41	0.01	
9	0.74	0.26	–	
10	0.72	0.28	–	
11	0.62	0.38	–	
12	0.39	0.61	0.01	

Nos. 1–8: Stage II; Nos. 9–12: Stage IV.

All of them have been deposited in the stage II mineralization and occur as crystal aggregates mainly enclosed by chalcopyrite. Tetradymite and galenobismutite, reported by Kovatchev (1979) and Popov (1993), respectively, were not recorded by us.

Tetrahedrite–tennantite

Members of this group reveal considerable compositional variations including pure tennantite and tetrahedrite as well as intermediate compositions. This is in good agreement with the fahlores from Madjarovo deposit (Tarkian & Breskovska 1990). However, in Zidarovo Fe-poor zincian tetrahedrites and tennantites predominate. They were deposited mainly in the fourth stage of mineralization. With the exception of pure tetrahedrite (Table 3, anal. 19–21) all other members of the fahlores carry only traces of Ag.

The Bi contents are of particular significance (Table 3). In the stage II mineralization only one generation of fahlores was found, exclusively as inclusions in chalcopyrite. Two analyses are devoid of Bi, while one carries 4.24 wt.% Bi

Table 2. Representative electron microprobe analyses of Bi minerals from Zidarovo.

No.	Sample	Cu	Ag	Pb	Bi	S	Total
1	27	0.45	0.01	–	98.12	0.06	98.64
2	126	0.47	0.11	–	78.61	19.44	98.63
3	126	0.38	–	–	79.09	19.43	98.90
4	7*	12.46	4.14	0.61	66.30	18.29	101.80
5	7*	12.99	3.33	0.51	67.06	18.56	102.45
6	126	19.02	–	–	60.36	19.80	99.18
7	1	19.84	0.03	–	60.83	19.60	100.30
8	27	19.48	0.07	–	59.84	19.82	99.21
9	27	35.41	5.55	–	39.69	19.75	100.40
10	7*	6.42	–	19.07	58.94	17.27	101.70
11	1	11.27	0.06	35.34	36.41	17.19	100.27
12	a-4	11.04	0.10	35.49	36.00	16.86	99.49
13	27	10.99	–	35.20	37.20	17.59	100.98
			Formula units				
1	27	0.01	–	–	0.99	–	1.00
2	126	0.03	0.01	–	1.90	3.06	5.00
3	126	0.03	–	–	1.91	3.06	5.00
4	7	7.84	1.54	0.09	12.69	22.84	45.00
5	7	8.11	1.22	0.09	12.70	22.88	45.00
6	126	0.99	–	–	0.96	2.05	4.00
7	1	1.02	–	–	0.96	2.02	4.00
8	27	1.01	–	–	0.95	2.04	4.00
9	27	2.76	0.25	–	0.94	3.05	7.00
10	7	1.09	–	1.00	3.06	5.84	11.00
11	1	1.00	–	0.98	0.99	3.03	6.00
12	a-4	0.99	0.01	0.99	0.99	3.02	6.00
13	27	0.98	–	0.95	1.00	3.07	6.00

1: Bismuth; 2–3: Bismuthinite; 4–5: Cuprobismutite; 6–8: Emplectite; 9: Wittichenite; 10: Krupkaite; 11–13: Aikinite.
* Analyst Yu. S. Borodaev, Moscow State University.

(Table 3, anal. 1–3). In the galena–sphalerite assemblage (stage IV) two different generations of fahlores were established. The first one occurs as small inclusions in galena and carries 0–3.86 wt.% Bi, while the second one was formed as rims around galena or as isolated grains with Bi-contents in the range of 0.52–11.22 wt.%. There is a clear tendency of Bi substitution in As-rich members of the fahlores (Fig. 3).

Cell dimensions of Bi-bearing fahlores

The cell sizes of the end members, tetrahedrite (a = 10.320 Å) and tennantite (a = 10.168 Å) increase with increasing Bi content (Breskovska & Tarkian 1994). With the exception of one single X-ray determination, a 10.470 Å, for Ag–Bi-bearing tetrahedrite with 1.16 Ag and 0.58 Bi atoms per formula unit (Mozgova & Tzepin 1983), no cell size data on Bi-bearing members of tetrahedrite–tennantite series have been published so far. However, substitution of

Table 3. Electron microprobe analyses of members of the tetrahedrite-tennantite series from Zidarovo.

No.	Cu	Ag	Zn	Fe	Sb	As	Bi	S	Total
1	42.31	–	6.87	2.29	–	21.49	–	28.50	101.46
2	42.11	0.05	7.12	2.15	–	21.95	–	28.59	101.97
3	38.17	0.36	7.15	1.27	17.51	6.28	4.24	25.47	100.45
4	39.02	0.54	7.34	0.65	4.40	13.19	7.84	26.30	99.28
5	40.78	0.16	7.10	0.82	1.37	20.39	0.52	27.90	99.04
6	38.13	0.57	7.34	0.82	5.13	13.69	6.77	26.67	99.12
7	38.86	0.39	7.32	0.88	7.21	14.02	3.50	26.97	99.15
8	39.90	0.20	7.35	1.03	2.71	15.27	6.36	27.01	99.83
9	36.89	0.65	7.41	1.14	11.96	6.17	11.22	24.98	100.42
10	38.12	0.38	7.26	2.43	11.14	12.00	1.77	26.26	99.36
11	39.24	0.30	7.26	2.32	8.70	14.33	2.14	26.75	101.04
12	42.11	0.02	7.49	0.67	0.61	20.30	0.08	28.21	99.49
13	42.02	–	7.29	0.51	0.82	21.16	–	28.43	100.23
14	42.09	–	7.60	0.54	4.39	18.59	–	27.99	101.20
15	38.93	0.39	7.35	0.65	15.47	9.89	0.23	26.42	99.33
16	39.72	0.23	7.13	0.80	14.48	10.25	0.93	26.19	99.73
17	39.01	0.24	7.21	0.51	17.21	8.86	–	26.16	99.20
18	41.78	0.06	6.89	1.67	0.01	21.82	–	28.59	100.82
19	29.53	10.43	6.87	–	27.91	–	–	23.32	98.06
20	28.98	10.99	7.06	–	27.58	–	–	22.77	97.38
21	25.32	16.44	4.98	0.35	26.93	0.14	–	23.07	97.23
22	41.92	0.02	6.60	1.38	2.23	19.49	–	27.72	99.36
23	41.94	0.01	6.78	1.29	3.95	17.66	–	27.71	99.34
24	40.23	0.02	6.74	2.24	0.35	18.77	3.86	27.84	100.05
25	42.68	0.30	7.72	1.14	0.95	19.96	–	28.31	101.06
			Formula calculated on the basis of 29 atoms						
1	9.72	–	1.53	0.60	–	4.18	–	12.97	29.00
2	9.63	0.01	1.58	0.56	–	4.26	–	12.96	29.00
3	9.80	0.05	1.78	0.37	2.34	1.37	0.33	12.95	28.99
4	9.82	0.08	1.80	0.19	0.58	2.82	0.60	13.12	29.01
5	9.82	0.02	1.64	0.22	0.17	4.11	0.04	13.12	29.14
6	9.56	0.08	1.79	0.24	0.67	2.91	0.52	13.24	29.01
7	9.60	0.06	1.76	0.25	0.93	2.94	0.26	13.20	29.00
8	9.79	0.03	1.75	0.29	0.34	3.18	0.47	13.13	28.98
9	9.71	0.10	1.90	0.34	1.64	1.38	0.90	13.03	29.00
10	9.47	0.06	1.75	0.69	1.44	2.53	0.13	12.93	29.00
11	9.53	0.04	1.71	0.64	1.10	2.95	0.16	12.87	29.00
12	9.88	–	1.71	0.18	0.07	4.04	0.01	13.11	29.00
13	9.80	–	1.65	0.13	0.10	4.18	–	13.13	28.99
14	9.87	–	1.75	0.14	0.54	3.70	–	13.01	28.99
15	9.74	0.06	1.79	0.19	2.02	2.10	0.02	13.09	29.01
16	9.92	0.03	1.73	0.23	1.89	2.17	0.07	12.96	29.00
17	9.83	0.04	1.76	0.15	2.26	1.89	–	13.06	28.99
18	9.65	0.01	1.55	0.44	–	4.27	–	13.08	29.00
19	8.30	1.73	1.88	–	4.09	–	–	12.99	28.99
20	8.25	1.84	1.95	–	4.10	–	–	12.85	28.99
21	7.33	2.80	1.40	0.12	4.07	0.03	–	13.24	28.99
22	9.92	–	1.53	0.37	0.27	3.91	–	13.00	29.00
23	9.97	–	1.57	0.35	0.49	3.56	–	13.05	28.99
24	9.58	–	1.56	0.60	0.04	3.79	0.28	13.14	28.99
25	9.88	0.04	1.74	0.30	0.11	3.92	–	13.00	28.99

Nos. 1–3: Stage II; Nos. 4–25: Stage IV.

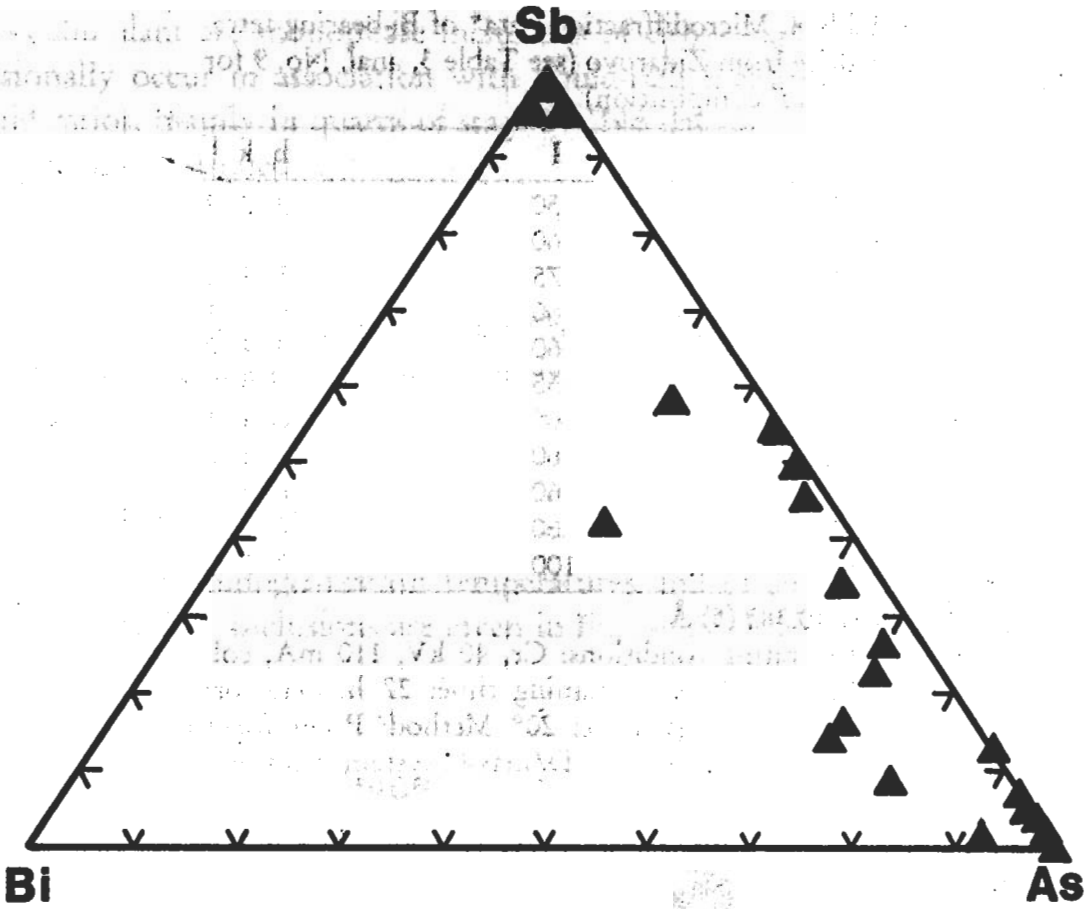

Fig. 3. Compositional range of Bi-bearing members of tetrahedrite–tennantite series in the Sb–As–Bi system.

Ag distinctly increases the cell size of tetrahedrite (Riley 1974, Pattrick & Hall 1983). For checking the effect of Bi substitution on the cell size, small crystals (35 × 25 μm) of the most Bi-rich, almost Ag-free tetrahedrite with 1.64 Sb, 1.38 As and 0.90 Bi atoms per formula unit (Table 3, anal. 9) were studied by X-ray microdiffraction (Table 4). The cell size obtained (a 10.383 Å) is much larger than those of Bi- and Zn-free (a 10.258 Å) and Bi-free zincian intermediate members (a 10.270 Å) with Sb/As ratios of about 1:1. Thus substitution of Bi for As and Sb considerably increases the cell size of fahlores. Further X-ray data, in particular of Bi-rich end members of the tetrahedrite–tennantite series, are necessary for correlation.

Galena

Galena is the most abundant ore mineral in Zidarovo, deposited exclusively in the fourth stage of mineralization, together with sphalerite. It often carries inclusions of tetrahedrite, tennantite or acanthite. 10 AAS analyses of large galena crystals devoid of mineral inclusions, revealed Ag, Bi and Sb contents of 270–451 ppm, 5–80 ppm, and 93–345 ppm, respectively.

Table 4. Microdiffraction data* of Bi-bearing tetrahedrite from Zidarovo (see Table 3, anal. No. 9 for chemical composition).

d	I	h k l
2.977	50	2 2 2
3.434	60	4 1 1
2.099	75	5 1 0
1.874	60	5 2 1
1.822	60	4 4 0
1.784	55	5 3 0
1.672	60	6 1 1
1.470	60	7 1 0
1.380	60	6 4 2
1.307	60	8 0 0
1.207	100	7 5 0

a = 10.383 (5) Å.

* Operating conditions: Cr, 40 kV, 110 mA, collimator: 30 μm, running time: 22 h, detector: OED, Omega angle: 20° Method: Point focus X-ray diffracotmeter D/max-C system, Rigaku.

Sphalerite

Sphalerite is an abundant mineral in Zidarovo. It was mainly deposited in the stage IV mineralization. Only rarely it is also found in stage II, in association with emplectite and aikinite. Microprobe analyses show that sphalerites from both stages of mineralization are extremely Fe-poor (in 13 analyses Fe = 0.08–0.89 wt.%, in 2 analyses Fe: 2.33–3.05 wt.%). AAS analyses revealed Cd and Mn values in the range of 3720–7230 ppm and 92–1220 ppm, respectively.

Fluid inclusion studies

Sixteen samples representing stages I–IV of ore mineralization from Kanarata and Yurta, were studied for fluid inclusions. The stages V and VI are devoid of ore minerals (Fig. 2). They were not included in the present study. A total of 192 inclusions (182 in quartz, 10 in sphalerite) were identified as primary and pseudosecondary according to Roedder (1984). In addition, about forty secondary inclusions were studied in quartz from different stages of mineralization.

Inclusion types

The majority of the inclusions is of common liquid-rich type with a vapor bubble which occupies between 15 and 40 percent of the total volume of the inclusions at room temperature. All of them homogenize to the liquid phase.

Less abundant are monophase inclusions of either vapor or liquid which occasionally occur in association with liquid-rich inclusions of various vapor/fluid ratios, mainly in quartz of stage IV. No daughter crystals were found in the inclusions studied.

Secondary inclusions

Most of the secondary inclusions were too small in size and not suitable for accurate measurements. Their homogenization temperatures are in the range of 105 to 145 °C. The salinities vary between less than 1.0 and 5.0 eq. wt.% NaCl.

Temperature and salinity data

Variations of homogenization temperatures and other data of primary and pseudosecondary inclusions are given in Fig. 4 and Table 5. There is a distinct

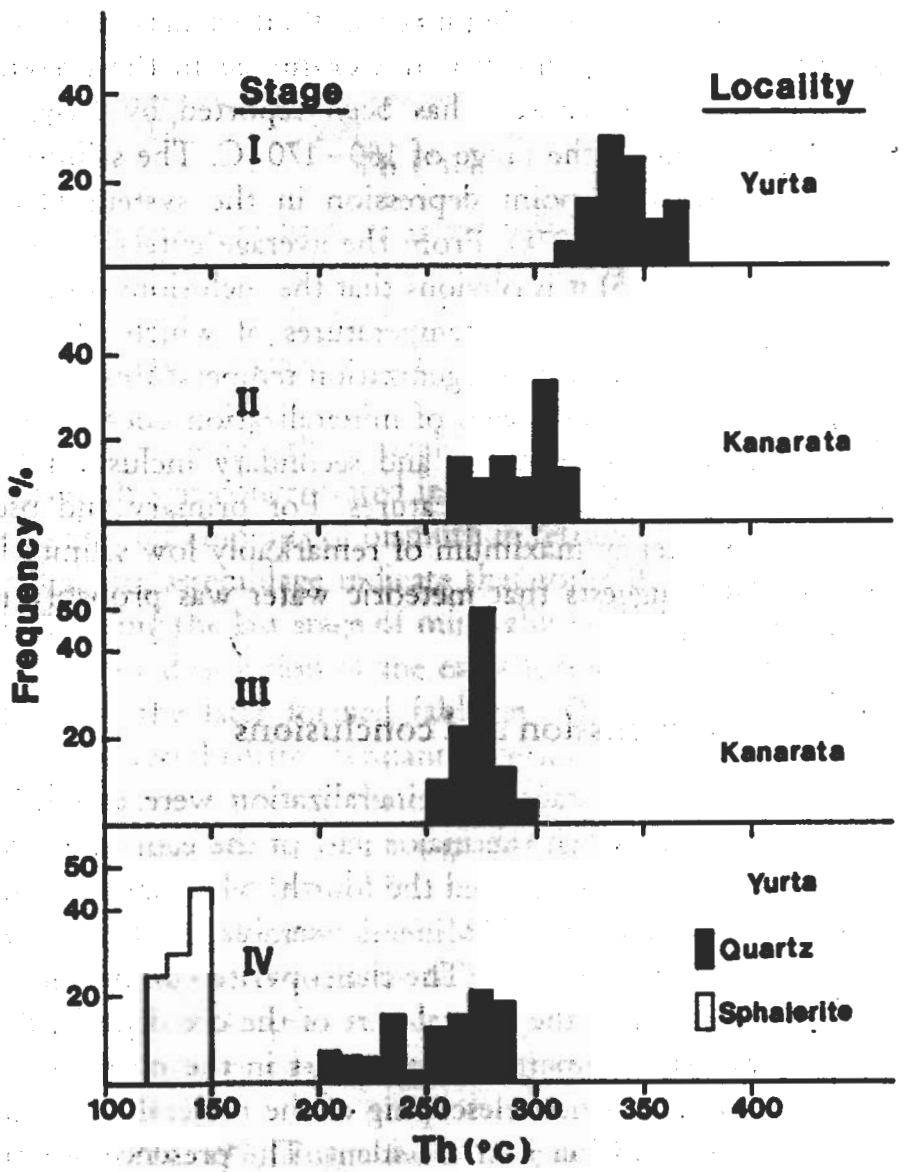

Fig. 4. Histograms showing the distribution of homogenization temperatures determined on the primary inclusions.

Table 5. Summary of fluid inclusion data.

Stage	Locality	Size (μm)	V/F	Th (°C)	Te (°C)	Mean Te	Tm (°C)	Salinity (eq. wt % NaCl)	Number of inclusions
I	Yurta	5×7 to 8×12	30/70 to 35/65	310–371	−15.2 to −24.3	−19.5	−1.7 to −2.2	3.3–4.3	22
II	Kanarata	6×6 to 10×12	20/80 to 30/70	258–316	−17.2 to −20.8	−19.0	−1.5 to −4.8	2.9–8.3	32
III	Kanarata	5×7 to 9×11	15/85 to 30/70	253–295	−14.8 to −22.2	−19.8	−1.6 to −2.2	3.1–4.3	36
III	Yurta	5×6 to 22×40	20/80 to 40/60	197–292	−15.6 to −24.9	−22.1	−1.3 to −4.5	2.0–8.3	92

V/F: vapor/fluid ratio; Th: homogenization temperature; Te: eutectic temperature; Tm: melting temperature.

decrease in homogenization temperatures from stage I to II, whereas temperature data determined for later stages show some overlaps. However, a general tendency of decreasing temperatures is obvious. The lowest homogenization temperatures (150–120 °C) were obtained for fluid inclusions in sphalerite from the last stage (Fig. 4). Calcite was not examined in the present study. However, its formation temperature has been reported by Kovatchev & Strashimirov (1979), to be in the range of 180–170 °C. The salinity data obtained are based on freezing point depression in the system H_2O–NaCl (Roedder 1962, Potter et al. 1978). From the average eutectic temperatures (−19.0 to −22.1 °C) (Table 5) it is obvious that the inclusions do not contain any $MgCl_2$ and $CaCl_2$, the eutectic temperatures of which are −33.6 and −49.8 °C, respectively. A plot of homogenization temperatures versus salinity data for fluid inclusions from all stages of mineralization does not show any correlation (Fig. 5). However, primary and secondary inclusions differ distinctly in their homogenization temperatures. For primary and pseudosecondary inclusions a frequency maximum of remarkably low salinity between 3 and 5 eq. wt. % NaCl suggests that meteoric water was probably involved during ore mineralization.

Discussion and conclusions

In the Zidarovo deposit four stages of mineralization were established. The main stages are the second, when the major part of the economically important copper and gold was deposited, and the fourth, when the base metal and the silver minerals were precipitated. Mineral assemblages of the main stages occupy different places in the ore field. The chalcopyrite–bismuthinite mineralization has been emplaced in the central part of the ore deposit (Kanarata), while the galena–sphalerite mineralization occurs in the northwestern periphery (Yurta). In spite of distinct telescoping of the mineral parageneses, lateral zoning of the mineralization is also evident. The presence of silver minerals, Ag-rich gold and Ag-rich tetrahedrite as well as the higher Ag-contents of chalcopyrite in the galena–sphalerite assemblage suggest that the hydro-

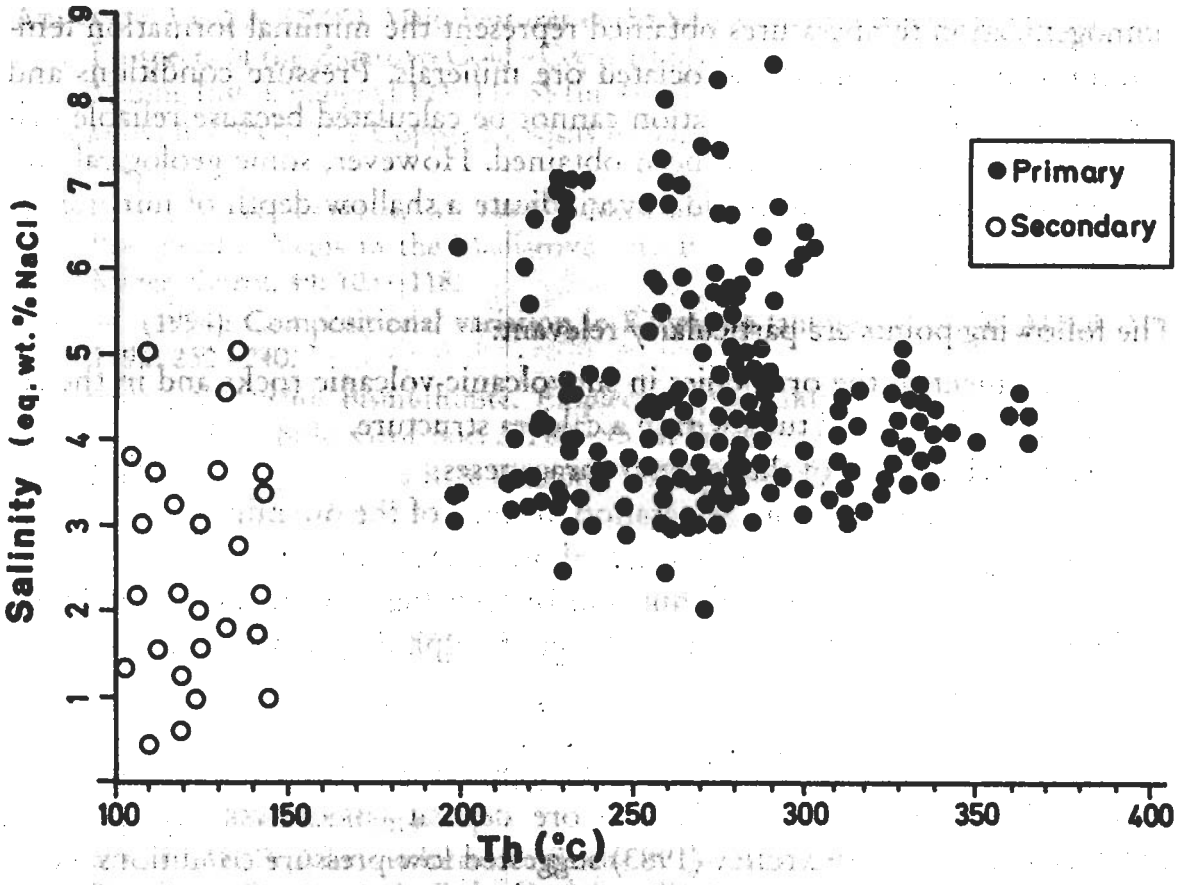

Fig. 5. Homogenization temperature versus salinity plot for primary and secondary fluid inclusions.

thermal fluids were enriched in silver during the last stage of ore mineralization.

The occurrence of bismuth minerals and Bi-bearing fahlores is specific to Zidarovo. Bismuth was concentrated in the early stage of mineralization. However, the significant amounts of bismuth in tetrahedrites and tennantites in the galena–sphalerite assemblage indicate that some Bi was also available or was redeposited during the last stage of mineralization. This may be due to partial decomposition or dissolution of the early formed bismuth minerals and their replacement by the later formed fahlores. The compositional variations of members of the tetrahedrite–tennantite series do not indicate any fluctuation of Sb and As concentrations in the ore fluids during their evolution.

Our fluid inclusion studies show a gradual decrease of homogenization temperatures from stage I (371–310 °C) to stage IV (292–197 °C) of mineralization. Formation temperatures in the range of 305–250 °C and 295–210 °C have been reported by Kovatchev & Strashimirov (1979) for chalcopyrite–bismuthinite and chalcopyrite–galena–sphalerite assemblage, respectively, which probably corresponds to the mineralization stages II and IV in the present study.

Kovatchev (1983, 1990) suggested zoning of the mineralization around the Zidarovo intrusion. Transition zones both in ore mineral parageneses and their formation temperatures (Fig. 4) are consistent with this assumption. The

homogenization temperatures obtained represent the minimal formation temperatures of quartz and the associated ore minerals. Pressure conditions and the primary depth of mineralization cannot be calculated because reliable evidence for fluid boiling has not been obtained. However, some geological and mineralogical peculiarities in Zidarovo indicate a shallow depth of mineralization.

The following points are particularly relevant:

1. Emplacement of the ore bodies in subvolcanic-volcanic rocks and in the related pyroclastics and tuffs within a caldera structure.
2. Distinct telescoping of the mineral parageneses.
3. Presence of more than one generation of some of the ore minerals.
4. Predominance of quartz in all stages of ore mineralization.
5. Periodical fluctuation of sulphur and oxygen fugacity in the mineralizing fluids which is indicated by alternation of sulphides, hematite and sulphosalts.

Almost all the above-mentioned mineralogical features are comparable to those encountered in the Madjarovo ore deposit (Breskovska & Tarkian 1993). Accordingly Kovatchev (1983) suggested low pressure conditions and a shallow depth of mineralization of 1300 m and 500 m in the central and outer zone of the Zidarovo deposit, respectively. Fluid inclusion data of the present study show that overall salinities of the fluids were very low during all stages of mineralization. This can be explained by interactions between ascending hydrothermal fluids and downward migrating dilute meteoric waters. Such processes are very likely in a subvolcanic-volcanic environment characterized by shalow-seated, fault controlled mineralized veins.

Acknowledgements

The paper reports part of a cooperative research program on the mineralogy and geochemistry of the hydrothermal polymetallic ore deposits in the Eastern Rhodope and the Srednogorie zone, Bulgaria. The project is jointly executed by the Universities of Sofia and Hamburg. We want to thank the administration of both universities for financial support. Thanks are due to Dr. Y. S. Borodaev, Moscow State University, and Mrs. B. Cornelisen, Hamburg University, for help with the microprobe analyses. We thank Mr. H. Tigges, Rigaku Company, Düsseldorf, and Dr. W. Liessmann, Hamburg University, for microdiffraction study of tetrahedrite, and Dr. V. Mladenova for her help with ore microscopy. Prof. E. F. Stumpfl, University of Leoben, kindly improved the English text.

References

Amov, B. G., Baldjieva, C. T., Breskovska, V. V., Kolkovski, B. G., Stoykov, H. M. & Todorov, T. A. (1985): Lead Isotopes, Genesis, and Age of Ore Deposits in South Bulgaria. – Geol. Ore Dep. XXV11: 3–17 (in Russ.).

Atanasov, Vess, A. (1990): Main Features in the Structure, Mineralization, Genesis and Prospects of the Zidarovo Gold–Copper-Polymetallic Deposit (Bulgaria). – Rev. Mining Inst. Leningrad 121: 43–55 (in Russ.).

Bogdanov, B. (1987): The Copper Deposits in Bulgaria. – "Technica" Sofia, 388 p. (in Bulg.).

Breskovska, V. & Tarkian, M. (1993): Mineralogy and Fluid Inclusion Study of Polymetallic Veins in the Madjarovo Ore Field, Eastern Rhodope, Bulgaria. – Miner. Petrol. 49: 103–118.

– – (1994): Compositional variation in Bi-bearing fahlores. – N. Jb. Miner. Mh. 1994: 230–240.

Kovatchev, V. (1976): Bismuthinite, Emplectite and Aikinite in the Zidarovo Ore Field. – Rev. Bulg. Geol. Soc. 37: 89–95 (in Bulg.).

– (1979): Tetradymite – a Rare Bismuth Telluride from Zidarovo Deposit. – C. R. Bulg. Acad. Sci. 32: 193–196.

– (1983): Ore Forming Processes in the Zidarovo Ore Field (Eastern Srednogorie). – XII Congress of Carpatho-Balc. Geol. Assoc., Bucarest, pp. 169–177 (in Russ.).

– (1990): The Form of Occurrence for Rare and Precious Elements in Zidarovo Ore Field. – Annual of the Higher Institute of Mining and Geology, part I, Sofia, pp. 131–145 (in Bulg.).

Kovatchev, V. & Strashimirov, S. (1979): Mineral Termometry Studies and Temperature Zonality in the Zidarovo Ore Field. – Review Bulg. Geol. Soc. XL, 1, pp. 101–108 (in Bulg.).

Marinov, T. (1980): Alkaline Intrusive Rocks in the Area of Zidarovo Village, Burgas District. – Review of the Bulg. Geol. Soc. XL1, 2, pp. 112–119 (in Bulg.).

Marinov, T. & Bairaktarov, I. (1981): Petrological Characteristic of the Subvolcanic Dyke Rocks from the Zidarovo Central Magmatic Complex. – Review Bulg. Geol. Soc. XL11, 1, pp. 56–66 (in Bulg.).

Mozgova, N. N. & Tzepin, A. I. (1983): Fahlores (Peculiarity of the chemical compositions and properties). – Moskov, Nauka, 280 p. (in Russ.).

Pattrick, R. A. D. & Hall, A. J. (1983): Silver substitution into synthetic zinc, cadmium, and iron tetrahedrites. – Miner. Mag. 47: 441–451.

Popov, P. (1981): Structure of the Zidarovo Ore Field. – Review Bulg. Geol. Soc. XL11, 1, pp. 45–55 (in Bulg.).

– (ed.) (1993): Geology and Metallogeny of Burgas Ore Region. – Sofia, Higher Institute of Mining and Geology, 93 p. (in Bulg.).

Potter, R. W., Clynne, M. A. & Brown, D. L. (1978): Freezing point depression of aqueous sodium chloride solution. – Econ. Geol. 73: 284–285.

Riley, J. F. (1974): The tetrahedrite–freibergite series, with reference to the Mount Isa Pb–Zn–Ag ore body. – Miner. Deposita 9: 117–124.

Roedder, E. (1962): Studies of fluid inclusions. I. Low temperature application of a dualpurpose freezing and heating stage. – Econ. Geol. 57: 1045–1061.

– (1984): Fluid inclusions, reviews in mineralogy, Vol. 12. – Mineralogical Society of America, Book Crafters Inc. Chelsea Michigan 48118.

Stanisheva, G. (1971): Upper Cretaceous magmatism in the Burgas syinclinorium. – C. R. Bulg. Acad. Sci. 24: 11, 1509–1512.

Tarkian, M. & Breskovska, V. (1990): Arsenic minerals and their genetic significance in the Madjarovo ore field, Eastern Rhodope, Bulgaria. – N. Jb. Miner. Mh. 1990: 433–442.

Todorov, T. (1986): Some aspects in the geochemistry of the elements in the Zidarovo polimetallic deposit, Burgas ore region. – Ore Forming Proc. Miner. Dep. 24: 3–17 (in Bulg.).